UNIVERSITÁ DEGLI STUDI DI PARMA

Dottorato di Ricerca in Scienze Mediche

Ciclo XXIX

Development of stem cell tissue engineered patches and assessment of their potential for corrective heart surgery using a cardiopulmonary bypass swine model

Coordinatore:
Chiar.mo Prof. Riccardo Bonadonna

Tutori:
Chiar.mo Prof. Federico Quaini
Dott. Mohamed Ghorbel

Dottoranda: Ambra Albertario

ABSTRACT

Congenital Heart Defects (CHDs) are the leading global cause of death in the first year of life. Truncus Arteriosus (TA) is a CHD characterized by a common aorta/pulmonary artery and a ventricular septal defect. When treating paediatric patients with CHD, corrective surgery often requires patches, conduits or valves to repair the defect. Right ventricular outflow tract (RVOT) reconstruction in patients with TA involves the use of a replacement patch. Synthetic and fixed grafts currently used in cardiac surgery are non-living, non-contractile and they lack growth potential, leading to increased risk of thrombosis, stenosis, calcification and reoperation. Several studies suggest that tissue-engineered grafts made from living, functional cells could grow and remodel in parallel with the patient, facilitate healing and help to recover cardiac function. To date, autologous stem cells represent the most promising cell source to engineer cardiovascular patches.

The aim of this study was to develop engineered cardiac patches with the potential to be used for correction of CHD. Additionally, we established a cardiopulmonary bypass recovery piglet model for RVOT reconstruction to test tissue-engineered grafts.

Mesenchymal stem cells (MSCs) were isolated from the thymus gland of both newborn piglets and children undergoing open-heart surgeries. Cell surface markers and functional characterization demonstrated the mesenchymal lineage of the thymus-derived stem cells. Three differentiation protocols were tested in order to identify the best strategy to generate cardiac committed cells from MSCs. Three scaffolds were developed and tested for their capability to allow cell engraftment and proliferation. Porcine pericardium and myocardium were decellularized and recellularized with undifferentiated and differentiated cells, which were cultured under static conditions. The biocompatibility of CorMatrix® was also investigated by culturing the seeded graft under either static or dynamic conditions. 20 - 25 kg piglets underwent general anaesthesia and the heart was accessed by sternotomy. Cardiopulmonary bypass was established by cannulating the ascending aorta and the inferior and superior vena cava. An incision over the RVOT and below the pulmonary valve was performed. The defect created was then patched using either an engineered-CorMatrix® or an unseeded control scaffold. The patches were stitched with the cell-seeded side facing the inner

side of the heart. Two animals were terminated 4 months after surgery and one was sacrificed after 24 hours. Histological and immunofluorescent stainings were performed on the explanted grafts and right ventricles in order to evaluate the grafts degradation and integration within the surrounding tissue, cells migration and penetration into the scaffolds, possible immune-response generated and to characterize the cellular content of the explants.

Human and porcine thymus-derived MSCs express the mesenchymal surface markers and efficiently differentiate into the three mesenchymal phenotypes. Cardiomyocyte-like cells were obtained from all the developed protocols as cardiac-specific markers were detected in the differentiated cells by immunocytochemistry and RT-PCR. No cellular nor nuclear materials were detected in the decellularized pericardium and myocardium, while the extracellular matrix structure and composition was well preserved, indicating that a successful decellularization was achieved. The recellularization of the decellularized materials and the CorMatrix® was efficient for both undifferentiated and differentiated cells. The optimal cell-scaffold-stimuli combination appeared to be CorMatrix® seeded with undifferentiated cells cultured under dynamic conditions. Two out of three piglets successfully recovered the surgical procedure. One animal was terminated prior the end point as the piglet was too anaemic after surgery. The histological examination of the 4 months-patches showed good integration of the scaffold within the surrounding tissue as the CorMatrix® was no longer detectable. New collagen-rich tissue built up from the implanted grafts and some cardiac-like areas were found in the graft-side of the explants. Immunofluorescent characterization of the samples confirmed that these areas expressed cardiac markers and that they were more abundant in the engineered-patch then in the unseeded scaffold. High degree of vascularization was observed in the newly formed tissue. The quantification of both the capillaries and the greater vessels demonstrated that there was more angiogenesis in the engineered graft then in the control. No major differences were observed in terms of endothelialisation as a mature layer of endothelium was observed in both samples. These data suggest that the presence of the seeded cells helped the remodelling of the graft and triggered the generation of new blood vessels. Evaluation of the engineered-graft that was explanted 24 hours post-surgery, showed the presence of a thick cell layer growing on the inner side of the scaffold. A strong inflammation process was on going, most likely due to the surgery performed on the day before.

In conclusion, with this study we have validated a protocol for isolation and differentiation of thymus-derived MSCs and the use of these cells to engineer living grafts from decellularized xenogeneic materials and commercially available scaffolds. These results allow the generation of cardiac patches that have the potential to be used in corrective heart surgery. Furthermore, the in vivo study established a cardiopulmonary bypass juvenile porcine model for RVOT grafting.

ACKNOWLEDGMENTS

Undertaking this PhD has been the most challenging experience of my life and it would not have been possible without the support that I received from many people.

Firstly I would like to say a very big thank you to my supervisor Dr. Mohamed Ghorbel for all the guidance he gave me during the three years I spent in Bristol. He has provided me valuable academic supports, suggestions and advice since even before I started working with him. I am also grateful to my co-supervisor Professor Massimo Caputo for his contributions in this project and his immense technical expertise in cardiac surgery. I would like to acknowledge them both for helping me to obtain a technician position to financially support my permanence abroad.

Similar, profound gratitude goes to my Italian supervisor Professor Federico Quaini for his constant support, availability and encouragements. He has been a truly dedicated mentor who always believed in me since when I met him during my bachelor and made it possible for me to obtain this PhD position.

I gratefully acknowledge The Sir Jules Thorne charitable trust for their generous financial support, without which this project would not have been completed. I would also like to thank our other founding bodies including The Enid Linder Foundation, The Mahoro Trust, the National Institute for Health, the Bristol Heart Institute and the University of Bristol.

A huge thank you goes to my research team, particularly to Megan Swim and Dr. Dominga Iacobazzi not only for their constant help, patience and good advices but also for being really good friends. The group of people working at Level 7 has been an incredible source of friendships. I am particularly pleased that I met Francesca, who soon became my greatest friend in Bristol.

I would like to acknowledge all the in vivo-team, the Langford Veterinary School and the TBRC for supporting us with surgeries and animal care. I am also thankful to the Wolfson Bioimaging Facility and the Flow Cytometry Facility for their technical help and precious feedbacks.

A heartfelt thank you goes to my mum and dad for encouraging me to follow my dreams and helping in whatever way they could during this period. I have always looked forward to going home to spend time with them and get looked after.

Finally, but by no means least, thanks go to my loving and supportive boyfriend Tommaso, who has been by my side throughout this entire journey. Living apart for three years has been an immense challenge, there are no words that can express my gratitude for his faithful love and endless patience. It is to him that I dedicate this thesis.

TABLE OF CONTENTS

ABBREVIATIONS

5-Aza	=	5-Azacytidine
AB	=	Alcian Blue
ACT	=	Activating Clotting Time
ACTA1	=	Actin alpha 1
AO	=	Aorta
ASC	=	Adult Stem Cell
ASD	=	Atrial Septal Defect
ASU	=	Animal Services Unit
aSMA	=	Alpha Smooth Muscle Actin
CCM	=	Cardiomyocyte Conditioned Medium
CD	=	Cluster of Differentiation
cDNA	=	Coding Deoxyribonucleic Acid
CHD	=	Congenital Heart Disease
CM/rCM	=	Cardiomyocyte / rat Cardiomyocyte
cMYH	=	cardiac Myosin Heavy Chain
CorMx	=	CorMatrix®
CPB	=	Cardiopulmonary Bypass
cTnI	=	Cardiac Troponin I
CX43	=	Connexin-43
DAPI	=	4',6-diamidino-2-phenylindole
Des/DES	=	Desmin
Diff-MSC	=	Differentiated Mesenchymal Stem Cell
DMEM	=	Dulbecco's Modified Eagle Medium
DMSO	=	Dimethyl Sulfoxide
ECHO	=	Echocardiogram
ECM	=	Extracellular Matrix
EDTA	=	Ethylenediaminetetraacetic acid
EDV	=	End-Diastolic Volume
EF	=	Ejection Fraction
EPC	=	Endothelial Progenitor Cell
ESC	=	Embryonic Stem Cell
ESV	=	End-Systolic Volume
EthD-III	=	Ethidium homodimer III
EVG	=	Elastic Van Gieson
FACS	=	Flow Cytometry
FBS	=	Fetal Bovine Serum
FS	=	Fractional Shortening
GATA-4	=	GATA Binding Protein 4

HLA-DR	=	Human leukocyte antigen-D Related
HLHS	=	Hypoplastic Left Heart Syndrome
HS	=	Horse Serum
hTMSC	=	Human Thymus Mesenchymal Stem Cell
ICC	=	Immunocytochemistry
IHC	=	Immunohistochemistry
IMDM	=	Iscove's Modified Dulbecco's Medium
IMS	=	Industrial Modified Spirits
iPS	=	Induced Pluripotent Stem Cell
Iso	=	Isolectin B4
ITS	=	Insulin-Transferrin Selenium
IVSd	=	Intraventricular Septum in diastole
IVSs	=	Intraventricular Septum in systole
LA	=	Left Atrium
Lin -	=	Lineage negative
LV	=	Left Ventricle
LVIDd	=	Left Ventricle Internal Diameter in diastole
LVIDs	=	Left Ventricle Internal Diameter in systole
LVPWd	=	Left Ventricle Posterior Wall in diastole
LVPWs	=	Left Ventricle Posterior Wall in systole
M199	=	Medium 199
MM	=	Master Mix
MSC	=	Mesenchymal Stem Cell
NMBA	=	neuromuscular blockade
NSAID	=	Non-steroidal anti-inflammatory drug
ON	=	Overnight
P	=	Passage
P/S	=	Penicillin/Streptomycin
PA	=	Pulmonary Artery
PBS	=	Phosphate Buffer Saline
PCL	=	Polycaprolactone
PET	=	Polyethylene Terephthalate
PFA	=	Paraphormaldehyde
PLA	=	Poly-L-lactic acid
PLG	=	Polyglycolic acid
PLGA	=	Poly-L-lactic-co-glycolic acid
PLLA	=	Poly-L-lactide
Post-op	=	Post-operative
pTMSC	=	Porcine Mesenchymal Stem Cell
RA	=	Right Atrium

RNA	=	Ribonucleic Acid
RT	=	Room Temperature
RV	=	Right Ventricle
RVOT	=	Right Ventricular Tract Reconstruction
SaA	=	Sarcomeric alpha Actinin
SC	=	Stem Cell
SDS	=	Sodium Dodecyl Sulphate
SEM	=	Scanning Electron Microscopy
smMYH	=	Smooth muscle Myosin Heavy Chain
SpO2	=	Oxygen Saturation
SV	=	Stroke Volume
TA	=	Truncus Arteriosus
TBRC	=	Translational Biomedical Research Centre
TE	=	Tissue Engineer
TGFβ	=	Transforming Growth Factor beta
ToF	=	Tetralogy of Fallot
TrV	=	Truncal Valve
Try	=	Trypsin
TX	=	TritonX-100
UCB-MNC	=	Umbilical Cord Blood Mononuclear Cell
ug	=	µg
VF	=	Ventricular Fibrillation
VSD	=	Ventricular Septal Defect

INTRODUCTION

1. THE HEART

1.1. Anatomy

The heart is a hollow muscular organ that pumps blood throughout the body. It is located between the lungs in the middle of the chest, behind and slightly to the left of the sternum. In mammals the heart is divided into four chambers: upper left and right atria (respectively LA and RA) and lower left and right ventricles (respectively LV and RV). The heart wall consists of three layers: endocardium, myocardium and epicardium (Figure 1).

Endocardium: is the innermost layer that covers the heart chambers and valves and is made of simple squamous epithelium. It is the equivalent of the tunica intima of the endothelium.

Myocardium: is the cardiac muscle, an involuntary and striated muscle that has the unique ability to initiate an action potential at a fixed rate. The myocardium is made of different types of cells, including muscle cells, consisting of the majority of the cells and that have the ability to contract; pacemaker cells, which form the conduction system of the heart; myocardial fibroblast and smooth muscle cells.

Epicardium: is the inner serous membrane of the pericardium, a conical sac of fibrous tissue that surrounds the heart. The epicardium is the equivalent of the tunica adventitia of the endothelium and it contains fibroelastic connective tissue, blood vessels, lymphatic and adipose tissue.

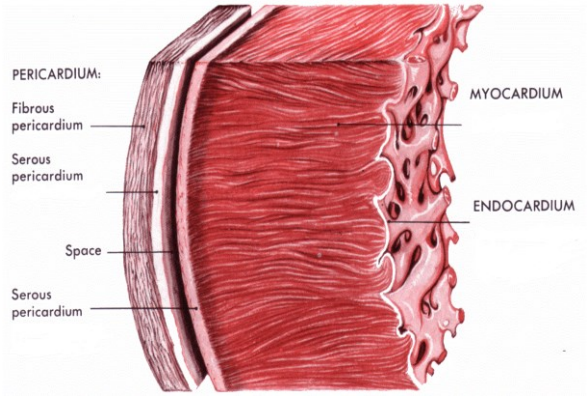

Figure 1 Section of the heart wall, showing the pericardium, constituting of the fibrous and serous pericardium; the myocardium and the innermost layer of the endocardium (Thompson 1984).

Four valves regulate blood flow through the heart: the tricuspid valve that lies between the RA and RV; the mitral valve (or bicuspid valve) that lies between the LA and LV; the pulmonary valve, which regulates the blood flow from the RV into the pulmonary artery and the aortic valve that controls the blood flow from the LV into the aorta (Thompson 1984) (Figure 2).

The heart receives deoxygenated blood from the systemic circulation through the superior and inferior vena cava. Here the blood enters the RA and goes to the RV through the tricuspid valve. The deoxygenated blood is pumped to the pulmonary circulation via the pulmonary artery and reaches the lungs where the exchange between carbon dioxide and oxygen happens. The oxygenated blood returns to the heart through the pulmonary veins, enters the LA and passes to the LV trough the mitral valve. From the LV, the blood is pumped to the systemic circulation via the aorta, where it will provide oxygen and nutrients to the body (Van Mierop 1965). The circulation system that supplies the heart with oxygen and nutrients and removes metabolic wastes is called coronary circulation. This system includes arteries, veins and lymphatic vessels. The nerve supply of the heart consists of the vagus nerve and several nerves arising from the sympathetic trunk. The heart rate and the heart contraction are more influenced rather than controlled, by the nervous system.

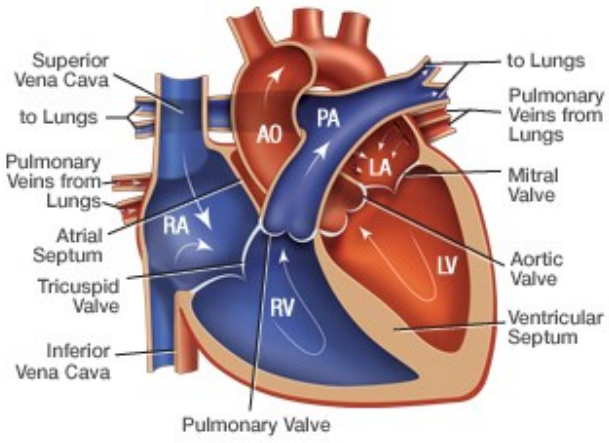

Figure 2 The normal heart. AO: aorta, PA: pulmonary artery, LA: left atrium, RA: right atrium, LV: left ventricle, RV: right ventricle (http://www.chop.edu/conditions-diseases).

1.2. Heart Development

The heart is the first functional organ to develop in vertebrate embryo. It derives from the mesodermic germ-layer cells. The process begins at around day 18 and 19 after fertilization, when two endocardinal tubes start to grow from the so-called cardiogenic region of the neural plate. By the third week, the two tubes migrate together and merge to form a single tube, called tubular heart. This structure is a primitive heart, which quickly forms five distinct regions: the sinus venosus, that will become the back part of the RA, the coronary sinus and the sinoatrial node; the primitive atrium and ventricle, that will develop respectively into the front parts of the LA, RA and LV; the bulbus condis, which will become the RV and the truncus arteriosus that will split to form the aorta and the pulmonary artery (Anderson and Brown 1996).

The human embryonic heart starts beating at around 22 day after conception. The heartbeats is initiated by the pacemaker cells that develop in the primitive atrium and in the sinus venus. Through a conduction pathway, the heartbeat spread from the pacemaker region to the rest of the heart.

2. CONGENITAL HEART DISEASE

Congenital heart disease (CHDs) consists of gross structural abnormalities of the heart or the intra-thoracic great vessels present at birth that have actual or potential functional significance.

2.1. Epidemiology

CHDs are the most common birth defect as well as the commonest cause of infant morbidity. The incidence ranges from 0.4% to 1.2% in live born babies, meaning that 4500 new cases are born every year in the UK (Krasuski and Bashore 2016). Without corrective surgery, about 60% of children with CHD die in the first year of life. This was the case until 30 years ago. However the enormous progress in the surgical treatments

over the last three decades, led to a situation in which 85% of infants with CHD can reach adulthood (van der Bom et al. 2011).

2.2. Aetiology

CHDs can be caused either by genetic or environmental factors, though usually are caused by a combination of both. Most of the genetic known causes are sporadic genetic changes, such as focal mutations, addition or deletion of genetic material. Large chromosomal abnormalities like trisomies 13, 18 and 21 are responsible of about 5-8% of cases of CHD (Gelb and Chung 2014). Also small chromosomal changes frequently lead to CHD. Microdeletion of the long arm of chromosome 1 (1q21), microdeletion of the short arm of chromosome 8 (8p23) and microdeletion of the long arm of chromosome 22 (22q11, DiGeorge syndrome) are just some examples (Pelech and Broeckel 2005). Among the environmental factors that predispose to a situation of CHD, there are: maternal illness, such as obesity, diabetes mellitus, phenylketonuria and systemic lupus arythematosus; medical drugs, like lithium, retinoic acid and some anti-epileptics and lastly infective embryopathies as rubella, cocksackie and HIV (Nora and Nora 1990).

Despite all what is known, in the 90% of CHD there are no detectable risk factors. That means that nowadays it is not possible to anticipate that a cardiac disease might occur in the 90% of cases of CHD (Gelb and Chung 2014).

2.3. Classification

A number of classification systems exist for CHD: alphabetical order, cyanotic and non-cyanotic, site of the defect, pathophysiological classification and so on. For example, the American Heart Association classifies the CHD into three great groups: septal defects, obstructive defects and cyanotic defects (Thiene and Frescura 2010).

2.3.1. Septal defects

In a normal heart there is no communication between the left and right side. If a hole is present in the septum, it means that the infant is affected by septal defect. The malformation can vary greatly in size, but they all allow oxygenated blood from the LV to mix with the deoxygenated one in the RV. Non-severe septal defects does not require corrective surgery. Whether a surgical repair is necessary, it is usually performed later in life rather than during the newborn period (Anderson and Wilcox 1992).

Atrial Septal Defect (ASD) accounts for approximately 5-10% of all the CHD. This malformation is characterized by a hole between the atria (Figure 3a). If a large defect is present, a great amount of oxygenated blood leaks from the LA back to the RA.

Ventricular Septal Defect (VSD) accounts for about 20-25% of all the CHD, making it the most common CHD. In VSD a hole between the two ventricles is present (Figure 3b). This allows the blood to pass from the LV to the RV.

2.3.2. Obstructive defects

In an obstructive cardiac defect, the blood flow is restricted or blocked. The obstruction can occur in any of the four cardiac valves, below or above one of the valve. The blockage, called atresia, or the narrowing, called stenosis, can occur either in veins or in arteries. According to the site of the disorder, it can be distinguished between aortic stenosis, pulmonary stenosis and coarctation of the aorta (Thiene and Frescura 2010).

Aortic stenosis accounts for 5% of all CHD and consists of a narrowing of the aortic valve. This cause a restriction of the blood that flow through the valve and consequently the heart needs to contract harder to pump enough blood into the aorta. Severe narrowing can lead to heart failure.

Pulmonary stenosis accounts for about 5 to 8% of all CHD and consists of a narrowing of the pulmonary valve. When this condition is present, the RV has to work harder to pump the blood through the narrow valve.

Coarctation of the aorta accounts for 8% of all CHD and it is a narrowing of specific portion of the aorta. The defect is usually found just past the arch of the aorta (Figure 3c). If the narrowing is severe, the LV might not be sufficiently strong to push blood through the coarctation. This can lead to a lack of blood in the lower part of the body

2.3.3. Cyanotic defects

The name of these cardiac defects is such because they result in cyanosis: a bluish-grey discoloration of the skin due to a lack of oxygen in the body. Therefore the blood that circulate in patients with cyanotic defects, is not adequately oxygenated.

Tetralogy of Fallot (ToF) accounts for around 10% of all CHD. It is characterized by a narrowing of the pulmonary valve that leads to have less blood pumped from the RV to the lungs. A large VSD is usually present, which allows the unoxygenated blood to pass from the RV to the LV without going to the lungs (Figure 3d). Corrective surgery needs to be performed in order to restore a normal blood flow (Jacobs 2000a).

Transposition of the great vessels accounts for 5% of all the CHD. It is characterized by an abnormal aorta, that instead of being connected to the LV, it connects to the RV. In this defect the blood is pumped back to the body, instead of being the RV to pump blood to the lungs (Utzon 1976).

Hypoplastic left heart syndrome (HLHS) accounts for about 1-2% of all CHD. This syndrome it is characterized by a smaller left side of the heart (Figure 3e). The structures that are usually affected are the LV, the aorta, the aortic valve and the mitral valve. Corrective surgery is needed to restore this malformation (Tchervenkov, Jacobs, and Tahta 2000).

Truncus arteriosus (TA) accounts for approximately 3% of all the CHD. This malformation combines the aorta and the pulmonary artery into one single vessel. TA is usually associated with valve abnormalities and VSD (Figure 3f).

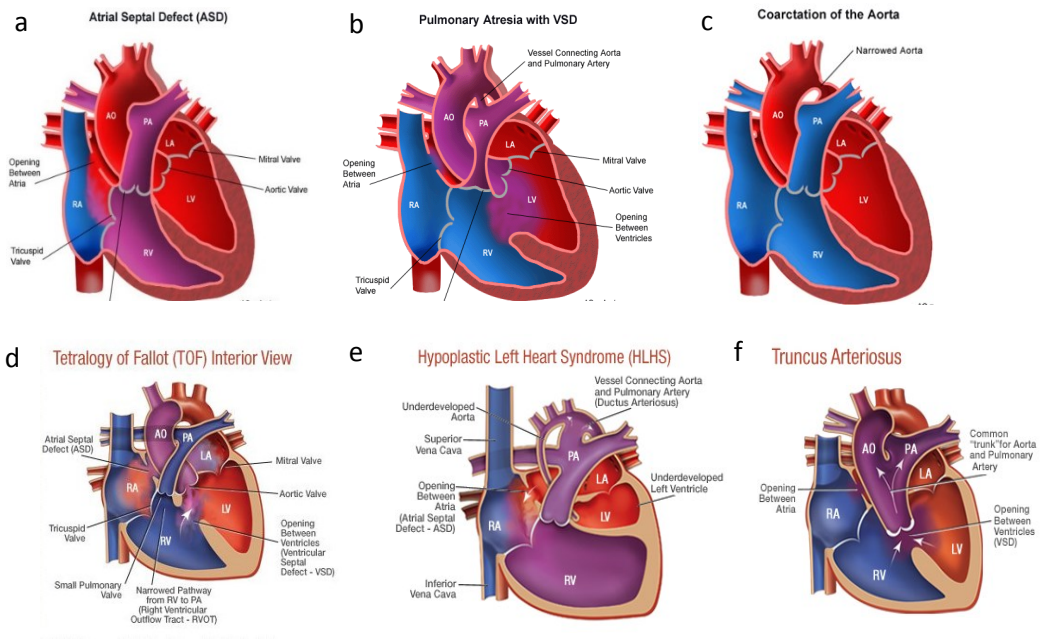

Figure 3 Anatomy of hearts with ASD, Pulmonary Atresia with VSD, Coarctation of the aorta, ToF, HLHS and TA (www.stanfordchildrens.org; http://www.chop.edu/conditions-diseases).

2.4. Treatments for CHDs

Some types of CHD can improve without surgery. Other malformations can be so small that no treatments are required. However, CHDs are usually serious conditions and surgery and/or medications are necessary. Some examples of medications include: diuretics, which help the body to eliminate water, digoxin, for strengthening the heart contraction and salts (Kaushal et al. 2009).

Most of the time medications are not enough and a surgical procedure is required to restore circulation back to normal. One-step corrective surgery is the ideal therapeutic option for patients with severe CHD, during which the cardiac surgeon closes holes in the heart using stitches or patch, repairs or substitute valves, widens narrowed arteries and restore the normal location of large blood vessels (Sun et al. 2015). Nevertheless, complex diseases normally require multiple open-heart surgeries in order to correct the malformation(s) (Woodward 2011). Palliative procedure may be indicated to relieve symptoms of acute heart failing, allowing more invasive procedures to be carried out when the infant has gained weight and his/her hemodynamic system will be stabilized. One of the main reason that cause the need of multiple interventions, is the deterioration of the implanted patch. In addition to that, current materials do not grow

with the patient and they need to be replaced (Said and Burkhart 2014). Patients with high risk of mortality and not suitable for corrective or palliative surgery, are candidate to heart transplantation. This extreme option is restricted due to a lack of suitable donor organs and, even in case of successful transplantation, life-long immune suppression would normally be associated with several serious side effects (Razzouk and Bailey 2014; Ishigami et al. 2015).

The socio-economic impact of CHDs is enormous. Thus, CHDs are considered a major healthcare burden. In fact patients usually need to undergo to more than one surgical procedure, their hospital permanency can be significantly long (from few days up to 2 weeks) and they need a life-long follow-up. This results in a huge challenge for the healthcare systems of the world. The World Health Organization calculated that CHDs cost about $ 60 million daily. Just in the US, approximately $ 400 million are spent per 1 million newborn baby with CHD (Krasuski and Bashore 2016).

2.5. Truncus Arteriosus

Truncus Arteriosus (TA) is rare congenital malformation that belongs to the cyanotic CHD. In a normal heart, the aorta comes out of the LV and the pulmonary artery arises from the RV and they are two distinct vessels. Patients suffering from TA, have a single large artery coming out from the ventricles that provides systemic, pulmonary and coronary circulation (Van Praagh and Van Praagh 1965). The common aorta/pulmonary artery is called truncus arteriosus. This name derives from a structure present during the embryonic development, where an arterial trunk originates from the two ventricles. This structure, should divide into the ascending aorta and the pulmonary trunk. Failure of the truncus arteriosus to divide, results in the pathological condition of TA.

Associated cardiac anomalies are normally present in patients with TA. The most common one is a VSD. A hole between the two ventricles is generally present below the arterial trunk. As a results, oxygenated and deoxygenated blood mix together. Some of this mixed blood is pumped to the lungs and some is pumped to the rest of the body. Most of the time more blood then usual goes to the lungs, overloading the respiratory apparatus. A single truncal valve (TrV) is contained within the single vessel. TrV dysplasia or dysfunction can occur as well as aortic arch and coronary artery anomalies. About

20% of patients with TA, have a DiGeorge syndrome, which is characterized by immune deficiency, bone disorder, facial deformity and hypocalcaemia (Ziolkowska et al. 2008; Momma 2010).

If TA was left untreated, about the 88% of patients would die within infancy (Sojak et al. 2012). This is mainly due to heart failure from TrV regurgitation, pulmonary overflow or shock from lower body hypoperfusion. In addition, the respiration can become difficult due to the surplus of blood circulating in the lungs that may cause extra fluid to develop in and around them. If too much blood flows to the lungs for a long time, it is possible that the blood vessels that goes to the lungs become permanently damaged. Over time, it becomes very difficult for the heart to pump so much blood to the lungs. As a result, pulmonary hypertension will develop, which could be life-threatening.

The symptoms of TA includes: bluish skin, typical of patients suffering from cyanotic defects; delayed growth or growth failure; lethargy; fatigue; poor feeding; rapid breathing (tachypnea), shortness of breathing (dyspnea) and widening of the finger tips (clubbing).

2.5.1. Classification

Two major classification systems are used to describe TA (Jacobs 2000b). The original one was developed by Collett and Edwards in 1949 and includes TA types I - IV, as follows:

Type I: the main pulmonary artery is present and comes out from the left lateral aspect of the common arterial trunk.

Type II: the right and left pulmonary arteries arise adjacent one to the other from the posterior aspect of the common trunk.

Type III: the right and left pulmonary arteries originate independently from the common trunk. They usually arise from the left and right lateral aspects of the trunk.

Type IV: true branch of pulmonary arteries are absent and the pulmonary blood flow derives from aortopulmonary collaterals. This type of TA is now recognized as a form of pulmonary atresia with VSD.

2.5.2. Treatments for Truncus Arteriosus

Surgical intervention is required to treat this condition. The procedure consists of a right ventricular outflow tract reconstruction (RVOT) that aims to create two separate vessels. Since 50 years ago this surgery carried a high mortality rate. Many advances have been done in the last decades and currently the early mortality after the RVOT has dropped to 5-10% (Thompson et al. 2001; Kalavrouziotis et al. 2006).

During the RVOT, the heart is accessed by median sternotomy and cardiopulmonary bypass is established. The common trunk is usually kept as the new aorta and a new pulmonary artery is created using either tissue from another source or a man-made tube. To this new artery, are sewn the branch pulmonary arteries. The VSD is closed with a cardiac patch (Urban et al. 1998).

More than one surgery may be required as the child grows. Multiple surgeries are required because the patch used to rebuild the pulmonary artery and the VSD will not grow with the patient (Lacour-Gayet et al. 1996). No known prevention is available for patients with TA. Though, early treatment can prevent the development of more serious complications.

3. STEM CELLS

Stem cells (SCs) are undifferentiated cells defined by their ability to self-renewal, which is the capacity to divide through mitosis maintaining the undifferentiated state; and to differentiate into more mature cell types. Two mechanisms ensure that a SC population is maintained throughout the time: stochastic differentiation, that happens when a SC divides into two differentiated daughter cells and a second SC divides into two SCs identical to the original; and obligatory asymmetric replication, consisting in the division

of a SC into one daughter cell identical to the original and another daughter cell that is differentiated. The differentiation potential of a SC is called potency (Gardner 2002). Depending on their potency, SCs can be classified as:

Totipotent: if the SCs can differentiate into both embryonic and extraembryonic cell types (e.g. cells from the morula);

Pluripotent: if the SCs can differentiate into all derivatives of the three germ layers of the embryo: ectoderm, mesoderm and endoderm (e.g. cells from the blastocyst);

Multipotent: if the SCs can differentiate into cell types of a closely related family (e.g. mesenchymal stem cells);

Unipotent: if the SCs can differentiate only into their cell lineage (e.g. progenitor cells).

3.1. Stem cell types

SCs are usually classified into three main groups: embryonic stem cells (ESCs), induced pluripotent stem cells (iPS) and adult stem cells (ASCs).

3.1.1. Embryonic stem cells

Embryonic stem cells (ESCs) are pluripotent SCs that derive from the inner cell mass of a blastocyst, a structure formed in the early development of mammals (Yamanaka et al. 2008). Human embryo develops the blastocyst after 4-5 days from the fertilization, at which time it accounts of about 50-150 cells. Being able to differentiate into the derivatives of the three germ layers, ESCs can develop into each of more than 200 cell types. Because of their high potency, ESCs require specific signals for a desired differentiation. If left undifferentiated, ESCs would give rise to a teratoma, a germ cell tumour (Thomson et al. 1998; Reubinoff et al. 2000). Moreover, ESCs cannot be autologous to the patient, leading to a risk of immune reactions (Drukker et al. 2002). Another concern regarding the use of ESCs is about the isolation process. In fact their

isolation requires the destruction of fertilized human embryo, hence the utilization of this cell type is ethically controversial.

It has been shown that ESCs can efficiently differentiate into cardiac cells (Maltsev et al. 1994; Laflamme et al. 2007; Lee et al. 2012). For example, spontaneously beating cardiomyocytes (CMs) can be found in embryoid body culture of ESCs (Zhang et al. 2009). Moreover, it has been shown that small molecule inhibitors of Wnt pathway can induce highly efficient (85%) cardiac differentiation in ESCs (Lian et al. 2012). However, ESC-derived CMs are functionally immature, myofilaments do not align in a preferential direction and they do not generate the same level of force found in mature CMs

3.1.2. Induced pluripotent stem cells

Induced Pluripotent Stem Cells (iPS) are pluripotent cell lines that are obtained from the reprogramming of fetal or adult somatic cells. iPS were first generated by the group of Yamanaka by transfecting differentiated cells with a combination of transcription factors, including Oct 3/4, Sox2, Nanog, Klf4 and Myc (Yu et al. 2007; Okita et al. 2008). These factors allow the reprogramming of differentiated cells, which shall revert back to a pluripotent stage, resembling the ESCs. Nowadays these very factors are still introduced within the cells, normally carried by retroviral vectors. These cells are characterized by a high plasticity, as they are able to differentiate into cells of the three germ layers (Takahashi et al. 2007). However, it has been shown that iPS may not retain their differentiation markers, implying that the differentiated phenotype might not be necessarily stable. In fact they are not able to reproduce daughter cells at the same rate (Young and Black 2004). The main clinical limitation of iPS consists in the risk of tumorigenesis deriving from the genomic integration of the viral vectors (Mayshar et al. 2010). In addition, human iPS have the potential to generate a teratoma when injected in mice (Yu et al. 2007).

3.1.3. Adult stem cells

Adult Stem Cells (ASCs) also called somatic stem cells, ASCs are a family of SCs whose function is to maintain and repair the tissue in which they are found. Most ASCs are multipotent and usually are referred to by their tissue or organ of origin. Stromal stem cells have been identified in several tissues, including bone marrow, adipose tissue, thymus, skeletal muscle and the heart (Beltrami et al. 2003; Laflamme and Murry 2005). Similarly to the iPS, the use of this type of cell is not as controversial as the use of embryonic SCs, because their production does not require the destruction of the embryo. Furthermore, ASCs do not allow the development of a teratoma as they cannot differentiate into the derivatives of the three germ layers. Not less relevant, ASCs have the potential to be autologous, as they could be isolated from the intended recipient, making the risk of rejection basically none existing. In comparison to iPS and ESCs, their plasticity is significantly lower, leading to a differentiation and transdifferentiation potential not as efficient (Taniguchi et al. 1997; Williams et al. 2008; Siebzehnrubl et al. 2011). Despite the promising potential of iPS and ESCs, so far most clinical and preclinical studies have employed ASCs mainly for safety reasons and easy accessibility (Patel, Shah, and Srivastava 2013).

3.1.3.1. Mesenchymal stem ells

Mesenchymal Stem Cells (MSCs) are a heterogeneous subset of ASCs that can be isolated from many tissues, such as the bone marrow, adipose tissue, thymus, skeletal muscle and the heart (Uccelli, Moretta, and Pistoia 2008; Roufosse et al. 2004; Kadner et al. 2002). Moreover, it is established that fetal tissues like the umbilical cord, cord blood, amniotic fluid and Warton's jelly, are a good source of MSCs (In 't Anker et al. 2003; Wang et al. 2004; Kern et al. 2006; Roura, Galvez-Monton, and Bayes-Genis 2014). MSCs are identified by their ability to adhere and grow on plastic; their capacity to differentiate into cells of the mesodermal lineage, such as adipocytes, osteocytes and chondrocytes (Dominici et al. 2006) and by the expression of specific Cluster of Differentiation (CD) markers (Majumdar et al. 2003; Barry and Murphy 2004): CD29, CD44, CD73, CD90, CD105 and CD166. (Table 1). In addition, MSCs do not express membrane or cytoplasmic proteins and transcription factors typical of mature cell types,

hence they are defined as Lineage negative (Lin-). MSCs stand out as an encouraging option for regenerative medicine due to their easy isolation, great expansion capacity, potential of being autologous, angiogenic properties and immune compatibility (Dimarino, Caplan, and Bonfield 2013).

3.1.3.1.1. Cardiac differentiation

The ability of the MSCs to transdifferentiate into cardiac cells, is still under a large debate. Many research groups have been trying to find out the optimum way to get the MSCs differentiate into CMs or cardiac-like cells. For example, in vivo studies have observed MSCs expressing cardiac lineage proteins such as Troponin, Nkx 2.5 and GATA4 when injected in infarct models (Toma et al. 2002; Kawada et al. 2004). Different groups have shown that MSCs can established electromechanical connections with native cells in the cardiac tissue of host animal models (Xu et al. 2004; Labovsky et al. 2010). Additionally, MSCs treated with the demethylating agent 5-azacytidine, seem to generate rhythmic calcium flux and potential electrical activities (Xu et al. 2004). Gao et al. provided a cocktail method to promote CM differentiation from bone marrow-derived MSCs. Their strategy was based on a combination of 5-Azacytidine, Salvianolic acid B and CM lysis medium to commit the MSCs by inhibiting the Wnt/beta-catenin signalling pathway (Gao and Jacot 2015). In fact the Wnt/beta-catenin signalling has been shown to regulate the cardiac differentiation. By inhibiting the glycogen synthase kinase 3 (GSK3) and stimulating the expression of beta-catenin shRNA, it is possible to produce functional CMs (Lian et al. 2013). Gnecchi et al. demonstrated that in vivo, MSCs can stimulate vascular and cardiomyocyte regeneration mainly acting by paracrine mechanisms. Also they might positively influence cardiac metabolism and contractility (Gnecchi et al. 2006; Gnecchi, Danieli, and Cervio 2012). However, a consistent generation of functional MSC-derived CMs has yet to be shown. The most common and easy way to verify if the differentiation has occurred, is to investigate whereas the treated cells express cardiac markers. For instance, immunocytochemistry techniques allow to establish if the cells exhibit specific antigens. The most commonly investigated cardiac markers are:

Sarcomeric alpha-Actinin (SaA), a cytoplasmic microfilament protein necessary for the attachment of the actin filaments to the Z-lines;

Marker	Description	Expression
CD29	also called integrin β1, it is a membrane receptor involved in cell adhesion	+
CD44	is a cell surface glycoprotein involved in cell to cell interactions, adhesion and migration mechanisms	+
CD73	also known as 5'-Nucleotidase, it is an enzyme that converts AMP to adenosine	+
CD90	also called Thy-1, it is a glycophosphatidylinositol anchor protein heavily glycosylated	+
CD105	also referred to as endoglin, it is a type 1 membrane protein that belongs to the TGFβ receptor complex. Thus it is involved in modulating a response to the biding of TGFβ1, TGFβ3, BMP2, BMP7 and Activin-A	+
CD166	is a transmembrane glycoprotein that belongs to the immunoglobulin superfamily of proteins	+
CD14	is a component of the innate immune system that is expressed mainly by macrophages and neutrophils	-
CD31	also known as PECAM-1, is expressed by monocytes, neutrophils and endothelial cells and it is involved in angiogenesis, integrin activation and leukocyte transmigration	-
CD34	typical surface marker of endothelial cells and vascular-associated tissue. It is a cell surface glycoprotein that functions as a cell-cell adhesion factor	-
CD45	is a tyrosine phosphatase receptor (PTPRC) which is present on all differentiated hematopoietic cells	-
HLA-DR	is a major histocompatibility complex, class II cell surface receptor that is found only on antigen-presenting cells	-

Table 1. *Cell surface markers for which the MSCs are positive: CD29, CD44, CD73, CD90, CD105 and CD166 and negative: CD14, CD31, CD34, CD45 and HLA-DR.*

Cardiac-Myosin Heavy Chain (cMYH), a MYH-beta isoform that is expressed mainly in the heart, where it plays a key role in cardiac muscle contraction. cMYH is the major protein of the thick filament in the sarcomeres of CMs. In human is encoded by the gene MYH7;

Desmin, is a type III intermediate filament found near the Z-line in sarcomeres. It is highly expressed in cardiac muscle. In humans, it is encoded by the gene DES;

Connexin-43 (Cx43), is a gap junction protein, consisting of a transmembrane protein that in cardiac muscle coordinates the membrane depolarization. Cx43 is the main cardiac connexin and is found mostly in the ventricular myocardium. In human is encoded by the gene GJA1.

Cardiac Troponin I (cTnI), is part of the Troponin complex, where it binds to actin in the thin myofilament in order to hold the actin-tropomyosin complex in place. cTnI is presented in the myocardium as a single isoform.

Quantitative Polymer Chain Reaction (qPCR) is a technic that allows to study the gene expression of cells and tissues. It is widely used to proof whether the differentiation has occurred by detecting the expression of cardiac-specific genes, including GATA-4, which is a transcription factor that regulates genes involved in myocardial differentiation and function; ACTA1 that encodes for one of the six different actin isoforms that are expressed in cardiac and skeletal muscle; Nkx 2.5 which is a transcriptional factor that plays critical role in cardiac differentiation; MYH -7; DES and GJA1.

4. STEM CELL-BASED THERAPY FOR CARDIAC REPAIR

As an alternative to reparative surgery and heart transplantation, stem cell therapy represents a favourable approach to the treatment of cardiac defects. The promise of this relatively recent technique is to facilitate the replacement of damaged cardiac tissue, leading to improved cardiac function and regeneration (Kaushal et al. 2009). This therapeutic strategy is based on the injection of dispersed stem cells directly into the damaged site, in order to stimulate the regeneration and remodelling of the compromised tissue and ideally to recover its function.

Different ways to deliver cells in the heart can be used (Steele and Steele 2006):

- Direct intramuscular delivery into the myocardium, which has been extensively applied in the clinical setting and allows cells to be directly delivered to the damaged area;
- Intravenous injection into the vascular system, which is associated with delay in delivery of the cells to the desire site, making the homing process of the injected cells not the most efficient;
- Trans-endocardial and trans-epicardial administration into respectively the endocardium and epicardium of the heart. This catheter-based technique may induce arrhythmias and requires electromechanical mapping;
- Intra-coronary administration, which involves cell delivery via a balloon-catheter that facilitates the cell flow through the damaged area (Wold et al. 2004).

The therapeutic effect of a SC-based therapy can be obtained in two ways: by a direct cellular effect, obtained with the transdifferentiation of the injected cells into cardiovascular lineage; or by a cytokine-paracrine effect. The second mechanism is triggered by the release of soluble factors from the injected SCs that recruit endogenous progenitor cells and help them differentiate into mature cardiac cells (Krause et al. 2010).

4.1. Preclinical and clinical studies

Currently there are not many animal models of CHD due to the complex nature of the diseases themselves and the difficulty to mimic them in vivo. However, in the last years, some progress have been done, especially to reproduce a volume overload and an increased pressure in the RV, which are common characteristics in patients with ToF and HLHS. For example, Hoashi et al. have developed a rat model with a pressure overload RV using a pulmonary artery banding. Skeletal myoblasts were injected in the rat hearts, inducing an improvement of RV function (Hoashi et al. 2009). A similar study was performed using cord blood SCs that were injected into the RV of a pressure overload right-heart ovine model. A promising outcome was achieved, as the function of the sheep right-hearts was enhanced (Davies et al. 2010). A juvenile porcine model was adopted to establish the feasibility of autologous cord blood mononuclear cells transplanted into piglet hearts. Cells were injected intramyocardially into the RV of the

animals, which were monitored for three months. All piglets survived without complications, confirming the safety of autologous UCB-MNCs collection and surgical delivery in a pediatric setting (Cantero Peral et al. 2015). In addition, another study performed in a ToF swine model, demonstrated the safety and positive effects of a cell therapy based on human ESCs-derived cardiac progenitors cells. Cells were administrated four months after the inducement of overloaded RV dysfunction, with multiple intramyocardial injections. Three months after the treatment, benefits regarding arrhythmic susceptibility were observed, although the improvement was not sufficient to obtain a significant change in the RV function (Lambert et al. 2015).

So far, in the cardiovascular regenerative field, SC-based therapies have been mainly applied to treat adult patients suffering from heart failure or myocardial ischemia (Sanganalmath and Bolli 2013). Nevertheless, in 2015 Burkhart et al. reported a case of cell therapy of intraoperative administration of autologous umbilical cord blood-SCs in a 4-month-old infant undergoing a second palliation surgery. After three months, the RV ejection fraction was increased from a mean baseline of 30 to 50% (Burkhart et al. 2015). Another study carried out in nine children affected by heart failure, demonstrated the safety and feasibility of intracoronary injection of autologous bone marrow mononuclear cells (Rupp et al. 2012). Only recently was concluded the first long term follow-up in paediatric patients with congenital disease. Autologous cardiac progenitor cells were isolated from seven babies with HLHS and were administrated via intracoronary injections one month after surgical palliation. All patients recovered well and no complications were observed. After 18 months, the treated children showed an increasing of the RV ejection fraction from 47 to 54% (Ishigami et al. 2015).

The experience accumulated with stem cell-based therapies for cardiac repair, suggests that dispersed cells might die soon after implantation. Since their therapeutic effect is thought to be attributed to the paracrine factors released during the initial post-transplantation phase, it is crucial that the cells remain alive after implantation. Yet, a cell therapy approach does not appear to be the most convenient strategy to repair complex CHDs. To restore normal anatomy to diseased heart it is generally required to use additional tissues that can be in various forms, such as patches, valves and conduits (Dean, Udelsman, and Breuer 2012; Kalfa and Bacha 2013; Smit and Dohmen 2015). Hence SCs might work more efficiently if embedded in some sort of scaffolds which

could help the development of biological tissue, that once implanted in the impaired heart, can grow and remodel in parallel with cardiac and whole body growth.

5. CARDIAC TISSUE ENGINEERING

Tissue engineering (TE) refers to a bioengineering technology that aims to generate biocompatible tissue substitute using three dimensional cell-seeded scaffold, to induce tissue remodelling and regeneration in the host's damaged organ.

Twenty years have passed since the first creation of an engineered heart tissue that was obtained by seeding a mix of collagen, extracellular matrix (ECM) various proteins and neonatal rat CMs into lattices or circular molds from embryonic chicken cardiomyocytes (Eschenhagen et al. 1997). After one week of culture, spontaneously and synchronously contractions were generated from the engineered heart tissue.

The last decade has seen a great progress in TE with new advances in interdisciplinary areas such as material and polymer sciences, developmental biology, genetic and bioreactor engineering. Every year more than 400 papers are published under the key words of cardiac tissue engineering (Hirt, Hansen, and Eschenhagen 2014). It does not surprise that this technique has come to the forefront as viable alternative for the treatment of heart diseases. For example, Steinert and collegues, developed a promising material made of rat CMs mixed with collagen and matrix factors, casted in circular molds and subjected to phasic mechanical stretch. Such construct reconstituted ring-shaped engineered heart tissue that displayed important cardiac markers and contractile properties (Steinert, Hendrich, and Zimmermann 2001). In 2007, a whole rat heart has been engineered for the very first time. After being decellularized by coronary reperfusion with detergents, the remained heart tissue was recellularized with another rat cardiac or endothelial cells, to obtain a construct able to generate pump function (Ott et al. 2008). Also, Shimizu et al. developed a temperature-sensitive coating material that allowed CMs to detach as intact monolayers from the culture dish where they were cultured in, by leaving the culture at room temperature. Stacking of many cell sheets can generate 3D tissues with beating potential and force generation (Shimizu et al. 2002).

5.1. Scaffold

TE relies extensively on the use of porous 3D scaffolds to provide the optimal environment for tissue and organ regeneration. The scaffold basically acts as a template for cell attachment and new tissue formation. The scaffold recolonization after implantation appears to contribute to the creation of living biological material well integrated with the surrounding tissue (Cheema et al. 2012). Scaffolds are frequently seeded with cells and frequently used growth factors. The cell-seeded scaffold (also referred to as patch) may facilitate the homing of resident cells and progenitor cells from the surrounding tissue by secreting chemoattractant factors (Smit and Dohmen 2015). The construct can be either cultured in vitro, to synthetize tissue which can be implanted later into the damaged site, or can be directly implanted in vivo in the injured site, exploiting the body's own mechanisms of regeneration and remodelling. This combination of cells, scaffolds, growth factors and stimuli is normally referred to as the tissue engineering triad (Figure 4).

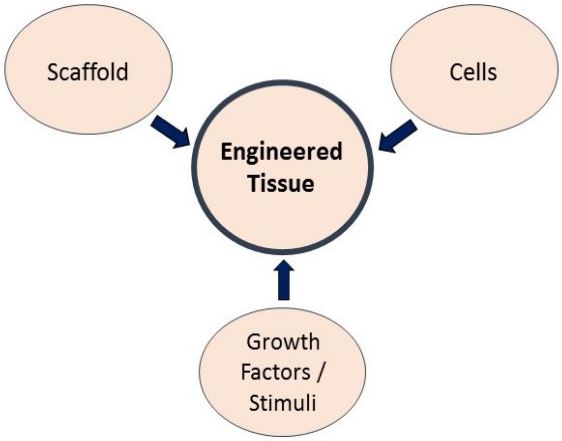

Figure 4 Tissue engineering triad of cells, scaffold, which act as a template for tissue origination and signals provided chemically by growth factors and physically by a bioreactor.

Several considerations are required when designing or determining the suitability of a certain scaffold for TE purpose. Some of the scaffold's needed requirements are:

Biocompatibility. First of all the seeded cells must be able to engraft the scaffold, function normally, produce their own ECM and eventually penetrate through the tissue. Biocompatibility of the patch with the seeded cells and the host's damaged organ is compulsory. Also, after implantation it is required that the patch induces a negligible immune response as it can reduce the healing process or provoke a rejection process.

Biodegradability. The scaffolds within the grafts are not intended to be permanent implants. Therefore the scaffold must be degradable to allow the seeded cells to produce their own ECM and the host's cells to populate and replace the patch over time. The scaffold should also be non-toxic and able to exit the host's body without interference with other organs and surrounding tissues. A little inflammatory response associated with controlled macrophages infusion, is required in order to allow the degradation process to take place in parallel with tissue formation (Brown et al. 2009; Lyons et al. 2010).

Scaffold architecture. To ensure cellular penetration and sufficient diffusion of nutrients throughout the construct, an adequate porosity is required. An interconnected pore structure is also necessary to allow diffusion of waste products out of the scaffold. The mean pore size of the scaffold is another key component. The pores need to be large enough to let cells migrate into the scaffold, where they eventually become bond to the ligands present within the construct, and at the same time small enough to establish an appropriate high specific surface to allow an efficient binding of a critical number of cells (Yannas et al. 1989; O'Brien et al. 2005). Thus, for each scaffold, a specific range of pore size exists, which can vary according to the engineered tissue and the cell type used (Murphy, Haugh, and O'Brien 2010; Murphy and O'Brien 2010).

Mechanical properties: the ideal scaffold should have mechanical properties consistent with the tissue or organ into which it has to be implanted. From a practical perspective, the construct must be strong and handling enough to allow surgical manipulation during implantation. The hydrodynamic function, elasticity, stiffness, compressibility and density of the scaffold have to be evaluated before proceeding with any preclinical validation (Ghanbari et al. 2009). Many materials have been developed with good mechanical behaviour and potential in vitro, which have failed when implanted in vivo. Often the cause of failing in vivo is the insufficient capacity of vascularization. The scaffold must enable the development of new vessels and adequate blood supply in order to contribute to the tissue remodelling (O'Brien et al. 2005). Therefore, a good balance between mechanical behaviour and porous architecture is a key factor for the success of any scaffold.

Ideally, the optimal reparative patch for pediatric cardiac corrective surgery, should possess the following characteristic: biocompatibility, biodegradability, growth potential consistent with the somatic enlargement, adequate porosity, resistance to calcification, good handling properties, minimal thromboembolism risk and absence of immunogenicity (Kalfa and Bacha 2013; Alsoufi 2014). To date, the ideal scaffold still does not exist. However many progress have been done towards this direction and several materials are currently under evaluation in the attempt of finding the optimized one.

5.2. Biomaterials

Great progress has been done in the field of biomaterials, which consist of those materials intended to be used as scaffold in TE. From being able to merely interact with the body, some biomaterials are now able to influence and promote biological process. Biomaterials can be either chemically engineered (synthetic materials) or derive from biological sources (biological materials).

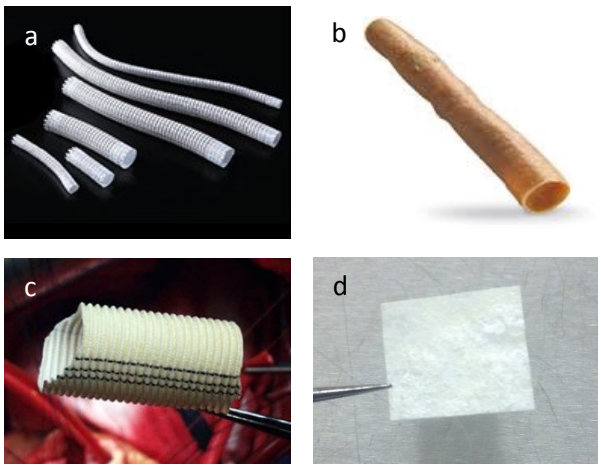

Figure 5 Biomaterials currently used in corrective surgery: Gore-Tex® (a), Contegra® (b), Dacron® (c) and CorMx (d).

5.2.1. Synthetic materials

Synthetic materials can be either biodegradable or non-biodegradable. Polymers are one of the most used type of synthetic materials. They are fabricated using synthetic biodegradable polymers such as poly-l-lactic acid (PLA), polyglycolic acid (PLG), polycaprolactone (PCL) and poly-dl-lactic-co-glycolic acid (PLGA). On one hand, these polymers have many advantages, as they can be limitlessly supplied, they are easy of shaping and their degradation characteristics can be controlled by changing the polymer itself or the composition of the individual polymers (Rowlands et al. 2007; Lu et al. 2000). On the other hand, the degradation process may affect the mechanical properties over time. Also, because the degradation happens by hydrolysis, it produces carbon dioxide that will lower the local pH which in turn might result in cell and tissue necrosis (Liu, Slamovich, and Webster 2006).

Gore-Tex® is a currently used non-biodegradable synthetic material for CHD corrective surgery (Figure 5Figure 5a). It is mainly applied to create conduits and vascular grafts. Gore-Tex® is durable, easy to handle, has a limitless supply and it lacks of structural deterioration. Disadvantages include the lack of growth potential, which applies also to all the synthetic materials, and the risk of thromboembolism.

5.2.2. Biological materials

Natural and natural-derived materials are commonly used biomaterials. Collagen, gelatine, fibronectin, various proteoglycans, alginate-based substrates and chitosan have all been used as supporting scaffolds for cells in TE (Nolan et al. 2008; Schneider et al. 2010; Hasan et al. 2016). Unlike synthetic polymer-based materials, natural polymers are biologically active and generally promote better cell adhesion and proliferation. Also, they are typically biodegradable which should allow over time, host cells to remodel the scaffold, by producing their own ECM that shall replace the degraded construct. However, generating scaffolds from biological materials with reproducible and homogenous properties represents a great challenge. In addition, this types of materials are more likely to have poor mechanical properties, which can limit their use in TE.

Decellularized materials have been largely used in cardiac corrective surgery. Decellularized tissues consist of naturally occurring materials, like pericardium, myocardium, veins and valves that have been processed in order to remove all cellular and nuclear components, leaving at the same time the ECM preserved. Decellularization is usually achieved with a combination of chemical reagents, like detergents, with enzymatic and physical methods, as freeze drying (Ott et al. 2008; Mirsadraee et al. 2006; Gardin et al. 2015). Different decellularization techniques have led to the development of various commercial products derived from different tissues with diverse physical and biological properties and applications. Regardless the applied technique, the developed materials have limited immunogenic effect due to the stripping of the ECM of cells and antigens that fuel the immune response. In fact the ECM is well conserved between species and if well decellularized, should not elicit a strong immune response.

CorMatrix® (CorMx) is an example of a decellularized material that is widely used in corrective surgery (Figure 5d). This biomaterial is developed using porcine small intestinal submucosa. CorMatrix® shows interesting properties for cardiac surgery, including low immunogenicity, easy handling and implantability, high mechanical strength, possible growth potential, good recruitment of host cells, remodelling without calcification and minimal scar formation (Quarti et al. 2011; Kalfa and Bacha 2013). CorMx-patches have been successfully used for CHD implantation, pediatric cardiac surgery and vascular reconstruction. For example, between June 2007 and May 2009, this material was used in 40 patients aged 2 days to 13 years. In 16 cases it was used for pericardial closure while in the remaining 37 for cardiac or vascular repair, including, atrial and septal defects, RVOT, superior vena cava, pulmonary monocusp valves and pulmonary arterioplasty. Mean follow-up was 7.85 months. Overall the explanted grafts displayed good resorption of the CorMx, re-endothelialisation and replacement of the matrix with new organized collagen (Scholl et al. 2010). More recently, a similar study was conducted in 37 paediatric patients that underwent cardiovascular reconstruction. A 411 days follow-up was carried out. Different surgical interventions were performed: septal defects, vascular augmentation, RVOT and valve reconstruction. Progressive stenosis was observed only in one case of RVOT and one case of circumferential pulmonary artery. All other grafts were fine and remained patent (Witt et al. 2013). Moreover, it has been shown by Badylak et al. that the non-cross-linked grafts like

CorMx, induce an immunoregolatory and proangiogenic macrophages response instead of an inflammatory, scar-forming response (Badylak et al. 2002).

5.2.2.1. Classification of biological materials

Autografts: which are fabricated using the patient's own tissue. Pulmonary autografts are commonly used in children with ToF or valve defects (Al-Halees et al. 2002). Autografts exhibit a good growth potential, they are not immunogenic nor are they associated with a thromboembolism risk. However, they might need to be replaced after many years and depending on the tissue type, they may be difficult to handle.

Homografts: are derived from humans, commonly cadavers. The most common used human-derived grafts are valves and vascular conduits. Cryopreserved decellularized homografts have been used for many years in CHD repair, for pulmonary and aortic substitution and for RVOT reconstitution (Gabbieri et al. 2007; Neumann et al. 2013). Decellularized homografts typically have good mechanical properties, their ECM is generally non antigenic and often repopulated after implantation. Disadvantages of homografts includes lack of growth potential, limited availability and if the decellularization is not completed, an immune response can be generate (Neumann et al. 2013).

Xenografts: consists of animal-derived constructs, generally bovine or porcine. They are widely used in corrective surgery due to the shortage of human substitutes. Decellularized porcine or bovine pericardium and valves are the most commonly fabricated xenografts (Yap et al. 2013). On one hand, their supply is almost limitless, their anatomical structure is adequate and they have good biological properties. On the other hand, they lack of growth potential, the decellularization weakens the construct and if it is not completed, can cause an immune response and they poses the risk of calcification and stenosis.

5.3. Bioreactor

Biophysical stimuli are sometimes applied to the scaffold in the form of a bioreactor, which consists of a device that applies different types of mechanical and/or chemical stimuli to the construct in order to ensure the biological environment of the heart and the circulatory system (Figure 5) (Martin, Wendt, and Heberer 2004). By mimicking the physiological mechanical forces, blood flow and shear stress, the bioreactor can allow the generation of patch that shall be functional after transplantation in vivo (Hecker and Birla 2007). When cell-seeded scaffolds are kept in culture for prolonged time, the tissue normally grow and reach a three dimensional structure, so that a static culture system would not be able to guarantee the perfusion of culture media uniformly. A dynamic bioreactor can maintain viable an engineered tissue by using both mechanical and biochemical conditioning. Furthermore, such a device can monitor not only the oxygen and carbon dioxide levels, pH, temperature and nutrient concentration, but it can also provide the control of flow waveform and physiological pressure. By doing this, the bioreactor keeps the culture medium under a pulsatile flow that allows the perfusion of the media within the whole scaffold (Carrier et al. 1999; Hecker and Birla 2007).

This dynamic tissue culture is gradually taking over to the static seeding. Since the beginning and until few years ago, the static system was the most commonly adopted. That was because of its simplicity, low cost and ease to be performed in a laboratory not being equipped with sophisticated devices. However, the efficiency of a static tissue culture is lower than the dynamic one. The cell distribution throughout the scaffold is not uniform, with the majority of cells attached to the outer side and just a few migrated to the inner part (Dai et al. 2009). Also, in a static system, the culture media would not be able to diffuse uniformly within the patch, generating area with low concentration of nutrients and oxygen.

5.4. Clinical and preclinical studies of TE-grafts

Before a developed engineered or non-engineered patch can be translated into clinic, it has to be tested in animal models in order to assess its safety and feasibility. Some preclinical studies have been carried out using both small and large models. Tissue

growth, histological and immunological properties of engineered material, usually can be successfully studied in small animal models, like rodents. Small animal models are easier to take care of and the cost of housing is relatively modest, however, due to their little size, they may not be adequate to perform complex surgery. Large animal models such as sheep, lamb, pig and dogs are the most commonly used animal to test TE-grafts for cardiac corrective surgery (Shinoka et al. 1995; Fuchs et al. 2002; Sadegh et al. 2014).

So far, bone marrow SCs and endothelial cells have been the most largely utilized cell type, probably due to their relatively easy accessibility and ease of harvesting. In these procedures, the generated scaffold, is firstly seeded with the desired cells and then is implanted in the animal model. Vincentelli et al. used lamb bone marrow SCs and MSCs to create in vitro TE-heart valves made of decellularized porcine pulmonary valves. The patches have been implanted in the pulmonary artery of 14 lambs. After four month, a great remodelling have been observed in the explanted samples, with the MSC-seeded valves being histologically closer to the native tissue (Vincentelli et al. 2007). Also, Dohmen et al. used autologous endothelial cells to engineer decellularized porcine jugular vein. The TE- and non-TE patches were implanted in the RVOT of 6 juvenile sheep. After three months, the recellularization density was higher in the TE-patches, but after six months, no such difference was seen (Dohmen et al. 2006). The potential of a TE-vascular graft made of PGA and coated with l-lactic and epsilon-caprolactone was evaluated in 7 juvenile lambs, plus 1 unseeded control. The patch was implanted in the superior vena cava and explanted after 6 months. All grafts were patent and increased in volume (Brennan et al. 2008). Dog models have been used to determine the viability of a wide variety of vascular grafts, including artificial vascular prostheses seeded with autologous cells derived from adipose tissue, epithelium and smooth muscle(Cook and Fox 2007). Dogs have also been successfully transplanted with decellularized conduits of bovine or porcine origin, showing patency and no complications (Scharn et al. 2002).

Encouraging results have been obtained also from clinical studies involving the application of TE-patch, conduits or valve in children suffering from CHD. For example, Shin'oka et al. reported a clinical trial with 42 patients with CHD that have received a TE-vascular graft seeded with autologous bone marrow cells (Shin'oka, Imai, and Ikada 2001). The applied scaffolds were made of PLLA/PCL and PGA and were degradable after 2 years. Mean length of follow-up was 16 months. No thrombosis, stenosis nor obstruction of the grafts were observed. The implants were patent and increased in size.

Another study was conducted in 25 patients with single ventricle physiology, in which PLLA/PCL/PGA grafts seeded with autologous bone marrow cells, were implanted as cavolpulmonary conduits. In 21 patients there was no failure of the grafts, while 4 required angioplasty due to graft obstruction (Hibino et al. 2010).

Despite all these positive results, the performance of engineered patches in patients with CHD requires to be further investigated. Main limitation of the clinical studies performed so far, is the lack of a long term follow up.

6. SWINE MODEL

Large animal models are essential for the translation of basic science into clinical practise. However, it is quite challenging to reproduce in animal the complex nature of CHD, making this a great limit in the translation of new therapies into clinic (Tarui, Sano, and Oh 2014).

The swine model has well been characterized in the literature as a crucial preclinical research model for studying cardiovascular diseases (Suzuki, Yeung, and Ikeno 2011; Ye et al. 2014; Mosala Nezhad et al. 2016). Pig anatomy, physiology and immunological system resemble those of humans to a remarkable degree. Porcine cardiovascular system is comparable to that of humans at the cellular level as well as in terms of electrophysiology, cardiac metabolism and function (Crick et al. 1998). Therefore pigs are one of the most successful large animal model used in cardiovascular research.

Thanks to their size and anatomy, it is possible to accomplish a cardiac surgical intervention that closely reflects the one performed in infants, as well as mimics the clinical setting.

Piglets have the tendency to grow at a really fast rate during their first six months of life and they reach considerable final size. This leads to a situation of cardiac exponential growth, which provides a viable model to test the feasibility and growth potential of a paediatric engineered patch. Validating TE cardiac or vascular grafts in such a model,

represents a real challenge, being the developed construct tested in a high growth rate environment.

7. CARDIOPULMONARY BYPASS

CBP is a surgical technique that temporarily takes over the function of the heart and lungs during an open-heart surgery. This technology allows to perform cardiac surgical procedures in a dry and motionless operative area. Because of the difficulty of operating on a beating heart, the bypass is routinely performed in cardiac surgery (Donmez and Yurdakok 2014). Thus, the bypass is aimed at maintaining the circulation of blood and oxygen content of the body while the surgeon is operating. The CPB system consists of a systemic circuit for oxygenating the blood and reinfusing it into the patient's body bypassing the heart. In fact this technique is a form of extracorporeal circulation (Figure 6).

A cannula in the RA, inferior/superior vena cava or femoral vein is placed to withdraw the deoxygenated blood from the body. This cannula is connected with tubing filled with isotonic crystalloid solution. Generally the venous blood is gravity drained to a reservoir, where is filtered, cooled or warmed and oxygenated before returning to the body. The cannula used to return the oxygenated blood can be inserted either in the ascending aorta or in the femoral artery (Hemli, Patel, and Subramanian 2012). An oxygenator is required to provide gas exchange to the blood and this happens through a membrane. According to the type of membrane, two different oxygenators exist: sheet-membrane and hollow-fibre oxygenator. Typically, the tubing and cannulae are manufactured of clear polyvinyl chloride, whereas the oxygenator casing and connectors are made of polycarbonate (Bell and Diffee 1991). The cardiotomy reservoir allows to recycle the suctioned blood from the surgical field. This reservoir includes a screen and a depth filter to reduce the risk of air and fat emboli and surgical contamination (Pradines et al. 2016) The blood is pumped back to the body thanks to a heart-lung machine that guarantees constant blood flow delivery. The blood pump has to generate blood flow and pressure against a certain degree of resistance, as described by the Hagen-Poiseuille equation:

Blood Flow rate = Pressure / Resistance

The pump should be made of biocompatible materials, be able to adjust for different size of extracorporeal tubing and create no area of blood turbulence or stasis. CPB pumps are operated by perfusionists.

To provide a bloodless and motionless surgical field, a cross-clamp is placed across the ascending aorta. Therefore, the coronary circulation is isolated and blood is prevented from entering the cardiac chambers. Hence, myocardial protection strategies are required to preserve cardiac function and prevent cell death (Weiland and Walker 1986). Two main approaches are generally used: cardioplegic and non-cardioplegic. Cardioplegic techniques for cardiac protection involve the delivery of cardioplegic solution to the heart, in order to provide diastolic electromechanical arrest. Potassium is the main agent used to induce cardiac arrest. The solution can be administered as cold or warm blood cardioplegia or as cold crystalloid cardioplegia. Non-cardioplegic techniques comprise the use of moderate systemic hypothermia with short periods of aortic cross-clamping and ventricular fibrillation (VF) (Whiting, Yuki, and DiNardo 2015). The CPB can be performed under systemic hypothermia or normothermia. Systemic hypothermia is achieved by cooling down the blood of the patients and it has been shown to reduce myocardial oxygen consumption, ensuring cardiac protection and increasing the tolerance for ischemia of vital organs after reperfusion (Bell and Diffee 1991).

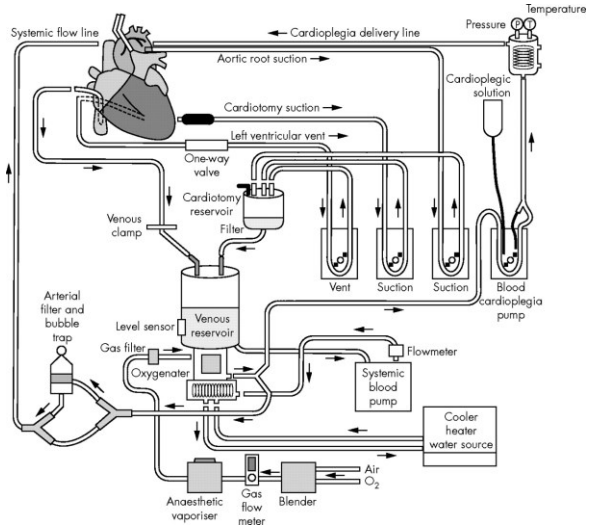

Figure 6 Cardiopulmonary bypass circuit (Field et al. 2006)

AIM OF THE STUDY

OBJECTIVES

Prosthetic replacement grafts are used in cardiac corrective surgery in the form of patch, conduit or valve. However, the current materials have several limitations, including low durability and lack of growth potential that requires to submit the patients to multiple surgeries and a lifelong follow-up. Tissue engineering holds great promises to generate viable biological materials with growth potential, remodelling and repairing capability.

The first section of the study was aimed to isolate, characterize and differentiate mesenchymal stem cells (MSCs) from the thymus-gland of newborn piglets and children undergoing open-heart surgery. MSCs were differentiated into cardiac-like cells in order to obtain cells with a phenotype coherent to the tissue where they may be implanted.

The second part of this thesis was focused at developing cardiac patches by engineering decellularized porcine tissues and a commercially available material with undifferentiated and differentiated MSCs, to generate grafts with the potential to be use in corrective cardiac surgery.

The last section of this study included the in vivo experiments. We aimed to establish a novel piglet model to test the safety and feasibility of our developed cardiac patches. The model consists of a cardiopulmonary bypass with recovery of the animal. Only few large animal models exist for CHD and heart failure. Therefore, the validation of our juvenile pig model is of significant importance to investigate the suitability of an engineered graft for cardiac repair in a paediatric setting.

MATERIALS AND METHODS

All the animal experimental protocols have been approved from the British Home Office. Animals were treated in accordance with the *Guide for the Care and Use of Laboratory Animals* of the National Academy of Science, published by the National Institute of Health in 1996. Neonatal rats were humanely sacrificed using a Schedule 1 procedure of the Animals (Scientific Procedures) Act published in 1986. Whereas, pigs were euthanized with an intravenous injection of barbiturate

In regards of human subjects, this study was performed in accordance with an accepted protocol from the University of Bristol and the National Health Service Consent from children's parents was obtained to collect discarded thymus tissue.

In vitro experiments, but when specified differently, were performed at the School of Clinical Sciences, in the Bristol Royal Infirmary and part of the University of Bristol.

1. CULTURE OF MSCs

1.1. Isolation

In an open-heart surgery, in order for the surgeon to access the heart, the thymus gland has to be discarded. Wasted thymus tissue from children aged few days up to 5 years old, with CHD undergoing corrective heart surgery, was used to isolate human MSCs.

The isolation and culturing of porcine MSCs, consist of the same protocols. The thymus gland was collected from newborn piglet, the very same day of delivery.

Collected samples were washed with 1% penicillin/streptomycin (P/S, Life Technologies) phosphate buffer saline (PBS, Life Technologies) and minced into small pieces. The washing solution was removed and a 1 mg/ml solution of Collagenase type I (Sigma Aldrich) was added to the tissue and incubate for 2 hours at 37°C. The cell suspension was then filtered through a 70 um nylon mesh to remove the stromal capsule and centrifuged at 1500 rpm for 5 minutes at room temperature (RT). The supernatant was removed and the pellet was resuspended in Dulbecco's Modified Eagle Medium (DMEM, Gibco, Life Technologies) supplemented with 10% Fetal Bovine Serum (FBS, Gibco, Life Technologies), 1% P/S and 0.2% Plasmocin (InvivoGen). Cells were seeded into an appropriate flask for cell culture (generally a T75) and kept at 37°C in a 5% CO_2 humidified atmosphere. 48 hours after seeding, non-adherent cells were removed, adherent cells were washed with PBS and fresh medium was added to the culture.

1.2. Cell expansion

When 70 to 80% confluence was achieved, cells were passaged (or splitted) from P0 to P1. Cells were firstly washed with PBS and enough Trypsin (Thermo Fisher) was added to cover the culture. Cells were incubated with the enzyme for about 5 minutes at 37°C in a 5% CO_2. Trypsin's activity was inhibited with culture medium containing at least 10% FBS, in order for the serum to stop the action of the enzyme. 10 ul of cell suspension were loaded into a chamber for cell counting. An automated cell counter was used for a consistent cell counting (Countess II FL, ThermoFisher). Cell suspension was centrifuged at 1500 rpm for 5 minutes at RT, the supernatant discarded and the pellet resuspended in the appropriate volume of culture medium. MSCs were kept in culture until passage 2, when they were either used for an experiment or, if not needed, frozen.

1.3. Cell freezing/thawing

In order to freeze the cells, they have to be trypsinized. After the cell suspension was centrifuged, the pellet was resuspended in a freezing mix made of 50% DMEM, 40% FBS and 10% Dimethyl Sulfoxide (DMSO, Sigma Aldrich) and transferred into a cryovial. The DMSO is a solvent used as cryo-protectant, thus it protects the cells from freezing damage. The cryovials were firstly put into a freezing container (Mr. Frosty, ThermoFisher) that allows the rate of cooling of -1°C per minute, which seems to be the optimal rate for cell preservation. Cells were kept at -80°C for short storage. If long storage was needed, cells were moved into liquid nitrogen tank (-196°C) after a couple of days.

Thawing the cells required to put the cryovials containing the cells of interest at 37°C until the suspension was defrosted. Then the cells were spin down at 1500 rpm for 5 minutes at RT and counted with an automated cell counter. The pellet was resuspended in the appropriate amount of DMEM with 10 FBS and 1% P/S. Plasmocin was used only for cells with a passage number of zero or one.

2. FUNCTIONAL CHARACTERIZATION OF MSCs

MSCs are functionally defined by their capacity to adhere on plastic, self-renew and differentiate into the three mesodermal phenotypes: osteocyte, adipocyte and

chondrocyte. Therefore the isolated human and porcine MSCs were differentiated into the three cell types.

2.1. Osteogenic and adipogenic differentiation

Low passage MSCs (P2 to P3) were trypsinized and $4x10^4$ cells (for the osteogenic differentiation) and $2x10^5$ cells (for the adipogenic differentiation) were seeded into each well of a 6-well plate. Per each differentiation experiment, three wells were used as negative control, where no supplements were added to the culture, and three wells were treated with the conditioning reagents and supplements. Cells were cultured with the basal alpha-MEM medium (Life Thechnologies) supplemented with 1% P/S. When cells reached 70 and 100% confluency, respectively for the osteogenic and adipogenic differentiation, the supplements were added to the treated cells (StemXVivo osteogenic/adipogenic supplements, R&D Systems). Every 3 days the media was changed to all the cells and the supplements were added to the treated cells.

After 3 to 4 weeks, cells were committed to the osteogenic lineage. At the end of the differentiation, cells were dyed with the Alizarin Red staining in order to detect the presence of any calcific deposition, typical of osteogenic cells. Cells were fixed for 1 hour with 70% ice-cold ethanol at 4°C. Then they were stained for 5 minutes at RT with Alizarin RedS (40 mM, pH 4.1, Sigma-Aldrich). At the end of the incubation, cells were washed five times with PBS and then they were observed under a bright field inverted microscope (Zeiss PrimoVert).

Regarding the adipogenic differentiation, after 3 weeks of differentiation, cells were coloured with the Oil Red O staining to detect any triglycerides or lipid vesicles which are typical of adipocytes. Cells were fixed with 4% paraphormaldehyde (PFA, Sigma-Aldrich) in PBS for 20 minutes at RT. After the fixation, cells were washed once with PBS and twice with 60% isopropanol (Sigma-Aldrich). Then they were stained with the Oil Red O solution made of 0.2 g Oil Red O (Fluka) in 40 ml isopropanol diluted in distilled water (3:2) for 30 minutes at RT. At this point cells were washed with 60% isopropanol and then observed under the bright field microscope.

2.2. Chondrogenic differentiation

Low passage MSCs (P2 to P3) were trypsinized and $2x10^5$ cells were resuspended in 5 ml of the completed StemXVivo Chondrogenic Base Media (R&D Systems). Cells were centrifuged at 200g for 5 minutes at RT and the supernatant was kept to culture the pellet of cells. Every three days the media was removed and replaced with fresh one.

After 3 to 4 weeks of differentiation, cells were fixed with 4% PFA for 20 minutes at RT. Cells were then washed with PBS and stained overnight (ON) at room temperature (RT) with the Alcian Blue solution (1% Alcian Blue 8GX, Sigma-Aldrich in 3% Acetic Acid, Sigma-Aldrich). The following day, cells were washed twice with 3% Acetic Acid and twice with PBS. Then cells were observed under the bright field microscope.

3. FLOW CYTOMETRY

Flow Cytometry (FACS) was used to investigate the expression of the surface markers of the isolated pig and human MSCs. Different antibodies were used due to the different species from which the cells were isolated (Table 2 and Table 3).

Antibody anti human	Dilution	Fluorophore Conjugated	Company
CD29	1:5	APC	BD Pharmingen
CD44	1:20	APC	BD Pharmingen
CD73	1:20	APC	BD Pharmingen
CD90	1:5	PE	R&D Systems
CD105	1:20	PE	R&D Systems
CD14	1:10	PE	BD Pharmingen
CD31	1:20	FITC	BD Pharmingen
CD34	1:40	FITC	BD Pharmingen
CD45	1:20	PE	R&D Systems
HLA-DR	1:20	APC	BD Pharmingen

Table 2. *Panel for hTMSCs characterization reporting the antigens investigated, the dilution of the antibodies used, the fluorophores conjugated with the antibodies and the companies from which they were obtained.*

Antibody anti pig	Dilution	Fluorophore Conjugated	Company
CD44	1:600	APC	eBioscience
CD73	1:10	(secondary antibody-APC)	R&D Systems
CD90	1:20	PE	Biolegend
CD105	1:5	PE	LSBio
CD31	1:10	PE	Bio-Rad
CD45	1:25	FITC	Bio-Rad

Table 3. *Panel for pTMSCs characterization showing the antigens that were analyzed, the dilution of the antibodies used, the fluorophores conjugated with the antibodies and the companies from which there were acquired. Since CD73 was unconjugated, the use of a secondary antibody was necessary to detect the construct.*

A suspension of cells is required for the staining. Thus, low passage cells (p3) were splitted and trypsin was inhibited by washing the cells with FACS buffer. Cells were re-suspended at 1000 cell/ul in FACS buffer. 200 ul of cell suspension were removed for a viability staining control and 100 ul were removed for unstained control. 100 ul of the 200 ul for the viability staining, were put at 95°C for 5 minutes in order to kill the cells. Then the dead cells were cooled down before they are added back to the other 100 ul of living cells. The viability marker used was conjugated with the fluorophore V450 (BD Horizon) and was used at 1:1000 in FACS buffer. Cells were incubated with the dye for 30 minutes covered at 4°C. At the end of the incubation, cells were washed with cold FACS buffer and spin down. The viability staining control was kept covered at 4°C until the end of the staining.

The initial pellet of total cells was re-suspended in FACS buffer in order to have at least 1500 cell/ul and cells were incubated for 30 minutes covered at 4°C with primary antibodies at appropriate concentrations. At the end of the antibodies incubation, cells were washed with cold FACS buffer and spin down. All cells, unstained control and viability staining control included, were fixed with 1% PFA and kept covered at 4°C until analysis.

FACS analysis was performed at the Flow Cytometry Facility, in the School of Cellular and Molecular Medicine of the University of Bristol. The Novocyte NovoSampler (ACEA Bioscience, Inc.) flow cytometer was used for data collection and the software

NovoExpress (ACEA Bioscience, Inc.) was used for data analysis. The unstained cells and the viability staining control are used to gate viable cells.

4. PRIMARY CULTURE OF RAT CARDIOMYOCYTES

4.1. Isolation of cardiomyocytes

Cardiomyocytes were isolated from 1- to 3-day-old Wistar rats (Charles River). A litter of neonatal rats was killed by means of decapitation, according to the schedule 1 of the Animals (Scientific Procedures) Act. The hearts were rapidly removed and placed in culture medium on ice. When all hearts were collected, they were washed with 1% P/S PBS in order to remove the blood. Hearts were minced into small pieces with fine scissors, filtered with a 70 um nylon mash and transferred into a sterile beaker with a magnetic bar. The tissue was dissociated with 0.05% Trypsin, 0.02% EDTA (Life Technologies) in PBS for 15 minutes at 37°C on a magnetic stirrer. At the end of the incubation, the cell suspension was filtered with a 70 um nylon mesh and the enzyme activity was stopped with FBS. This first fraction of cells was kept aside. A solution of 0.1% Trypsin, 0.02% EDTA was added to the tissue and incubated for 15 minutes at 37°C on the magnetic stirrer. . At the end of the incubation, the cell suspension was filtered with a 70 um nylon mesh and the enzyme activity was stopped with FBS. This second fraction of cells was kept aside and the same procedure was repeated for other three times. All the five isolation fractions were mixed together and centrifuged at 100 g for 5 minutes at RT. The pellet was resuspended into 10% FBS, 1% P/S DMEM and cells were seeded into a T75 flask. The cells were kept for 1 hour at 37°C in a 5% CO_2 to allow the cardiac fibroblasts to attach and remove the majority of them from the cardiomyocyte culture. At the end of the incubation, non-adherent cells were removed and centrifuged at 100 g for 5 minutes at RT. The pellet was then re-suspended into an appropriate volume of DMEM mixed with Medium 199 (M199, Gibco) at a ratio 1:1 and supplemented with 1% FBS and 1% P/S. Cells were finally seeded into a T25 flasks previously coated. After 48 hours, non-adherent cells were washed away and fresh growing medium was added to the culture. Cells usually started beating after 3 or 4 days and after a week the majority of them were beating in a synchronized way.

Different ECM components were tested to find out the best coating material. Gelatine, collagen type I and fibronectin were applied. The beating rate and growing potential of the cardiomyocytes were monitored to identify the optimum coating component.

4.2. Preparation of cardiac conditioned medium

Every time the primary culture of rCMs was fed, the old wasted medium was not thrown away. Instead it was collected as conditioned medium and centrifuged at high speed in order to allow all debris and dead cells to sediment in the pellet. The supernatant was then filtered through a 0.22 um filter and either used to feed culture of hMSCs or stored at -20°C until needed.

4.3. Characterization of cardiomyocytes

To assess if the isolated cells were actually CMs, they were either stained for cardiac proteins, or lysed in order to isolate the RNA on which the expression of cardiac-specific genes was examined. When confluence was achieved, cells were trypsinized and seeded onto coated coverslips, previously inserted into a 24-well plate. After approximately one week of culture, cells were fixed and stained with the following primary antibodies (protocol is described in paragraph 6): Mouse anti-Sarcomeric alpha-Actinin, Mouse anti-cardiac Myosin Heavy Chain, Rabbit anti-Desmin and Rabbit anti-Connexin-43 (antibodies' specifications are reported in Table 5).

To investigate the gene expression of the isolated cells, a quantitative Real Time-PCR was performed to study the expression level of the genes GATA-4, ACTA1, DES and cMYH (protocols are reported in paragraph 7).

5. CARDIAC DIFFERENTIATION

Cell differentiation into cardiac-like cells was performed. Three different lines of low passage (P2 to P4) human and porcine MSCs were used in three independent experiments. Cells were seeded at low density (2500 cell/cm^2) into both 6-well plates and 24-well plates. Cells seeded onto the 6-well plates were used for RNA extraction and qPCR, while cells seeded onto the 24-well plates were fixed and used for

immunocytochemistry (ICC). A glass coverslip was inserted into each well of the 24-well plates to allow cells' ultimate staining. Three different protocols were set up and optimized.

5.1. Chemical protocol (T1)

The first protocol (treatment 1, T1) was based on the paper published by Smits et al., where human cardiac progenitor cells were differentiated into mature cardiomyocytes (Smits et al., 2009). Cells' differentiation was achieved by adding to the cells a combination of supplements. The demethylating agent 5-Azacytidine (5uM; Sigma Aldrich) was added to the culture for the first three days of differentiation in order to stop cells from proliferating. The Transforming Growth Factor-beta 1 (TGF-β1, R&D Systems) was supplied twice per week, from the 6th day of differentiation at the concentration of 1 ng/ml. Ascorbic Acid (0.1mM, Sigma-Aldrich) was added every other day from the 6th day of differentiation. The differentiation medium was obtained from a combination 1:1 of Iscove's Modified Dulbecco's Medium (IMDM; Gibco, Life Technologies) and Ham's F12 (Gibco, Life Technologies) and supplemented with 2% Horse Serum (HS; Gibco, Life Technologies), 1% Insulin-Transferrin Selenium (ITS), 1% MEM non-essential amino acids and 1% P/S.

5.2. Conditioned medium (T2)

With the second treatment (T2) cell differentiation was obtained due to the cytokines and growth factors present in the medium conditioned from a separate culture of rat cardiomyocytes (CCM). The rationale of this technique is to mimic in a bland way the in vivo environment, in order to see if it helps the differentiation process of the MSCs. The CCM was mixed 1:1 with DMEM, 2% HS and 1% P/S. No supplements were added to the culture but 5-Aza (5 uM for the first three days of differentiation) in order to inhibit cell proliferation.

5.3. Coculture (T3)

In the third treatment (T3) MSCs were differentiated in the presence of rat cardiomyocytes (rCMs). The two cell types were maintained separate by a cell culture insert (Millicell®, Millipore, Figure 7), made of a membrane of Polyethylene Terephthalate (PET) with 0.4 um pores to allow molecules only to pass through it. An insert was placed into each well of the 24-well plates and 6-well plates. The MSCs were seeded at the bottom of the wells, while the rCMs were seeded onto the inserts previously coated with 1% gelatine. The rationale of this condition was to mimic in a more realistic way the in vivo cardiac environment and see if the presence of the cardiomyocytes is enough to commit the MSCs. 5-Aza (5 uM for the first three days of differentiation) was the only supplement added to the culture in order to inhibit cell proliferation. The differentiation medium was given by a combination 1:1 of DMEM and M199, supplemented with 2% HS and 1% P/S.

Figure 7 24-well plate cell culture insert. rCMs were cultured on the inserts, while MSCs were growing on the bottom of the well.

For each differentiation experiment, an untreated condition was used as negative control in order to compare the cells submitted to the differentiation protocols to those that have not been treated with any supplements or particular media. These untreated cells were cultured in the normal growing medium (DMEM with 10% FBS and 1% P/S) until confluence was reached. Then the cells were either fixed for immunological staining or lysed for RNA extraction.

Cells were checked every day and pictures were taken at least once a week to monitor morphological changes. The differentiation was stopped after 3 weeks of culture from the seeding day. Treated and untreated cells were either stained for cardiac markers, or

lysed to extract RNA and investigate their gene expression. Additionally, in T3 was assessed that the rCMs were alive on the inserts. A viability/cytotoxicity assay was performed to establish cell viability (a detailed explanation of the technique is reported in paragraph 10.).

Each differentiation protocol has been performed with at least three different cell lines of both human and porcine MSCs. In addition, each individual experiment was carried out in triplicate for both ICC and qPCR.

6. FLUORESCENT IMMUNOSTAINING

Cells were fixed with 4% PFA for 20 minutes at RT. Fixed cells were washed twice with PBS and cell membranes were permeabilized with 0.01% TritonX-100 (Millipore) in PBS for 10 minutes at RT. Cells were then washed and incubated with 10% Normal Goat Serum (Sigma Aldrich) PBS for 30 minutes at RT. This incubation allows to block any antigens that might bind an antibody raised in goat. Because all the secondary antibodies used were produced in goat, a goat serum has to be used. At the end of the blocking, cells were incubated with the cardiac-specific primary antibodies Mouse anti-Sarcomeric alpha-Actinin, mouse anti-cardiac Myosin Heavy Chain, Rabbit anti-Desmin and Rabbit anti-Connexin-43 ON at 4°C (antibodies' details are reported in Table 5). The following day, cells are washed three times with PBS and secondary antibody solutions were prepared. Goat anti-Mouse conjugated with Alexa Flour 488 was used to detect the primary antibodies raised in mouse, while a Goat anti-Rabbit conjugated with Alexa Flour 54 was used to detect the rabbit antibodies (antibodies' information are reported in Table 5). Both secondary antibodies were incubated for 1 hour, cover and at RT. At the end of the incubation, cells were washed three times with PBS and nuclei were counterstained with 4',6-Diamidino-2-Phenylindole, Dihydrochloride (DAPI; 1:3000; ThermoFisher) for 10 minutes, covered at RT. Cells were then washed three times with PBS and in the end the coverslips were transferred onto microscope slides where were mounted with DPX mounting medium (Vectashield). Samples were analysed using a fluorescent inverted microscope (Zeiss Observer.Z1).

7. GENE EXPRESSION ANALYSIS

7.1. Total RNA extraction from animal cells and tissues

A RNeasy mini kit (Qiagen) was used to isolate RNA from samples. Cells were washed with PBS and lysed with QIazol Lysis Reagent, a phenol-based solvent. If RNA was to be extracted from tissue, it was necessary to weight the specimen in order to use a piece not heavier than 0.025g. The tissue was transferred into a 2 ml tube with ceramic beads and 700 ul of QIazol. The tubes were inserted into a homogenizer (Bertin Technologies, Minilys) to allow complete tissue destruction.

140 ul of chloroform (Fluka Analytical) were added to the cell/tissue samples and the tubes were shaken vigorously for 15 seconds. Tubes were placed on the benchtop for 2 minutes and then centrifuged at 12000g for 15 minutes. The upper aqueous phase containing RNA was transfer into a new collection of tubes and the volume of each sample was estimated. 1.5 of that volume of 100% ethanol (Sigma-Aldrich) was added to the samples, which were mixed by pipetting. Up to 700 ul of the above solutions were transferred into RNA-extraction column tubes and centrifuged at 10000 rpm for 15 seconds. The flow-throws containing QIazol were discarded and the operation was repeated if necessary. 350 ul of RWT Buffer were added to each column and the samples were centrifuged at 10000 rpm for 15 seconds. To digest any DNA residues, a digestion with DNase I was performed. 10 ul of enzyme were mixed with 70 ul of RDD Buffer for each sample. The solution was then added to the samples, which were incubated for 15 minutes at RT. At the end of the incubation, 350 ul of RWT buffer were added to each sample and the tubes were centrifuged at 10000 rpm for 15 seconds. Two washes with 500 ul of RPE Buffer were performed, during which samples were centrifuged at 10000 rpm for 1 minute each. The columns were transferred into a new collection of tubes and 40 ul or RNase-free water were added to each of them. Samples were centrifuged at 10000 rpm for 2 minutes to elute the RNA.

RNA analysis was performed using a NanoDrop® spectrophotometer (Thermo Fisher Scientific Inc.) in order to quantify RNA concentration (expressed as ng/ul) and calculate RNA purity. A 260/280 ratio was detected as indicator of protein contamination, whereas a 260/230 ratio was detected to show possible chemical contaminations (e.g. with the guanidine salts from QIazol). RNA samples were stored at -80°C.

7.2. Retrotranscription

The QuantiTect Transcription kit (Qiagen) was used to convert the RNA into cDNA. The reaction was prepared on ice. 800 ng of RNA were normally used, and RNase free-water was added to each sample up to 12 ul. 2 ul of gDNA wipeout buffer were added to each sample for effective elimination of genomic DNA contamination from starting RNA. Samples were incubated for 2 minutes at 42°C.

A master mix solution (MM) was prepared containing, per each sample: 4 ul of Quantiscript RT buffer, 1 ul of Quantiscript Reverse Transcriptase and 1 ul of RT Primer mix. 6 ul of the MM were added to each samples, which were incubated for 30 minutes at 42°C and 3 minutes at 95°C to inactivate the enzyme. cDNA samples were then moved to ice and either stored at -20°C or used straightaway for qPCR.

7.3. Capillary Real-Time PCR (RT-PCR)

The QuantiTect SYBR® Green PCR Kit was used to quantify cDNA targets. The reaction was prepared on ice. Due to the limited capacity of the capillary PCR machine to allocate 34 capillaries maximum, it was necessary to perform a reaction for each single primer. A master mix solution (MM) containing SYBR Green, RNase-free water and Primers, was prepared according to Table 4. The MM was then aliquoted into as many tubes as the number of samples. Then to each tube was added the appropriate cDNA.

<table>
<tr><th>Reagents</th><th>ul</th><th>Triplicate</th><th></th><th></th><th>Error</th></tr>
<tr><td>SYBR Green</td><td>5</td><td rowspan="4">x 3</td><td rowspan="3">x No. of samples</td><td rowspan="2">x No. of Primers</td><td rowspan="4">+ 10%</td></tr>
<tr><td>RNase-free water</td><td>3</td></tr>
<tr><td>Primer</td><td>1</td><td></td></tr>
<tr><td>cDNA</td><td>1</td><td></td><td></td></tr>
</table>

Table 4. *Summary of the reagents used in the qPCR with the respective used volume.*

The MM was then distributed to each sample, where the appropriate cDNA was added. 10 ul of each samples were then transferred to a single capillary (La Roche). When all samples were moved to the capillaries, there were centrifuged at 2000 for 30 seconds,

in order to allow the solution to reach the bottom of the capillary. The capillaries were then inserted into the capillary PCR (LightCycler 1.5, La Roche) and the reaction set up as follow:

Denaturation: 95°C (x 1 cycle)

Amplification: Denaturation: 95°C / Annealing: 60°C / Synthesis: 72°C (x 50 cycle)

Melting: 95°C (x 1 cycle).

At the end of the reaction, the melting curve and the standard amplification curves were generated and the crossing point (Ct) of each sample analysed. A relative quantification was performed and as the 18s housekeeping gene was used to normalise the Ct value of the genes of interest. Thus the expression of the genes of interest was compared to the one shown by the housekeeping gene. The Student's T-test was used to verify if any real difference existed between different conditions (e.g. treated cells vs untreated cells). Additionally, a standard error and a standard deviation were calculate.

Regarding the differentiation experiments, the expression level of cardiac-specific genes was investigated. The expression detected in the untreated cells (negative control) was compared to that exhibited by the treated cells. The targeted genes were: GATA-4, ACTA1, DES and cMYH. The primers for the human genes were commercially available and they were all obtained from Qlagen. Whereas, the primers for the porcine genes were not available on the market, thus they were designed.

7.4. Porcine primers design

The NCBI genomic database was used to generate the primers of interests. Two primer pairs were designed per each gene, in order to choose the optimal pair. In Table 5 are reported only the primer pairs that showed better results and that were used in the differentiation experiments. Primers were firstly tested with a non-quantitative PCR reaction. cDNA extracted from porcine heart was used in the tests. At the end of the amplification process, the products were separated according to their size in a 1.2% agarose gel (Sigma Aldrich) supplemented with Ethidium Bromide (COMPANY) to allow samples' revelation. At the end of the electrophoresis, the gel was transferred into an imaging system (ChemiDoc, Bio-Rad) to develop the DNA bands.

Name	Forward primers	Reverse primers	Product length
Pig GATA-4	CGACACCCTAATCTCGATATGTT	CAGTTGGCACAGGAGAGGC	221
Pig ACTA1	TACAAAGATGTGCGACGACGA	CCTTCTGACCCATACCCACC	164
Pig DES	GGCTCAGTACGAGACCATCG	GCATCGATCTCGCAGGTGTA	177
Pig MYH-7 β	AGGTCAAGGCCTACAATCGC	CTTAGTTGCGCCCTCAGGAT	232

Table 5. *Primers designed for porcine cardiac-specific genes. The table shows the nucleotide sequences of both the forward and reverse primers, as well as the length of the amplification product in terms of base pairs.*

8. TISSUE DECELLULARIZATION

Porcine pericardium and myocardium were collected from approximately 60 kg adult pigs. Tissues were washed several times with 1% P/S PBS and cleared from any other tissues. All following steps were performed in sterile conditions and over a shaker, in order to keep the solutions in movement.

8.1. Decellularization of the pericardial membrane

Being extremely thin and soft, the pericardium has the tendency to fold easily on itself. To keep the tissue flat, cell crowns (CellCrown inserts, Sigma-Aldrich) were used to fix the pericardium over them (Figure 8). Two different protocols were applied in order to identify the optimal decellularization strategy. The first protocol was based on the activity of the enzyme Trypsin (Try, 0.1% Life Technologies) that was incubated with the samples for 48 hours at 37°C. Whereas the second protocol was based on the action of the detergent TritonX-100 (TX, 1%, Millipore) that was let in contact with the samples for 48 hours at RT. Both solutions were refreshed after 24 hours. At the end of the incubations, all samples were treated with DNase I (25 ug/ml, Sigma Aldrich) for 48 hours at 37°C, in order to remove any residual of nuclear materials. Then tissues were washed with 1% P/S PBS for 10 days at RT. The washing solutions were changed at least once per day. At the end of the protocols, the samples were stored at 4°C until needed.

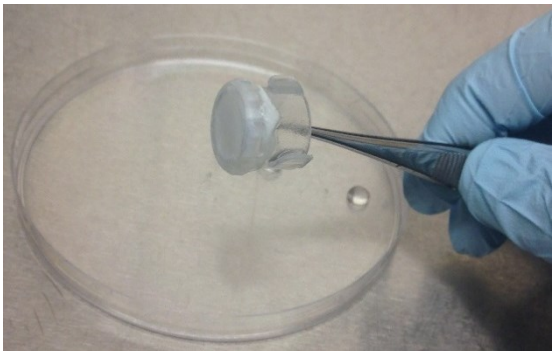

Figure 8 Pericardial membrane mounted over a cell crown to keep the tissue flat. Both the decellularization and the reseeding of the pericardium occurred with the tissue mounted over the insert.

8.2. Decellularization of the myocardium

Little pieces of myocardium were cut from the pig heart. The size of the pieces was approximately 1 cm^2 and the thickness of few millimetres. To wash away the cellular and nuclear material from the tissues, the samples were firstly treated with the detergent Sodium Dodecyl Sulfate (SDS, 1%, Sigma-Aldrich) for 36 hours at RT. Tissues were then washed with 1% P/S PBS for 24 hours at RT and incubated with the detergent TritonX-100 for 1 hour at RT. A week of washing with 1% P/S PBS followed the procedure and the washing solution was changed at least once a day. At the end of the protocol, samples were stored at 4°C until needed.

9. CELL SEEDING OVER SCAFFOLDS

9.1. Recellularization on acellular pericardium and myocardium

Cells were seeded at high density ($1x10^5$ cell/cm^2) over the Try- and Tx- decellularized pericardia and SDS-decellularized myocardia. The pericardial tissues were kept mounted over the inserts in order to maintain a flat surface and cells were seeded inside the crowns. Differentiated and undifferentiated hTMSCs were used to test both the reseeding potential of the developed scaffolds and the cells' ability to adhere over them. Cells were cultured in DMEM supplemented with 10% FBS and 1% P/S, which was refreshed three times per week. Cells were cultured over the decellularized materials for up to 2 weeks under static condition. Then the patches were analysed with different techniques, including viability/cytotoxicity assay, histology and scanning electron microscopy.

9.2. Cell seeding on clinical-grade scaffold

CorMatrix® (CorMx, ECM Technologies) is a clinically used decellularized material that we also employed as scaffold to generate cardiac patch. This material derives from the porcine small intestinal submucosa and consists of a thin and elastic tissue that looks like a sheet of paper. Hence, prior its utilization, it has to be soaked ON in culture medium. Differentiated and undifferentiated hTMSCs were seeded over the CorMx at high density ($1x10^5$ - $5 x10^5$ cell/cm^2) and were cultured in normal medium for up to two weeks under static conditions.

Scaffold	Decellularization technique	Cell seeded	Environment
Pericardium	Trypsin / DNase I	hTMSCs	Static
		Diff-hTMSCs	
	TritonX-100 / DNase I	hTMSCs	
		Diff-hTMSCs	
Myocardium	SDS / TritonX-100	hTMSCs	
		Diff-hTMSCs	
CorMx	Ready-to-use	hTMSCs	
		Diff-hTMSCs	
		hTMSC	Dynamic (bioreactor)
		Diff-hTMSCs	
		pTMSCs	

Table 6. *Summary of the different combination of utilized scaffolds, decellularization technique, and cell types applied to engineer the material and the condition of culture.*

In addition, differentiated and undifferentiated hTMSCs and undifferentiated pig TMSCs were seeded on the matrix and cultured for one week under static condition and one week in a rotating bioreactor (Harvard Apparatus). The bioreactor generates a dynamic system that allows culture medium to be equally dispersed throughout the construct and at the same time, it applies mechanical forces to the patch, such as sheer stress (Figure 9). The patches were stitched around a little tube that was set up to rotate at 2 rpm. 150 ml of normal medium were added within the bioreactor the first day of

culture. The bioreactor was placed at 37°C in a 5% CO_2 humidified atmosphere for one week.

After two weeks of culture, the patches were dismounted from the bioreactor and analysed with viability/cytotoxicity assay, histology and scanning electron microscopy. Unseeded scaffolds were used as negative control. In addition, the pTMSCs-seeded CorMx was tested in a cardiopulmonary bypass recovery piglet model.

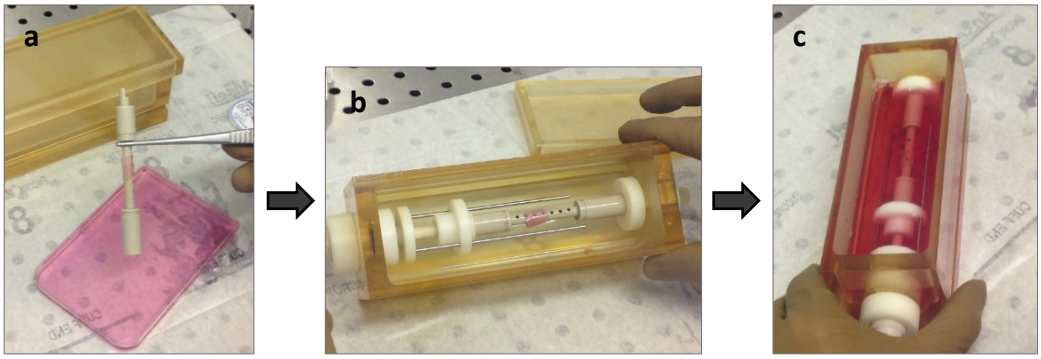

Figure 9 Bioreactor installation. The graft was stitched to the rotating arm of the bioreactor and stitched back to itself so as it fashions a tube shape (a). The arm is then inserted within the chamber (b), which was filled with growing medium (c). The bioreactor was placed into an incubator at 37°C for one week.

10. VIABILITY/CYTOTOXYCITY ASSAY

The Viability/Cytotoxicity assay kit for animal live and dead cells (Biotium), provides green and red fluorescence for live and dead cells respectively. The technique uses probes (Calcein AM) for intracellular esterase activity in viable cells, while takes advantage of compromised plasma membrane integrity in dead cells.

Calcein AM is a membrane-permeable, non-fluorescent esterase substrate that can enter the cytoplasm, where is cleaved by esterases in viable cells, producing the green fluorescent dye calcein. This product is cell membrane impermeable and is retained in the cytoplasm of live cells with intact plasma membrane. Dead cell either do not stain due to the lack of esterase activity, or fail to retain calcein in the cytoplasm due to their compromised plasma membrane. The working concentration of Calcein AM used was 4 uM.

Ethidium homodimer III (EthD-III) is a plasma membrane-impermeable dye that is excluded by viable cells. This dye does not fluoresce until it binds molecules of DNA. EthD-III penetrates dead cells with damaged plasma membrane and then it stains the nucleus with red fluorescence. The working concentration of EthD-III applied was 2 uM.

Cells were incubated with the dyes for 40 minutes at 37°C. At the end of the incubation, cells were washed with PBS and observed with an inverted fluorescent microscope.

11. HISTOLOGICAL EXAMINATION

11.1 Sample preparation

Tissue samples were washed with PBS and fixed with 4% PFA PBS and incubated ON at 4°C. The following day, samples were washed with PBS and transferred in histological cassettes (Histosette I, Simport). Samples were then processed ON in the Excelsior AS processor (Thermo Fischer). The day after, samples were embedded in paraffin using a Histo Star embedding machine (Thermo Fischer). Samples were cut using a Reichert-Jung 2030 Biocut microtome and sections of 4 um thickness were produced. The sections were then incubated ON at 37°C and stored at RT. The same preparation protocol was applied to process samples for immunohistochemistry.

11.2. Hematoxylin and Eosin

Hematoxylin and Eosin (H&E) H&E is a histological stain that colours the nuclei of the cells and the calcified material in blue to purple thanks to the oxidation product of hematoxylin, haematin. Cellular and nuclear materials are counterstained with eosin, an alcoholic solution that colours the eosinophilic structures in various shades of red/pink.

This staining was performed using a Shandon Varistan 24-4 automated machine (Thermo Fischer). The procedure included a dewaxing step into clerene (Leica) and rehydration with different concentration of Industrial Methylated Spirits (IMS, Gente Medical) to tap water. Slides were then moved into hematoxylin (Pioneer Research Chemicals) and washed in distilled water. Samples were transferred into Scots Tap Water Sub (Atom Scientific) and washed with running tap water. Slides were stained with 0.5% eosin (Atom Scientific) and washed in running tap water. Finally, slides were dehydrated in IMS and rinse with clerene.

11.3. Elastic Van Gieson

Elastic Van Gieson (EVG) is a staining procedure that forms a variety of bounds with elastin that in turn has high affinity for the iron-hematoxylin complex formed by the reagents in the stain. Thus, elastin retains the dye longer than other tissue elements, becoming the only stained tissue. In fact remaining tissues are decolorized. Van Gieson' stain is used to counterstain the principal one. This dye colours the collagen fibers in red, whereas all other tissue elements such as cytoplasm, red blood cells and muscular tissue, are stained in yellow.

An automated machine was used to perform the histological stain. Slides are firstly dewaxed in clerene and then rehydrated to tap water. Samples were then moved into 0.5% Pot Permanganate (Sigma Aldrich), rinsed in distilled water, incubated with 1% Oxalic acid (Sigma Aldrich) and washed again with distilled water. Then, slides were moved into IMS before and after being incubated with Millers Elastin (Pioneer Research Chemicals). Samples were washed with tap running water and stained with Van Gieson solution (Pioneer Research Chemicals). Finally, slides were dehydrated in IMS and rinsed in clerene.

11.4. Alcian Blue

In order to detect the glycosaminoglycans (GAG) left in the tissues, Alcian Blue (AB) staining was performed manually. This protocol allows the visualization of acid mucosubstances, acetic mucins and cellular material. Strongly acidic mucosubstances are stained blue, nuclei are stained pink to red and cytoplasm are coloured in pale pink. Samples were deparaffinised in clerene and hydrated to distilled water. Then samples were stained for 30 minutes at RT with alcian blue solution (1% alcian blue in 3% acetic acid solution). At the end of the incubation, samples were washed under tap running water for 10 minutes and rinse in distilled water. Nuclei were counterstained with nuclear fast red solution for 5 minutes (0.1% nuclear fast red, 5% aluminium sulfate in distilled water). Samples were washed under tap running water for 5 minutes and rinsed in distilled water. Then samples were dehydrated in IMS and rinsed with clerene.

At the end of the H&E, EVG and AB stainings, samples were mounted with DPX mounting medium (Thermo Fischer Scientific) and let dry ON. Slides were observed with a bright field inverted microscope (Zeiss Observer.Z1).

12. IMMUNOHISTOCHEMISTRY PROCEDURES

Sections of paraffin-embedded samples were incubated for one hour at 60°C in order to let the tissues attach better to the slides. Then samples were dewaxed with three washes in Clerene. Samples were rehydrated with gradually lower concentrations of alcohol: two washes with 100% IMS, one with 90% IMS, one with 70% IMS and lastly one wash with distilled water. Tissue antigens retrieval was performed with Sodium Citrate buffer (10mM, with 0.05% Tween 20 (Sigma Aldrich), pH 6) by microwaving the samples three times at 700 w. Samples were let cool down in tap running water for 20-30 minutes and then washed twice with 0.5% Tween-20 PBS. Samples' antigens were blocked with 5% goat serum in PBS for 40 minutes at RT. Different primary antibodies were used, depending on the sample and on the purpose of the experiment. All the primary antibodies used in this study are reported in Table 7 with the relative concentrations. Sarcomeric alpha-Actinin, Desmin, cardiac-Myosin Heavy Chain and Connexin-43 consist of cardiac markers, while smooth muscle-Myosin Heavy Chain and alpha-Smooth Muscle Actin are smooth muscle antigens and Isolectin-B4 is an endothelial marker. The following day, samples were washed three times with Tween-PBS and then incubated covered for 1 hour at RT with the appropriate secondary antibodies (Table 8). At the end of the incubation, tissues were washed three times with Tween-PBS. To counterstain the nuclei, samples were stained with DAPI (1:3000) for 10 minutes covered at RT. Tissues were then washed three times with Tween-PBS and mounted with fluorescent mounting medium. Samples were observed with an inverted fluorescent microscope.

Antibody	Dilution ICC / IHC	Source	Company
Sarcomeric alpha-Actinin	1:100 / 1:100	Mouse	Abcam
Desmin	1:200 / 1:150	Rabbit	Abcam
Connexin-43	1:150 / 1:100	Rabbit polyclonal	Santa Cruz Biotechnology
Cardiac-Myosin Heavy Chain	1:150 / 1:100	Mouse	Thermo Fischer
Smooth muscle-Myosin Heavy Chain	Ready-to-use	Mouse	Dako
Alpha-Smooth Muscle Actin	1:200	Mouse	Abcam
Isolectin B4 - biotin	1:100	/	Life Technologies

Table 7. *Primary antibodies used in this study. The table shows the antigens detected, the dilution of the antibodies, the animal in which the antibodies have been produced and the company that sells them.*

Antibody	Dilution	Host animal	Company
Mouse - AF488	1:400	Goat	Abcam
Mouse – Cy3	1:300	Goat	Jackson Immuno Research Labs
Rabbit – AF 546	1:400	Goat	Abcam
Streptavidin - AF488	1:200	/	Life Technologies

Table 8. *Secondary antibodies applied in this study. The table reports the name of the antibodies along with the conjugated fluorophore, the concentration at which the antibodies were used, the animal into which the antibodies were raised and the Company from which they were obtained.*

13. SCANNING ELECTRON MYCROSCOPY ANALYSIS

Sample structure, morphology and topography were analysed with a Quanta 200 FEI field emission scanning electron microscope, in the Walfson Bioimaging Facility of the University of Bristol. For SEM examination, tissues of about 0.5 cm^2 were fixed with 4% PFA ON at 4°C. A 0.1 M phosphate buffer solution was prepared by mixing a di-sodium hydrogen phosphate dehydrate (1M, Fluka) with sodium dihydrogen phosphate anhydrous (1M, Fluka). This buffer was used to wash the tissues three times, before carrying out a second fixation with 1% osmium tetroxide (1 part of osmium 4% (Electron Microscopy Sciences), 1 part of 0.4 M phosphate buffer and 2 parts of distilled water)

for 20 minutes at RT. Samples were then washed three times with the 0.1M phosphate buffer and dehydrated in alcoholic solutions with progressive concentrations: 25%, 50%, 70%, 80%, 90%, 95% and 100%, 10 minutes each. To allow the samples to be wholly dry, a critical point dryer was used (Leica EM CPD300). At this point, samples were mounted over little pegs and then coated with Argon to make them electrically charged. The Emitech K575X sputter coater machine was used.

All specimens were examined with the SEM either at an opening voltage of 10 kV and spot size of 3, or at an opening voltage of 5 and a spot size of 1, depending on the tissue observed.

14. IN VIVO STUDY

A swine model of recovery CPB was established to test the engineered CorMx in vivo. A piece of approximately 7 cm^2 of scaffold was seeded with undifferentiated pTMSCs and culture for 2 weeks as explained in paragraph 9.2. Surgical procedures were performed at the Translational Biomedical Research Centre based at the Langford Veterinary Campus, Bristol.

Five-week-old Landrace female piglets of approximately 20-25 kg, were used in this study. The choice of this breed is due to their rapid growth, which lead to an increased stress on the early graft.

14.1. Cardiopulmonary Bypass

The CPB was designed in order to reproduce as close as possible what is routinely done in the operating cardiac theatre for children undergoing RVOT. All drugs administered to the animals were provided from the Translational Biomedical Research Centre and were supplied by NHS internal pharmacy. Surgical procedure was performed under general anaesthesia and neuromuscular blockade that were administered and controlled by an anaesthetic machine (Figure 10a). The neuromuscular blocking agent (NMBA) Pancuronium Bromide (2 mg/ml) was used to relax the residual muscle tone and diaphragmatic paralysis that would be present despite the anaesthesia and was administered via the jugular vein. Anaesthesia was inducted by intramuscular injection of ketamine (100 mg/ml) and midazolam (5 mg/ml). Occasionally Propofol (10 mg/ml)

was administered intravenously to reach a deeper anaesthesia. Then anaesthesia was maintained with inhalation of 1-2% Isoflurane. Throughout the surgical procedure were also administered intravenously Fentanyl (50 mg/ml, analgesic), Cefuroxime (750 mg, antibiotic), Pancuronium Bromide (2 mg/ml) and Heparin (5000 i.u./ml, anticoagulant) to ensure that the activating clotting time (ACT) was above 450 during the CPB.

Piglets were placed in a supine position in order to have better access to the thorax. An endotracheal tube was inserted to provide mechanical ventilation that was started with 10 ml/kg tidal volume, 100% oxygen and 0 mmHg of end-expiratory pressure. The right carotid artery and vein were exposed to monitor the arterial pressure and to insert a central line catheter for drug infusion and monitoring of the central nervous system. This single-stage venous catheter allows the monitoring of the piglet's hemodynamic profile by passing a thin tube into the superior vena cava that entered the right side of the heart and exited through the pulmonary artery.

Figure 10 Anaesthetic (a) and cardiopulmonary bypass machine (b) used in our surgical procedures.

The heart was then exposed via median sternotomy, hence a cut over the sternum was performed. CPB was established by cannulating the inferior and superior vena cava and the ascending aorta. The deoxygenated blood was drained from the heart and lungs to a reservoir via venous cannulation and returned oxygenated to the cannulated ascending aorta thanks to a mechanical pump and an oxygenator. Cardiac monitoring of the heartbeat, blood pressure and arterial oxygen saturation (SpO_2) were performed to measure the depth of anaesthesia and NMBA. A non-cardioplegic technique was carried out, hence the heart was not stopped from beating, so that no cardioplegic arrest was needed, in order to avoid any ischemic damage of the heart after reperfusion. Short

periods of aortic cross-clamping and VF were performed by applying directly on the heart fibrillating patches that keep the ventricle in VF. The flow, mean arterial pressure and rectal temperature during the bypass were maintained respectively between 85 and 100 ml/kg, 55 and 65 mmHg and 37°C, thus the CPB was performed under normothermia conditions.

An incision over the right ventricular outflow tract and below the pulmonary valve annulus was performed (Figure 11a). The defect created was then patched using either a control CorMatrix, or an engineered one that were stitched to the RV (Figure 11b). The engineered patch was placed with the cells facing the outer side of the heart. After anastomotic haemostasis was assured, the cannulae were removed and the incisions closed (Figure 11c). When surgery was completed, full rewarming and strong analgesia (based on a combination of opioids, paracetamol and NSAIDs) were established before the piglet was allowed to wake.

Post-operative (post-op) monitoring was intense for the first 48 hours after surgery in order to identify any changes in the physiological condition or evidence of poor pain control (Figure 11d). A combination of the following drugs were administered intravenously during the intensive care: Paracetamol (300 mg, every 6 hours, analgesic), Morphine (5 mg, every 4 hours, analgesic), Cefuroxime (400 mg, every 8 hours) and Meloxicam (8 mg, every 24 hours, NSAID). Additionally, intramuscular injection of Buprenorphine (0.3 mg/ml, every 12 hours, vetergesic) were performed when piglets returned to the Animal Services Unit (ASU). Regular checks were made in the subsequent two days, being this the critical period during which serious post-operative complications were likely to occur. This mistake caused a lot of blood loss during the surgery leading to a situation of anaemia. During the night following the operation, the anaemia got worse and we decided to terminate the animal. Data from this piglet allowed us to evaluate the integration of the scaffold right after the bypass and the host's immediate reaction to the patched material.

Before termination, pigs were checked with echo. Euthanasia was then performed with an intravenous injection of Euthatal (200 mg/ml, pentobarbitone), a short-acting barbiturate.

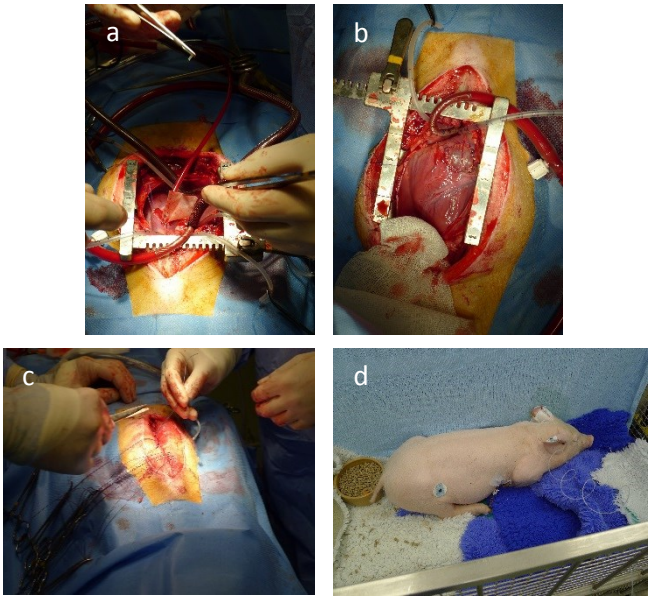

Figure 11 CPB surgical procedure. The adopted operating conditions were mimicking the clinical standards of pediatric procedure. The heart was accessed by sternotomy and after the bypass was established, a cut was performed on the RVOT and the patch was stitched to it (a, b). The sternum was closed (c) and the piglet recovered in the intensive care unit for 48 hours (d) until it was moved to the animal services unit.

14.2. Two-dimensional doppler echocardiography

Two-dimensional doppler echocardiography (Echo, VividQ, GE Healthcare) was performed in the short-axis view to observe the cross section of the RV and LV. The animals were laid down on the right side and the probe was placed in correspondence of the heart. The M-mode measuring allowed to calculate several parameters, including the thickness of the Interventricular Septum in diastole and in systole (respectively IVSd and IVSs), the LV Internal Diameter in diastole and in systole (respectively LVIDd and LVIDs) and the LV Poster Wall in diastole and in systole (respectively LVPWd and LCPWs). Furthermore, it was determined the volume of the end-diastole (EDV) and end-systole (ESV), the Ejection Fraction (EF), the Stroke Volume (SV) and the Fractional Shortening (FS).

Echo was performed immediately before surgery and after two, three and four months post-op in order to monitor the animals' cardiac functions until the termination. Prior the echo, pigs were anaesthetised with Ketamine (100 mg/ml), Midazolam (5 mg/ml) and Azoperone (40mg/ml) to sedate the animal during the procedure. Anaesthesia was then maintained with inhalation of 1-2% Isoflurane.

14.3. Evaluation of the explants

Pigs were dissected in order to collect the patched-heart as well as the liver, kidneys and spleen for future possible examinations. The heart was further dissected to isolate the implanted graft. All the collected tissues were either fixed with 4% PFA to be embedded I paraffin, or flash-frozen for OCT-embedded cryosections (OCT-embedding matrix, Cell Path). Sections of paraffin-embedded LV, RV and grafts were examined with histological and immunofluorescent stainings. H&E and EVG histological stainings allowed to visualize the cellular distribution through the explants, the possible degradation and integration of the grafts with the surrounding cardiac tissue, the immune response raised by the implants and the collagen and elastin composition of the samples. Immunofluorescent stainings was performed to investigate the expression of cardiac, endothelial and smooth muscle markers in the explanted grafts and relative RV as positive controls. Three different double stainings were carried out. The expression of smooth muscle Myosin Heavy Chain (smMYH) was study along with Desmin (Des), Connexin-43 (CX43) with cardiac Myosin Heavy Chain (cMYH) and alpha-Smooth Muscle Actin (aSMA) with Isolectin B4 (Iso).

14.3.1. Blood vessels quantification

The double staining for aSMA and Iso allowed to visualize the vasculature present in the stained samples and to distinguish between capillaries and greater vessels. In fact the capillaries are made of a monolayer of endothelial cells and they lack of a layer of smooth muscle cells. Based on this assumption, we considered as capillaries all the small vessels that were positive for Iso (showing a single layer of endothelial cells) but negative for aSMA. The vascularization of the TE-patch 4m was compared to that one exhibited by the unseeded scaffold, in order to verify if the presence of the seeded cells made any difference in terms of angiogenesis. Ten random pictures were taken per each sample and the two vessel types were counted separately.

RESULTS

CHAPTER 1: IN VITRO STUDY

OBJECTIVES

In the first section of the in vitro study, we aimed to isolate MSCs from the thymus gland of both children undergoing heart surgery and newborn piglets, in order to generate a line of human and porcine thymus-derived MSCs. Cells were characterized for the expression of mesenchymal surface markers and for their ability to differentiate into cells of the mesodermal lineages. MSCs were then submitted to three optimized protocols of cardiac differentiation and the cardiac commitment was assessed by evaluating the expression of cardiac-specific markers in the form of proteins and genes.

In the second part of the in vitro study, we focused on the development of xenogeneic scaffolds and viable grafts. Porcine pericardia and myocardia were decellularized with either enzymatic- or detergent-based techniques. Two different approaches were compared to decellularize the pericardial membrane: a Trypsin-based protocol and a Triton X-based technique. The reseeding potential of the developed scaffolds was assessed by recellularizing them with undifferentiated and cardiac-committed MSCs in order to verify and compare the capability of both cell types to engraft the developed materials. Moreover, the biocompatibility of CorMatrix, a clinical-grade material, was evaluated and the engineered scaffold was cultured under static and dynamic conditions.

1. MSC ISOLATION, EXPANTION AND CHARACTERIZATION

The enzymatic isolation of human and pig thymus-derived MSCs produced viable spindle-like shaped cells as shown in Figure 12. Both cell lines efficiently adhered to non-coated cell culture plastic flasks after few hours from seeding. The growing rate in 10% FBS medium was relatively high. In fact the cells normally reached confluence after five/six days of culture.

1.1. Functional characterization

To functionally characterize the human and pig TMSCs, their ability to differentiate into cells of mesenchymal origin (osteocytes, adipocytes and chondrocytes)-was verified. The direct differentiation of the MSCs was carried out in vitro using appropriate media and ready-to-use supplements specific for each differentiation protocol. Terminally differentiated cells were histochemically stained to determine their respective commitment. Untreated cells that were cultured without any supplements, were used as negative control.

1.1.1. Osteogenic differentiation

The osteogenic differentiation of the human and porcine TMSCs was established by staining the cells with Alizarin Red (Figure 13 from Dr. D. Iacobazzi). This staining allowed to detect any deposition of mineralized matrix from the differentiated cells. Our data showed that both human and pig differentiated TMSCs, were positive for the staining as several red spots of calcium deposits were detected. No positivity for Alizarin Red was observed in the untreated cells. These results confirmed the ability of both hTMSCs and pTMSCs to differentiate along the osteoblastic lineage.

1.1.2. Adipogenic Differentiation

The adipogenic differentiation potential of the human and pig thymus-derived MSCs, was evaluated by staining the cells with Oil Red O (Figure 14 from Dr. D. Iacobazzi). This histological stain allowed to identify intracellular lipid vesicles that are typically present in large numbers within mature adipocytes. Triglyceride accumulation in the cytoplasm of differentiated cells, was clearly visible and stained in bright red by the Oil Red O dye.

This indicated that both hTMSCs and pTMSCs were able to differentiate into mature adipocytes. Control cells cultured in the absence of any adipogenic supplements, did not yield lipid-filled cells.

1.1.3. Chondrogenic differentiation

The chondrogenic potential of human and porcine TMSCs was accessed using the pellet-culture system and chondrogenic-inducing medium. Control pellets were cultured in the same medium without supplements. After 21 days of culture, the 3D spheroid cultures were stained with the copper-containing dye Alcian Blue to verify the cartilage formation (Figure 15 from Dr. D. Iacobazzi). Chondrogenic pellets were positive for AB and showed cartilage-specific proteoglycans stained blue, while control cells were negative for the staining. These results confirmed the chondrogenic potential of the hTMSCs and pTMSCs.

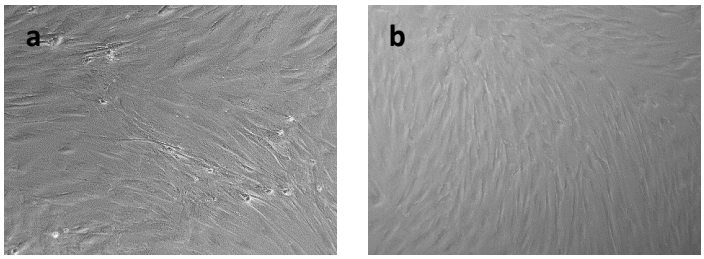

Figure 12 Human (a) and pig (b) thymus-derived MSCs growing on plastic. After few hours of culture, cells attached to the plastic and started to proliferate. Magnification: 100X.

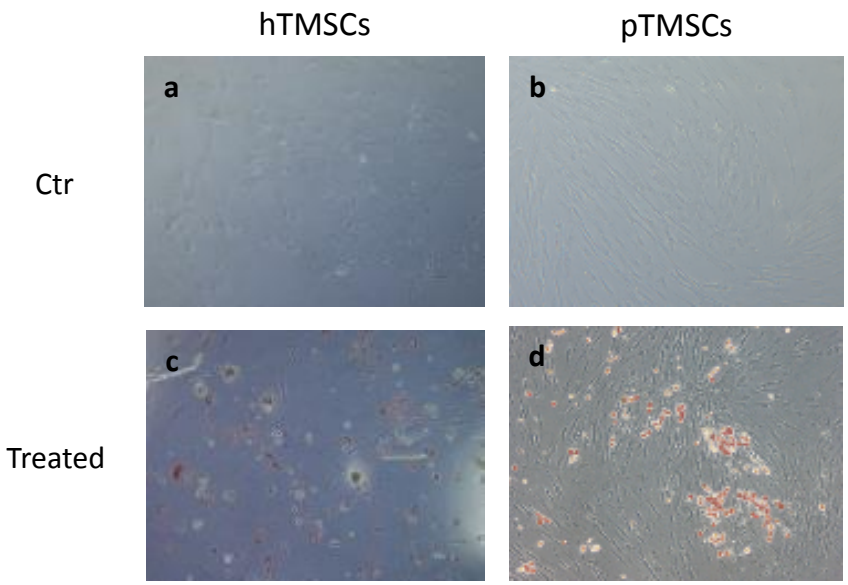

Figure 13 Human and pig thymus-derived MSCs can differentiate among the osteogenic lineage if conditioned with osteocyte-inducing medium (c, d). Positivity for Alizarin Red demonstrated the presence of calcium deposition in treated cells, in contrast with untreated control cells, where no positivity was detected (a, b). Magnification: 100x (From Dr. D. Iacobazzi).

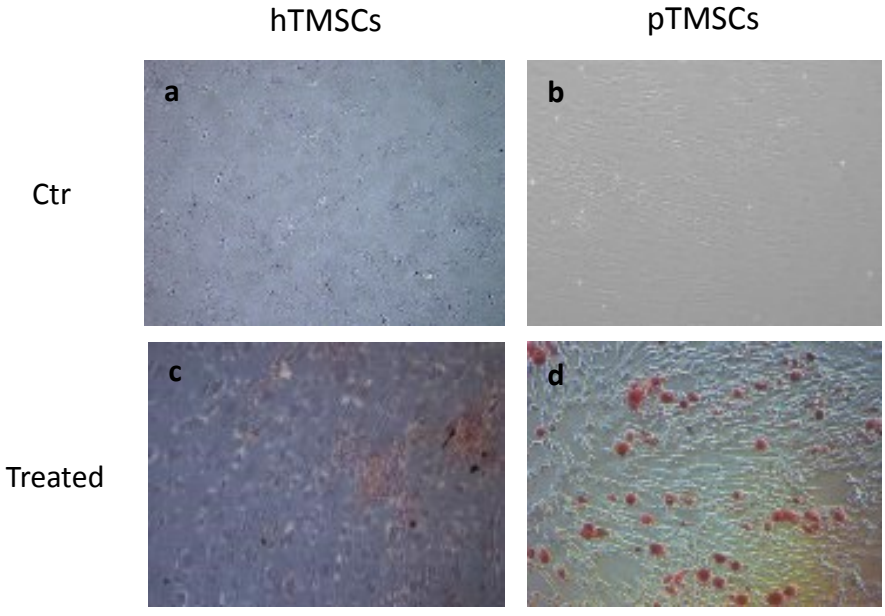

Figure 14 Oil Red O staining confirmed the adipogenic potential of human and porcine thymus-derived MSCs (c, d). Treated cells exhibited accumulation of triglyceride droplets typical of mature adipocytes that appeared with a bright red colour. Control untreated cells did not show positivity for the staining (a, b). Magnification: 100x. (From Dr. D. Iacobazzi).

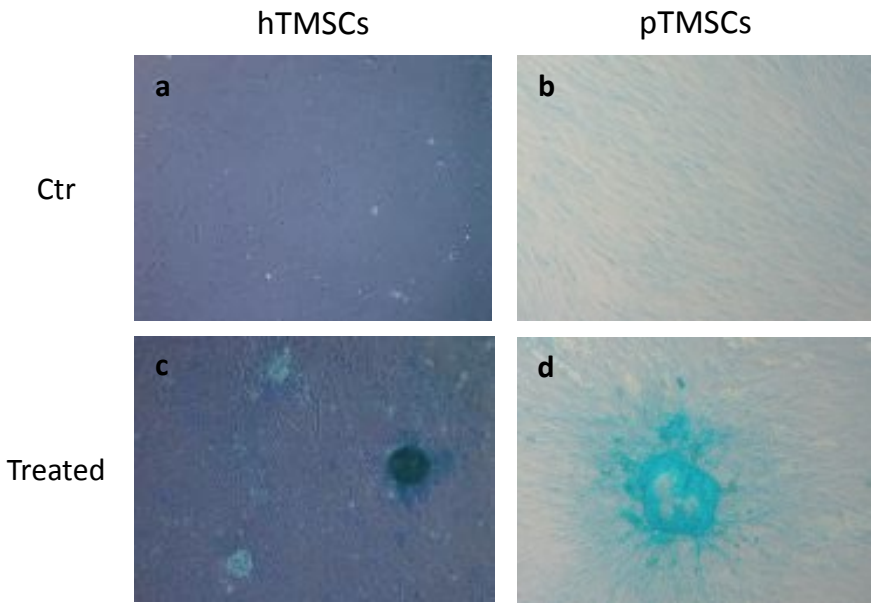

Figure 15 Human and pig thymus-derived MSCs undergo chondrogenic differentiation if cultured in appropriate stimulating medium (c, d). Chondrogenic pellets showed cartilage-specific proteoglycans that were positive for Alcian Blue staining. In contrast, unstimulated controls were negative for the staining (a, b). Magnification: 100x. (From Dr. D. Iacobazzi).

1.2. Surface markers characterization

Flow cytometry (FACS) allowed to investigate the expression of both surface and nuclear markers. A combination of positive and negative markers was used to characterize the MSCs. Dominici et al. suggested that the minimal criteria for MSC surface phenotyping is expression of CD73, CD90 and CD105, accompanied by the lack of CD14, CD34, CD45 and HLA-DR (Dominici et al. 2006). To characterize the human thymus-derived MSCs, the research panel originally proposed by Dominici was applied and implemented with additional markers. Indeed, the hTMSCs were also tested for the expression of CD29, CD44 and for the lack of CD31. Due to the poor availability of FACS porcine antibodies, the research panel for the porcine cells included less markers. pTMSCs were examined for the expression of CD44, CD73, CD90 and CD105, accompanied by the lack of CD31 and CD45.

Cells were gated using an unstained control and a live/dead control. In the unstained control no antibodies were used, while in the live/dead control an antibody that binds viable cells only, was used. Three different cell lines were used for the characterization of both the human and porcine cells (n=3). In Figure 16a are reported the histograms of the percentage of the human viable cells that were positive for CD29, CD44, CD73, CD90, CD105, CD14, CD31, CD34, CD45 and HLA-DR. These data confirmed that the

hTMSCs highly expressed CD29, CD44, CD73 and CD105 (> 91%) and were positive for CD90 (83%). Furthermore, no expression of CD14, CD31, CD34 and HLA-DR was detected. Low percentage of hTMSCs was positive for CD45 (< 5%). In regards of the porcine MSCs, Figure 16b shows the histograms of the percentage of the cells positive for CD44, CD73, CD90, CD105, CD31 and CD45, indicating that the pTMSCs highly expressed CD44, CD90 and CD105 (> 95.5%) and were positive for CD73 (90%). No positivity was detected for the endothelial and hematopoietic markers CD31 and CD45.

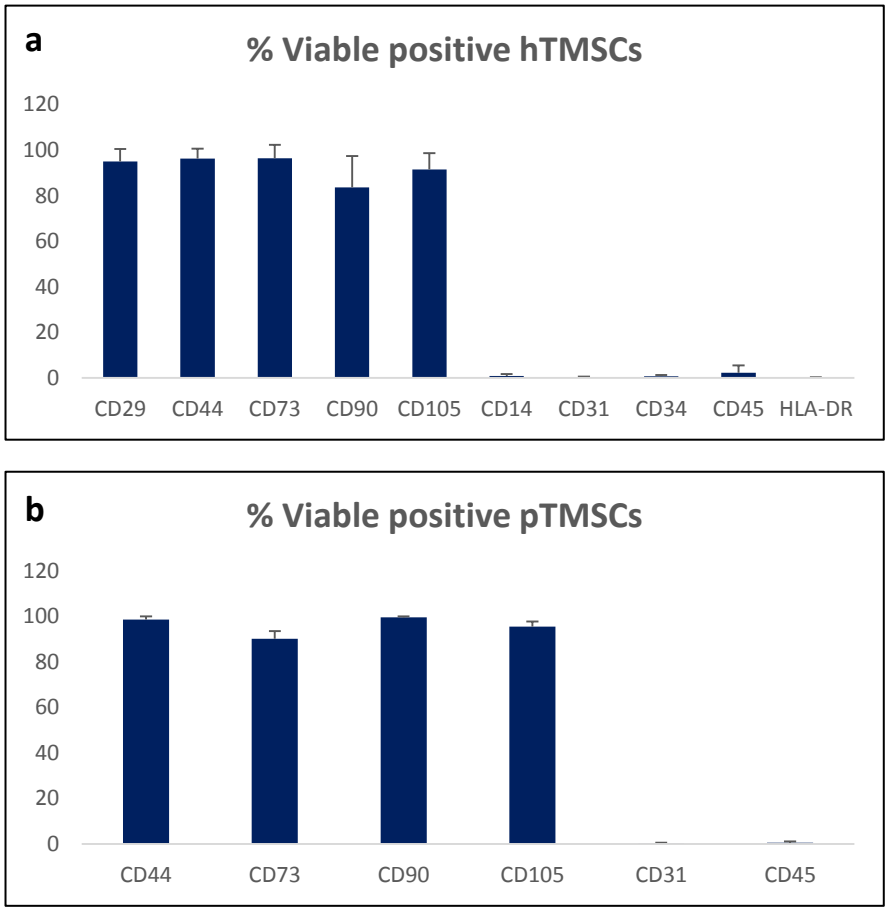

Figure 16 Flow cytometry characterization of the surface markers expressed by the human and porcine thymus-derived MSCs. hTMSCs highly expressed the typical mesenchymal markers CD29, CD44, CD73, CD90 and CD105 while were negative for the immune-system proteins CD14, CD31 and HLA-DR, the endothelial marker CD34 and the hematopoietic marker CD45 (a). Porcine cells were demonstrated to strongly express CD44, CD73, CD90 and CD105 wile no expression was detected for CD31 and CD45 (b). N = 4 for both cell lines.

2. rCM ISOLATION AND CHARACTERIZATION

Cardiomyocytes were isolated from the heart of neonatal rats (1 to 3 days old) using a trypsin-digestion protocol. Adherent cells exhibited a rod-shape or a multiangular morphology (Figure 17). Different ECM components were used to coat the plastic plate, such as gelatine, fibronectin and collagen. The gelatine-coated plates, showed better cell behaviour in terms of colony-forming capability, beating rate and cell growth. On the gelatine-coated flasks, cells started to arrange themselves into colonies after 2-3 days of culture and beating cells were observed within the colonies as soon as they formed. At this stage, about 18-22 beats/minutes were recorded. Over time, the contractions of the colonies became more frequent and synchronous. Confluency was normally achieved after one week. Monolayers of CM were usually beating in a synchronized fashion and the contraction rate was approximately 35-40 beats/minutes.

CMs were characterized with immunocytochemistry and RT-PCR. To verify the expression of proteins typical of mature cardiomyocytes, cells were stained for Sarcomeric alpha-Actinin (SαA), cardiac Myosin Heavy Chain (cMYH), Desmin (Des) and Connexin-43 (Cx43). Positivity for all the four markers was detected (Figure 18). In the staining for SαA, cMYH and Des, it was clearly observed the striations characteristic of the sarcomeric structures of muscle cells. IHC showed that the isolated cells were not a homogenous population of CMs as few cells did not express any of the cardiac markers. Those non-cardiac cells could most likely be cardiac fibroblasts, epicardial and endothelial cells. For the purpose of this study it was not necessary to obtain a homogenous culture. In fact it was a good thing to have such contamination as it has been shown that in order to keep healthy and mature CMs it is advised to culture them with non-cardiac cells as they support and stimulate cardiac growth.

RT-PCR assays showed that the cardiac-specific genes GATA-4, ACTA1, cMYH and DES were highly expressed in the isolated CMs (Figure 19). The transcripts of the same genes were undetectable in the undifferentiated MSCs that were used as negative control. The difference of expression between the negative controls and the CMs was significant for GATA-4, DES and cMYH ($p < 0.05$), while the expression of ACTA1 appeared to increase.

These results showed that the optimized protocol to isolated primary culture of rat cardiomyocytes allowed to obtain cardiac cells with high yield. Most of the isolated cells highly expressed cardiac-specific markers both in the form of proteins and as transcripts.

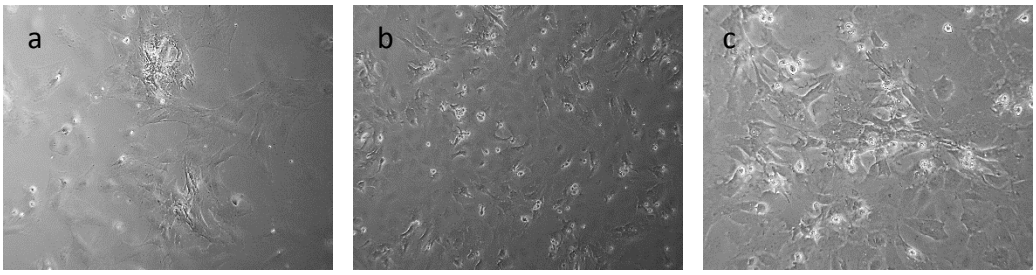

Figure 17 Two different pattern of contracting structures in the primary culture of rat neonatal cardiomyocytes. After 2-3 days in culture, cells aggregated in contracting colonies (a). Confluent monolayer of contracting cardiac myocytes were obtained after a week of culture on gelatine-coated plates (b, c). Magnification: 100x

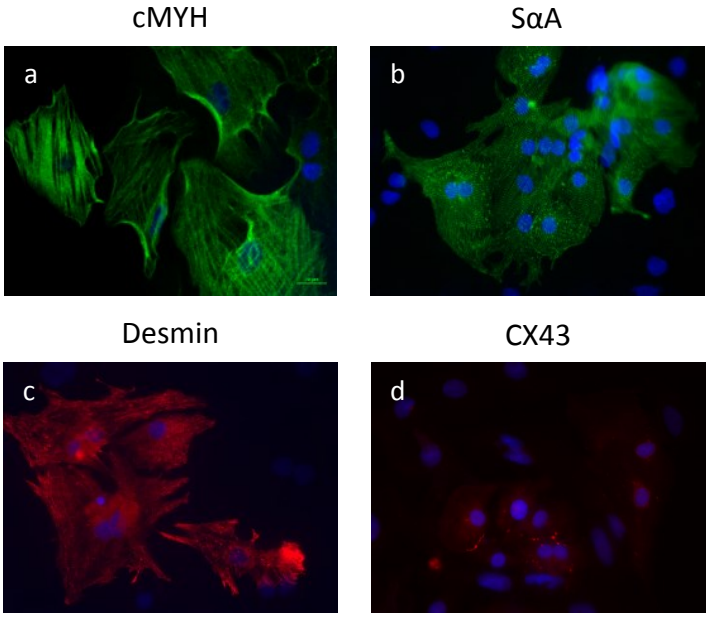

Figure 18 Cardiomyocytes isolated from neonatal rats expressed cardiac-specific proteins, such as cardiac-Myosin Heavy Chain (a) stained with green fluorescence, Sarcomeric alpha-Actinin (b) in green fluorescence, Desmin (c) and Connexin-43 shown by red fluorescence (d). Magnification: 200x.

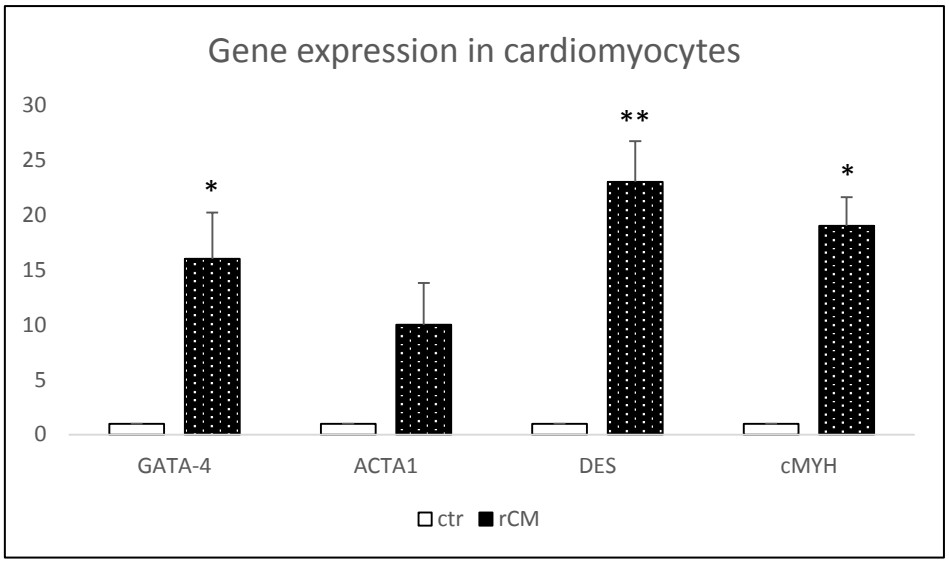

*Figure 19 Expression of cardiac-specific genes in cardiomyocytes isolated from neonatal rats (white-on-black dotted bars) compared to undifferentiated mesenchymal stem cells as negative control (white bars). The expression level of GATA-4, Desmin (DES) and cardiac Myosin Heavy Chain (cMYH) was detected to be significantly higher in the cardiac cells then in the control cells. ACTA1 was also found to be more expressed by the cardiomyocytes. * $p < 0.05$; ** $p < 0.005$.*

3. DIFFERENTIATION OF MSCs INTO CARDIAC-LIKE CELLS

Human and porcine thymus-derived MSCs were induced to differentiate into cardiac-like cells. Three different protocols were applied: T1 that was based on a combination of chemical agents, T2, which was based on the cardiomyocytes conditioned medium (CCM) and T3 that was based on the coculture of the MSCs with cardiomyocytes isolated from neonatal rats. Untreated MSCs were used as negative control of the differentiation.

3.1. Morphological changes

During the differentiation periods, pictures of the cells were taken once a week to record any morphological changes. Regarding protocols T1 and T2, immediately after the 5-Aza induction, few cells died due to the toxicity of the demethylating agent. The proliferation of the survived cells was not completely stopped, but rather inhibited as cells were growing at a lower rate. The morphology of the treated cells changed gradually after the induction of the differentiation. After a week, both human and

porcine cells started to lose the spindle-like shape typical of mesenchymal cells (Figure 20; Figure 21). A more rod-like shape was observed, as cells enlarged and adopted an elliptical conformation. After two weeks of differentiation, cells exhibited many cytoplasmic processes and branches characteristic of cardiac cells. After 2 weeks of differentiation, human cells treated with T2 began to aggregate themselves into colonies that were visualized only after three weeks in the porcine cells. At the end of the differentiation treatments, some cells showed granularity and multinucleation, which are typical of cardiomyocytes. No colonies were detected in the T1-treated cells. Since the control cells were not treated with 5-Aza, their proliferation was not inhibited. Control cultures were stopped after two weeks when 100% confluency was achieved.

No pictures were taken of the T3-treated cells as it was not possible to visualize to the cells growing at the bottom of the well due to the inserts present in each well.

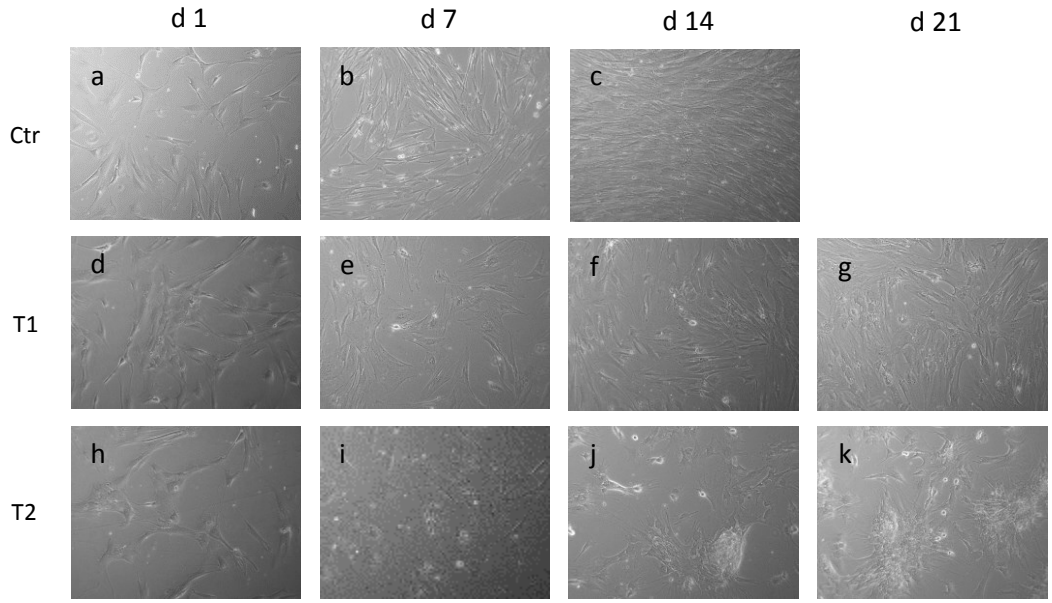

Figure 20 Morphological changes from human thymus-derived MSCs (d, h) to cardiomyocyte-like cells induced by two different protocols, T1 and T2. The morphological differentiation evolved gradually after 5-Aza treatment. At one week after induction, treated cells started to lose their spindle-shape and a more rod-like shape was acquired (e, i). After two weeks of differentiation, cells conditioned with T2 began to aggregate themselves into high-density colonies (j). By the end of the differentiation, most of the cells were part of colonies (k). No colonies were observed in the cells treated with T1 (f, g) but most of them exhibited long cytoplasmic process and showed multinucleation. Untreated cells were used as negative control (a, b, c). These cells proliferated with the standard rate of MSCs. After two weeks of culture 100% confluency was reached (c) and the cells were stopped from being cultured. Magnifications: 100x.

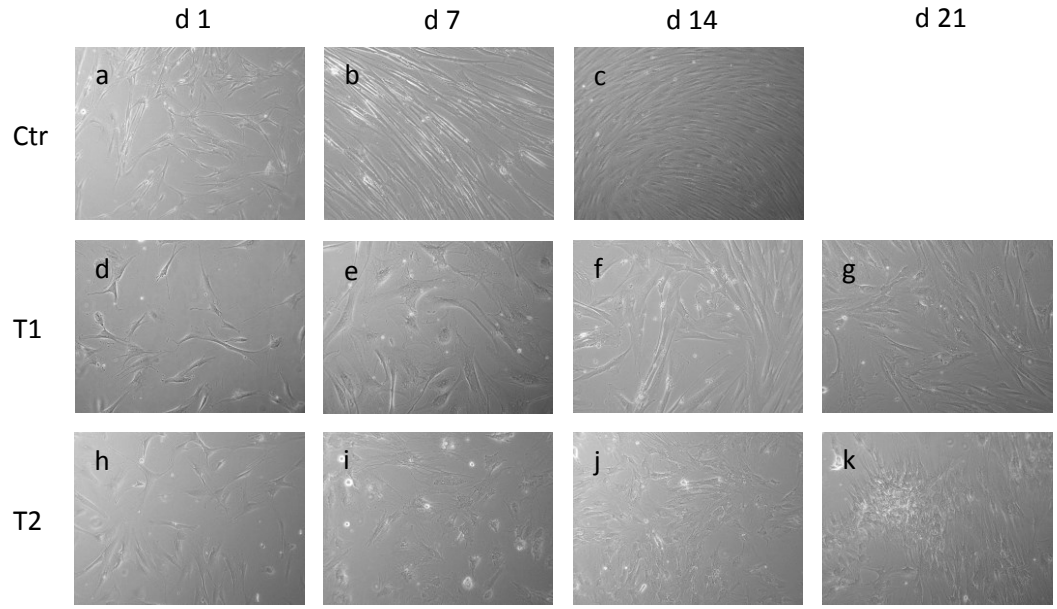

Figure 21 Morphological changes exhibited by the pig thymus-derived MSCs (d, h) during the differentiation into cardiomyocyte-like cells. Cells were treated with two different protocols, T1 and T2. Pictures were taken after 7, 14 and 21 days from induction with 5-Aza. Control untreated cells were compared to the treated ones (a, b, c). After two weeks of culture, the control cells reached confluence and the culture was stopped. The morphology of the treated cells changed gradually. At one week after induction, cells treated with T1 and T2 started to enlarge and a more elliptical shape was adopted (e, i). After two weeks of differentiation, treated cells showed cytoplasmic elongations and granularity typical of cardiac cells (f, j). At the end of the induction, some of the T2-treated cells were aggregated in colonies (k), while T1-treated cells maintained the elongated shape and few branches were observed between cells (g). Magnifications 100x.

3.2. Assessment of the differentiation by fluorescent immunocytochemistry

Monoclonal antibodies against cMYH, SαA and Des were used to analyse the expression of cardiac specific proteins in the human and porcine cells (respectively Figure 22; Figure 24). Untreated cells revealed an absence of staining for the examined antibodies. Human cells treated with all the three applied protocol were strongly positive for cMYH. Almost all the treated cells expressed the cardiac marker, which allow to visualize the striations typical of the sarcomeres of muscle cells. SαA was expressed by approximately 40% of the T1- and T2- differentiated cells. More positivity was detected in the T3-treated cells (about 50%). Several clusters of SαA-positive cells were observed, while individual cells expressing SαA were relatively rare. Desmin was detected to be highly expressed in the cells treated with all protocols. The fluorescent signal was strong and allowed to visualize the cells' cytoplasmic process and branches that connected the cells to each other's.

rCMs viability over the inserts was checked at the of the experiments with a live/dead staining assay. Most of the cells were viable after three weeks of culture and some beating cells were detected (Figure 23).

Immunostaining of the porcine cells revealed strong positivity for cMYH in the cells treated with all protocols. As for the human cells, nearly all the treated pTMSCs expressed the cardiac marker. The staining against SαA showed a lot of positive cells treated with T1 and T2, however the fluorescent signal was relatively weak in comparison with the other markers. Only a few T3-treated cells expressed SαA. High expression was detected for Des in most of the T2- and T3- treated cells. A slightly weaker fluorescent signal was observed in the T1-treated cells, though many pTMSCs were positive for the examined protein.

3.3. Evaluation of the gene expression

Three different cell lines were induced to differentiate into cardiomyocyte-like cells and three independent experiments were carried out for both human and porcine cells. Total RNA was isolated from treated and non-treated cells and analysed by RT-PCR. The expression of four cardiac-specific genes was investigated: GATA-4, ACTA1, DES and cMYH.

Regarding the human cells, the expression of the examined cardiac genes, strongly increased at the end of the differentiation (Figure 25). GATA-4 was significantly more expressed in the T3-treated cells in comparison with the untreated cells (5.3 times more). In T1- and T2- treated cells GATA-4 was respectively 3.2-fold and 2.7-fold more expressed than the control. The expression of ACTA1 increased in the committed cells but not much difference was observed between the three treatments. Although not statistically significant, data analyses indicated an increase of 5.7, 6.3 and 7.6 in the T1-, T2- and T3- committed cells respectively.

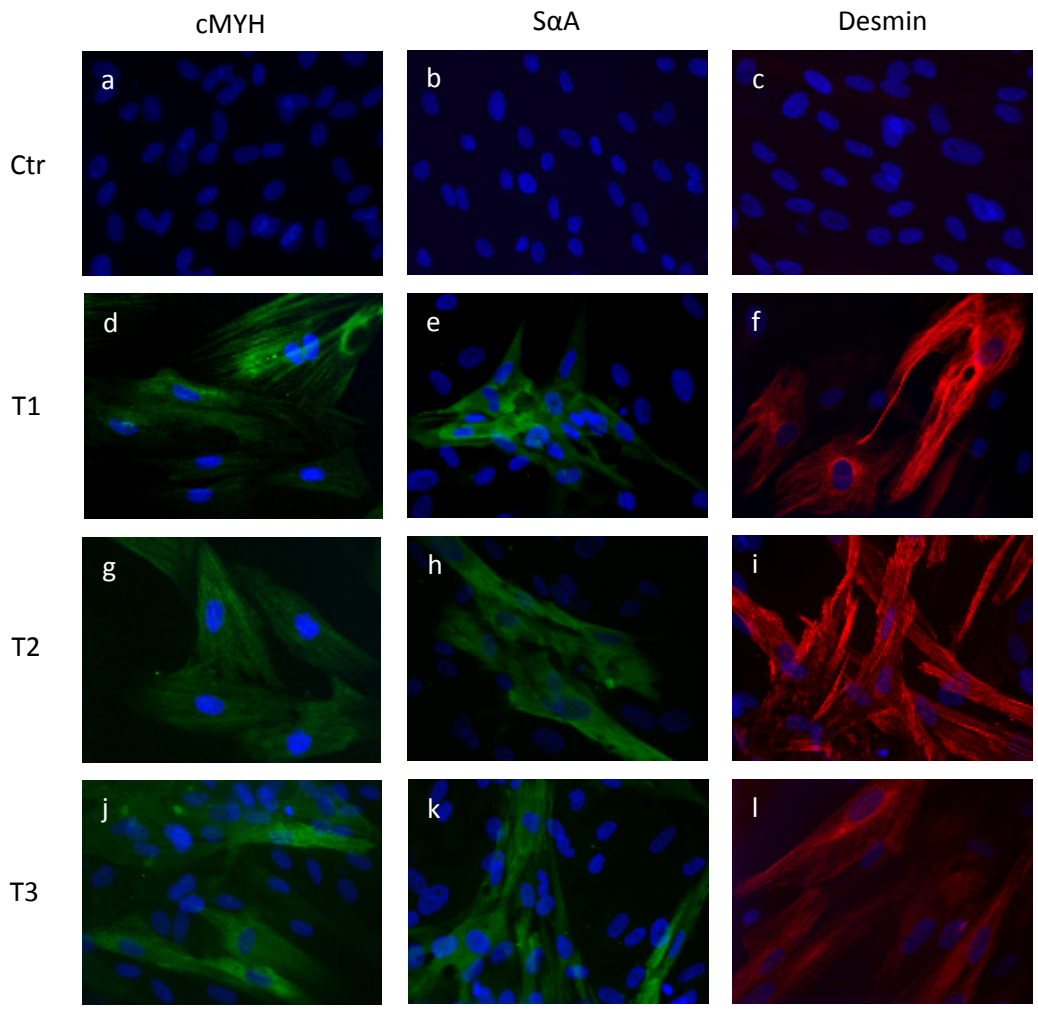

Figure 22 Immunofluorescent staining for cardiac Myosin Heavy Chain (cMYH, first column), Sarcomeric alpha-Actinin (SαA, second column) and Desmin (Des, third column) in the untreated human control cells (a, b, c); T1-treated (d, e, f); T2-treated (g, h, i) and T3-induced human cells (j-l). cMYH is indicated by green fluorescence and was strongly expressed by most of the treated cells. Clusters of positive cells were found for SαA (green fluorescence). Des was highly expressed by most of the differentiated cells (red fluorescence). Absence of staining for the three markers was detected in the control cells. Magnification: 200x.

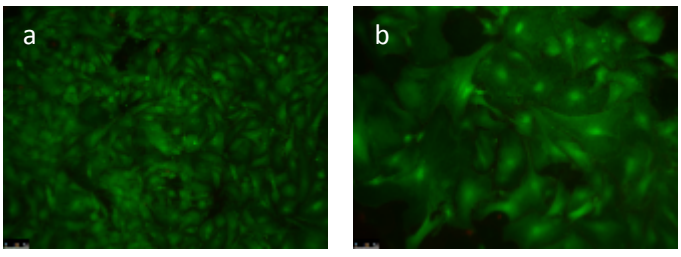

Figure 23 Live/Dead staning of rat cardiomyocytes cocultured with the MSCs. The assays showed viable cells growing on the inserts (green fluorescence). Many beating cells were found even after three weeks of culture. Very few dead cells were detected (red fluorescence). Magnification: 100x (a); 200x (b).

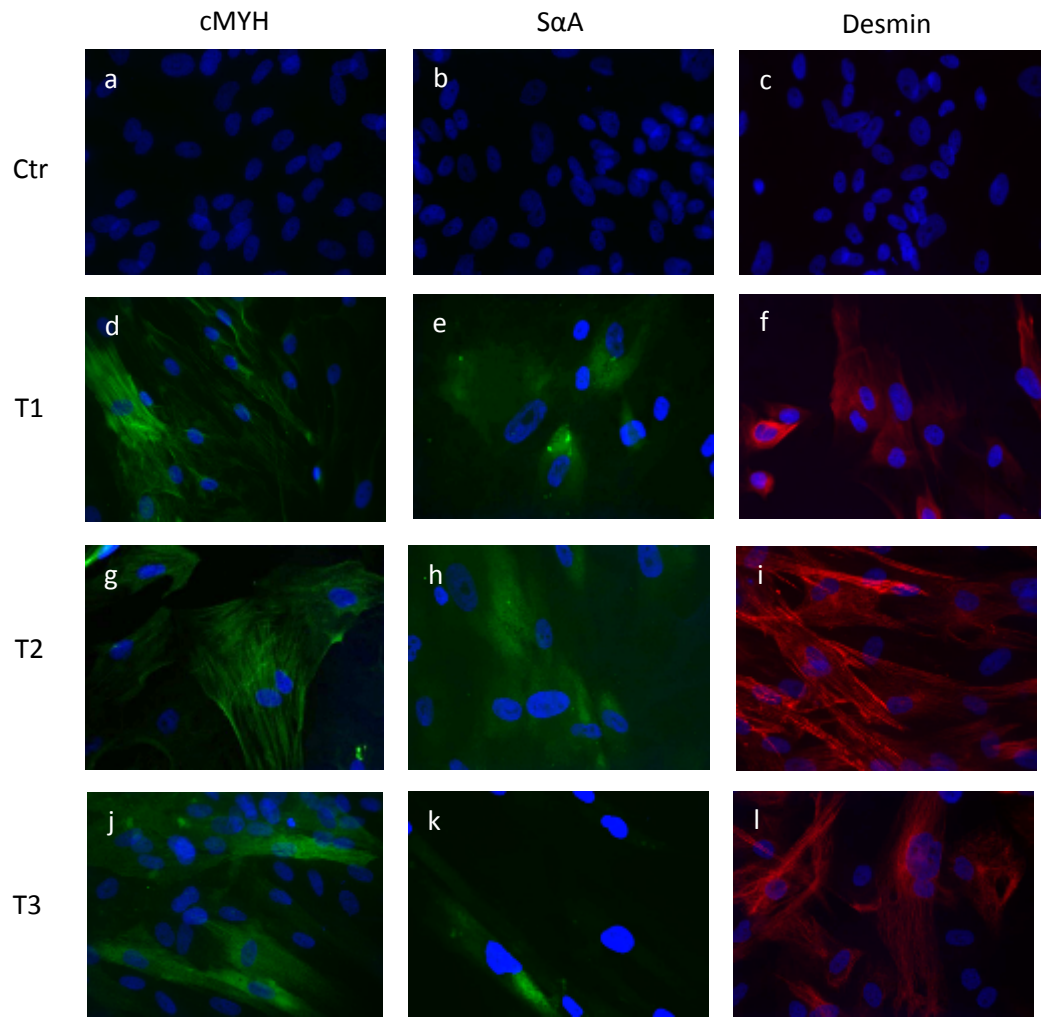

Figure 24 Fluorescent immunostaining for the proteins cardiac-Myosin Heavy Chain (cMYH, first column), Sarcomeric alpha-Actinin (SαA, second column) and Desmin (Des, third column) in the porcine untreated cells (a, b, c); T1-treated (d, e, f); T2-induced (g, h, i) and T3-treated pig cells (j-l). cMYH is shown by green fluorescence and was highly presented in most of the treated cells. Few positive cells were found for SαA and the fluorescent signal (green) was relatively weak. Des was strongly expressed by most of the treated cells (red fluorescence). No staining was detected in the control cells for the three cardiac markers. Magnification: 200x.

No statistical significance was observed between the treated and untreated cells, probably due to the high variability between each experiment. DES was significantly more expressed in the T2-treated cells then in the control cells (13.5 times more). Even though no statistical significance was observed, T1- and T3- induced cells increased 9.4-fold and 11.3-fold respectively. A higher expression level than the control was also found for cMYH. This gene was 6.8 times more expressed in the T1-treated cells and 4.2 and 5.3 times more expressed in the T2- and T3- treated cells respectively. In summary, T3-committed cells showed the highest expression of GATA-4 and ACTA1, while DES was most expressed by the T2-induced cells and cMYH by the T1-treated cells.

Because of the lack on the market of primers complementary to porcine cardiac genes, new primers were designed to recognize the same genes studied in the human cells. Two primer pairs were designed per each gene. The electrophoresis that followed the PCR, showed that both primer pairs recognized the genes GATA-4 and DES, while only one pair recognized ACTA1 and cMYH (Figure 27). As for the human cells, the expression of the examined gene strongly increased in the committed cells (Figure 26). T2-treated cells showed significantly higher expression of GATA-4 in comparison with the negative control (10.3 times more). Although not statistically significant, an increase of 5.8-fold and 8.7-fold was observed respectively for the T1- and T3- treated cells. ACTA1 was found to be 4.9 times more expressed in the T1-committed cells and 2.8 and 6.6 times more expressed respectively in the T2- and T3-induced cells. The expression of DES was significantly higher in both the T2- and T3- treated cells then the untreated (15-fold and 13.3-fold respectively). In T1-treated cells DES was found to be 7.4 times more expressed than the control. cMYH was significantly more expressed in the T3-induced cells (17.8 times more). An increase of 10.5-fold and 12.7-fold was detected for the T1- and T2-induced cells. In summary, T2-commetted cells showed the highest increase of GATA-4 and DES, while T3-induced cells exhibited the highest expression of ACTA1 and cMYH.

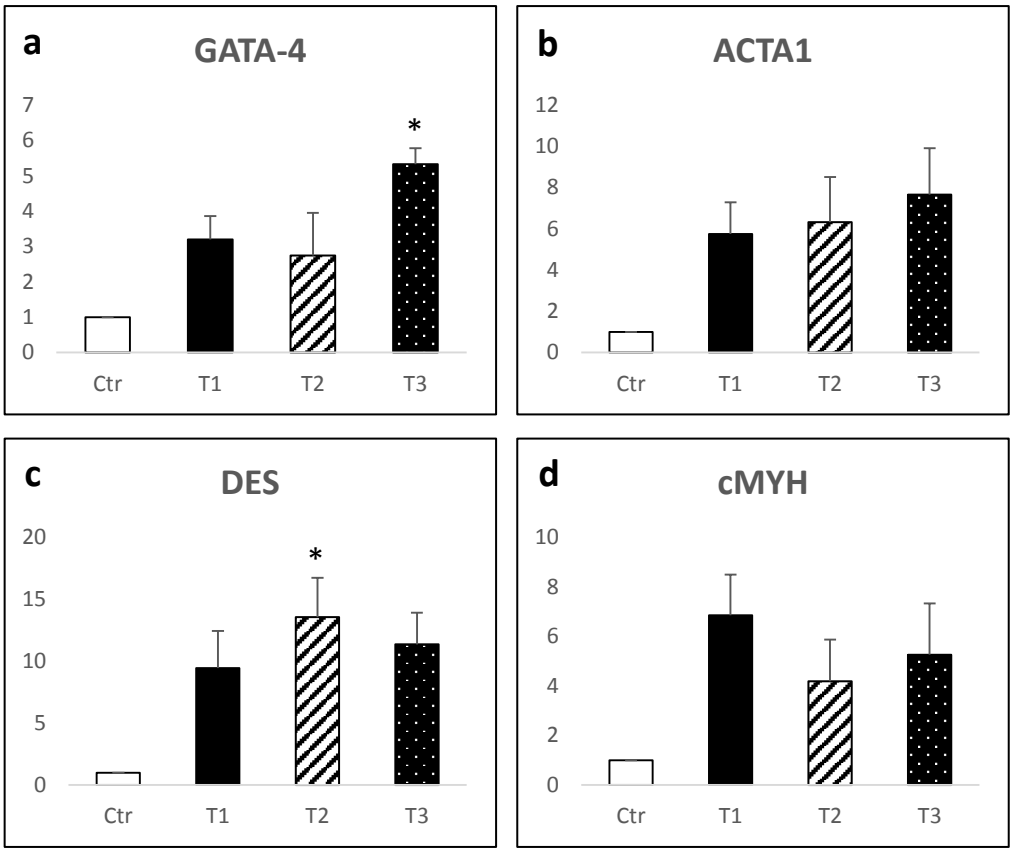

*Figure 25 Expression of cardiac-specific genes in the human cells at the end of the differentiation treatment. Untreated control cells (white bars) were compared to cells treated with protocol T1 (black bars), T2 (diagonal stripes) and T3 (white-on-black dotted bars). The expression of GATA-4 (a), ACTA1 (b), DES (c) and cMYH (d) was strongly higher in the cardiac-committed cells than in the control cells. Statistical significance was observed for GATA-4 in the T3-induced cells and for DES in the T2-treated cells. * $p < 0.05$; n=3.*

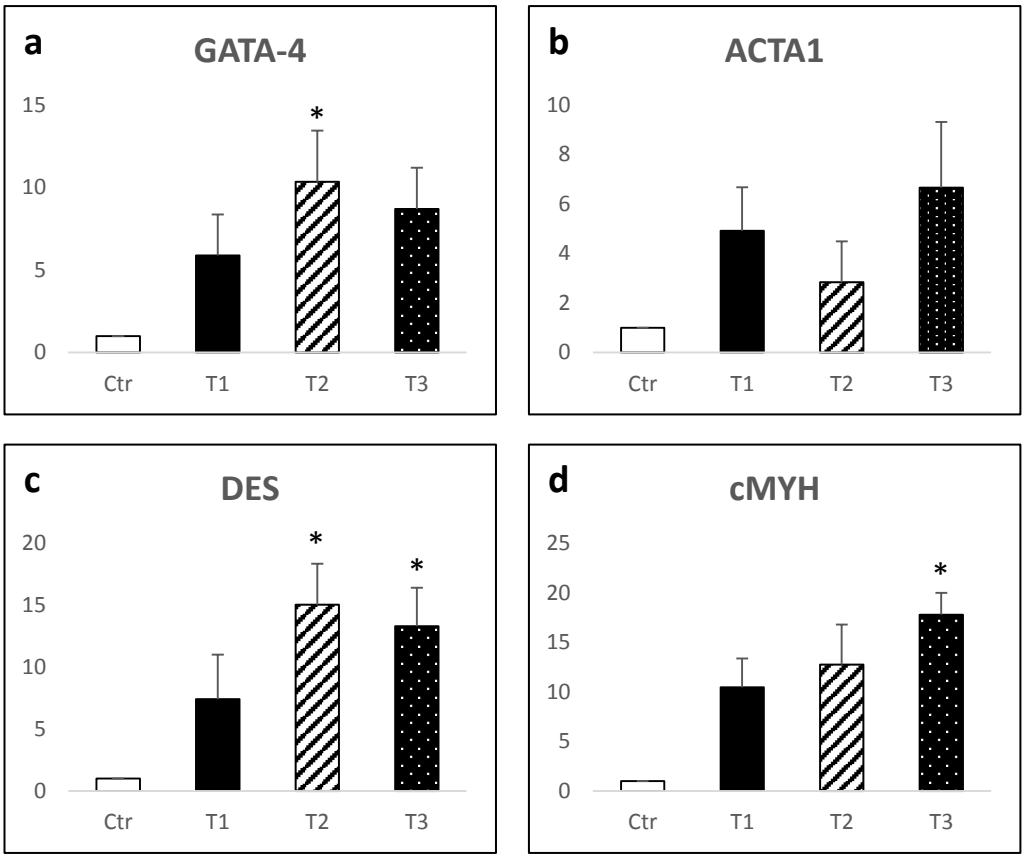

*Figure 26 Expression of cardiac-specific genes in the porcine-derived MSC at the end of the differentiation protocols. Untreated control cells (white bars) were compared to cells conditioned with protocol T1 (black bars), T2 (diagonal stripes) and T3 (white-on-back dotted bars). The expression of all the investigated genes, GATA-4 (a), ACTA1 (b), DES (c) and cMYH (d) was much higher in the differentiated cells in comparison with the undifferentiated cells control. Statistically significance difference was found for GATA-4 in the T2-treated cells, for DES in the T2- and T3-induced cells and for cMYH in the T3-treated cells. * $p < 0.05$; n=3.*

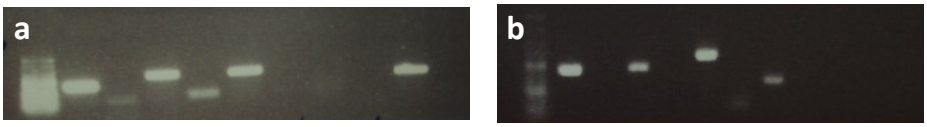

Figure 27 Gel electrophoresis of the PCR-amplification products of the cDNA isolated from porcine myocardium and subsequently recognized and amplified by the designed porcine primers. In the first gel (a) samples were loaded as follow (from left to right): 18s, neg ctr, GATA-4 I, neg ctr, GATA-4 II, neg ctr, ACTA1 I, neg ctr, ACTA1 II, neg ctr (a). In the second gel (b) samples were loaded in the following order (from left to right): DES I, neg ctr, DES II, neg ctr, MYH I, neg ctr, MYH II, neg ctr.

4. GENERATION OF DECELLULARIZED SCAFFOLDS

4.1. Characterization of the acellular pericardium

Two decellularization protocols were applied to decellularize the porcine pericardium. The first protocol was based on a treatment with the enzyme Trypsin, while the second one was based on a treatment with the detergent Triton-X. Both treatments were followed by a digestion with a nuclease. During the decellularization process the pericardial membranes turned completely white, suggesting that blood and cellular content were removed. In order to access the effect of the two protocols on ECM structure and components, histological analyses and SEM were performed. Native porcine pericardium was used as positive control. Histological findings from H&E staining demonstrated that both decellularization treatments were successful as there was no evidence of whole cells or cell fragments in the tissue sections (Figure 28). Examination of the samples stained for elastin and collagen (EVG) showed that the major histoarchitecture of the ECM had been retained in both the Try- and TX-decellularized pericardia. AB staining confirmed that the GAG content was unaltered in the decellularized tissues. In addition, it did not appear to be a significant difference between the native tissue and the decellularized ones in terms of remaining GAG and collagen tissue content. All the histological stainings showed that the TX-decellularized pericardium was more compacted than the Try-decellularized one. Furthermore, it seemed that the detergent TX removed the adipose tissue present within and/or outside the pericardial membrane more efficiently than did the enzyme. SEM images demonstrated that the morphology of the decellularized tissues was not altered by the applied protocols, indicating that the ECM was well preserved after the decellularization treatments.

Both protocols were successful in removing all cellular and nuclear materials from the pericardium, retaining the composition and morphology of the cardiac matrix.

4.2. Evaluation of the acellular myocardium

Pieces of porcine myocardium were decellularized using a SDS/TX- protocol. After 3 days of treatment, the pieces of myocardium showed a whitish coloration, suggesting that blood and cellular content were removed. Histological stainings confirmed that a

total decellularization was achieved as no cellular or nuclear materials were detected (Figure 29). Native porcine myocardium was used as positive control. Histological and SEM analyses of the decellularized tissue confirmed that a complete decellularization was achieved as no presence of cells was detected and the ECM structural components remained intact. Examination of the sections stained for H&E showed a complete lack of nuclei and myofibers within the decellularized tissue. Histological findings from the EVG staining demonstrated that the acellular myocardium was a collagen-rich tissue with fibers of elastin, implying that the ECM was well preserved after the treatment. The AB staining showed the presence of a large amount of GAG left in the matrix, suggesting that the major histoarchitecture of the ECM was retained. SEM examination of the treated tissues, confirmed that the cardiac surface was denuded of cells, while the reticular network of the ECM was retained intact. These results established the efficiency of the developed protocol in removing the cellular and nuclear content from the tissue and at the same time preserving the composition and structure of the cardiac matrix.

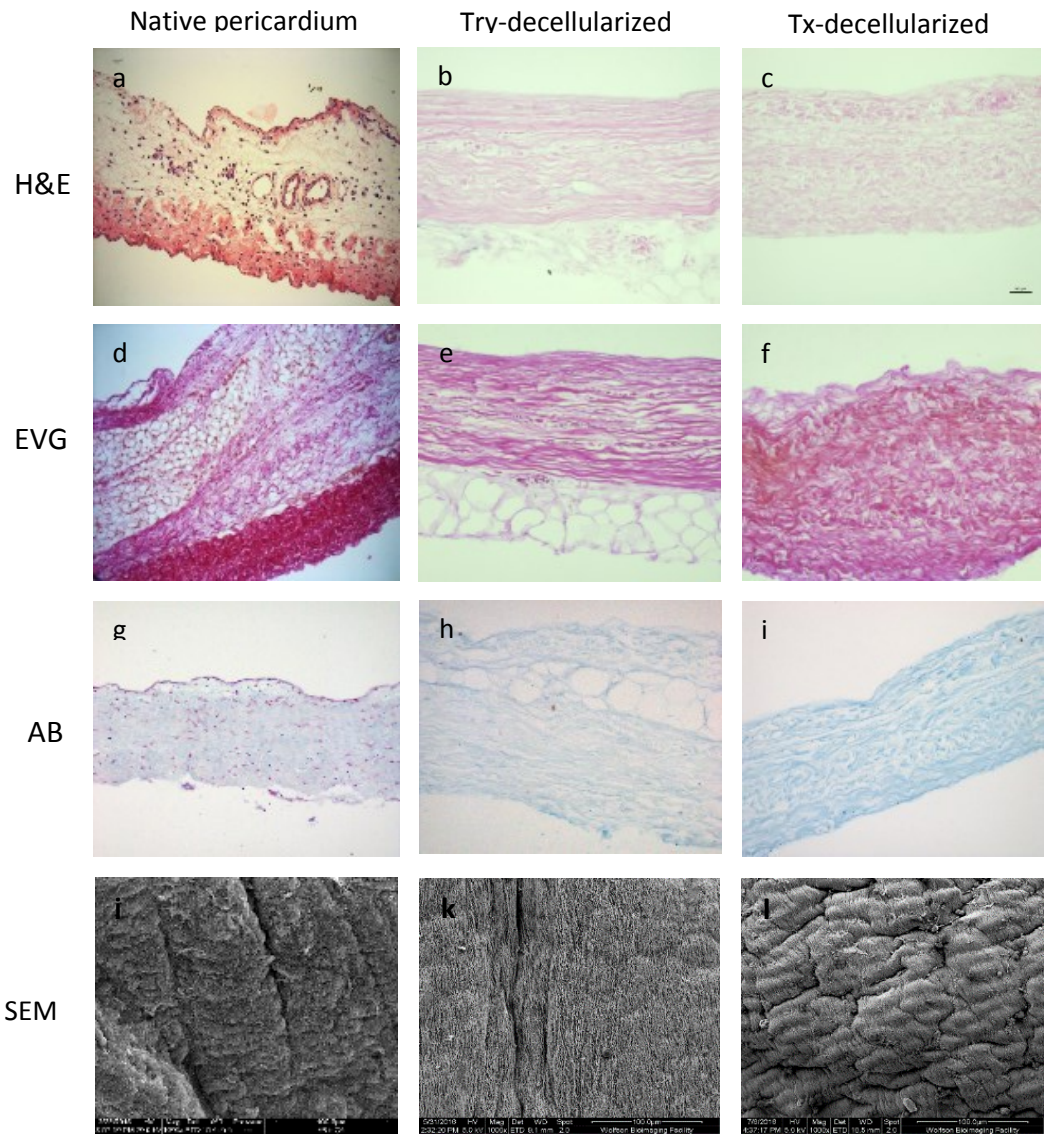

Figure 28 Successful decellularization of porcine pericardia with Trypsin or TritonX. The histological stainings of the native pericardium showed a tissue rich in collagen and GAG, constituted of a dense cellular content (a, d, g). As shown in the H&E staining of the decellularized tissues, all cellular and nuclear materials were removed from the tissues (b, c). EVG stainings demonstrated that the ECM remained intact after the treatments and the collagen content did not differ from the native tissue (e, f). AB staining illustrated that the GAG were retained in the decellularized tissues (h, i). SEM images confirmed that the cellular components were absent from the surface of the decellularized pericardia (k, l). No major differences were observed between the matrix of the native pericardium and that of the decellularized tissues (j-l). Magnifications: 200x (a-i); 1000x (j-l).

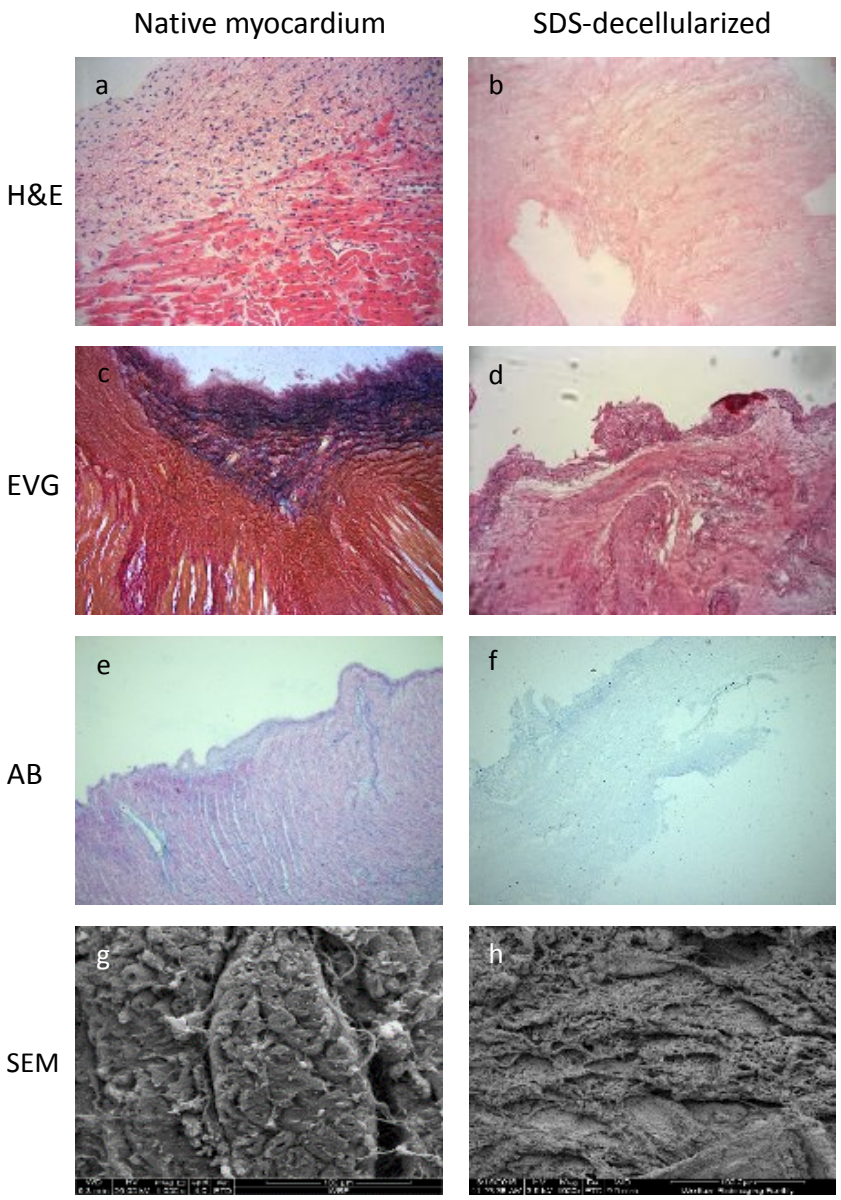

Figure 29 Successful decellularization of porcine myocardium was achieved with SDS. As shown in the H&E histological staining, all cellular and nuclear components were removed from the native tissue and a pale pink matrix was obtained at the end of the treatment (a, b). EVG examination illustrated that collagen (pink) and elastin (purple) were retained after the decellularization (c, d). In the AB histological staining it was observed that the GAG content of the myocardium has not been altered (e, f). The morphology of the native and decellularized myocardium was analysed with the SEM, which confirmed that the surface of the decellularized tissue was clear of cells and the ECM fibers were retained in the treated tissue (g, h). Magnifications: 200x (a-f); 1000x (g, h).

5. EVALUATION OF THE SEEDING POTENTIAL OF DECELLULARIZED SCAFFOLDS AND A CLINICAL GRADE-GRAFT

Human thymus-derived MSCs were seeded onto the Try- and TX-decellularized pericardia, on the SDS-decellularized myocardium and on the clinical-grade graft CorMx. Differentiated (cardiac-like) and undifferentiated MSCs were tested for their ability to adhere and proliferate onto the decellularized tissues.

5.1. Recellularization of acellular pericardium

With the aim to identify the protocol that generates the most suitable scaffold for the development of a cardiac patch, the histological, morphological and biocompatibility properties of the Try- and TX-decellularized pericardia, were investigated. At this stage of the study, the most important criteria to evaluate was the biocompatibility of the scaffolds. After two weeks of culturing the cells over the decellularized pericardia, the constructs were analysed with histological stainings, SEM and viability/cytotoxicity assay.

The H&E staining revealed a monolayer of hTMSCs growing over the Try-decellularized pericardium (Figure 30). No cells were found deep in the tissue. The diff-hTMSCs have adhered in a similar way as a single layer of cells was growing on the surface of the tissue. The AB staining confirmed the presence of GAG within the acellular tissue and the undifferentiated and differentiated cells growing on top of the Try-treated scaffolds. In agreement with the histological analyses, the results of the SEM indicated that the cells were attached and well distributed on the surface of the tissues. A confluent layer of cells was observed for both cell types. This monolayer was found to be made of aligned undifferentiated cells, while the diff-hTMSCs did not align themselves over the scaffold. In addition, SEM images confirmed that the morphology of the two cell lines was significantly different. hTMSCs exhibited an elongated shape, while the diff-hTMSCs had a more elliptical shape, being wider and shorter than their undifferentiated progenitors. The viability/cytotoxicity assay demonstrated that most of the cells growing on top of the scaffolds were alive. Very few dead cells were detected.

Histological findings from the H&E staining of the TX-decellularized-reseeded pericardium revealed that both hTMSCs and diff-hTMSCs grew on the acellular tissue (Figure 31). Examination of the section stained with EVG and AB confirmed that both cell lines engrafted on to the TX-decellularized pericardium as a clear layer of cells was visible on top of the scaffolds. No cells penetrated within the tissue but in some area they proliferated into multilayers. In addition, hTMSCs appeared to grow more than the diff-hTMSCs, as a thicker layer of cells was observed. Cell morphology was verified by SEM analyses, which showed high affinity of the both cell types for the TX-decellularized tissue. Indeed, a confluent and oriented layer of cells was growing on the surface of the scaffold. In comparison with the Try-decellularized pericardium, a denser layer of cells seemed to be present on the TX-decellularized pericardium. The viability assay demonstrated that the layer of hTMSCs and diff-hTMSCs was mainly made of viable cells. Only few dead cells were observed. The assay also confirmed that the undifferentiated cells proliferated more than the differentiated ones. Additionally, it appeared that both cell lines had a stronger affinity for the TX-decellularized pericardium in comparison with the Try-decellularized pericardium.

5.2. Recellularization of acellular myocardium

To investigate the reseeding potential of the SDS-decellularized myocardium and the interaction between the scaffolds and the cells, histological analysis and SEM were performed. H&E staining was performed in order to visualize the distribution of the hTMSCs and diff-hTMSCs into the developed scaffolds (Figure 32). Few cells adhered the decellularized myocardium and penetrated deeper in the tissue. The EVG staining of the reseeded tissue showed an amount of elastic fibers similar to the unseeded. The AB staining displayed the presence of several nuclei of hTMSCs engrafted in the tissue, while a smaller amount of diff-hTMSCs was found in the scaffold seeded with the committed cells.

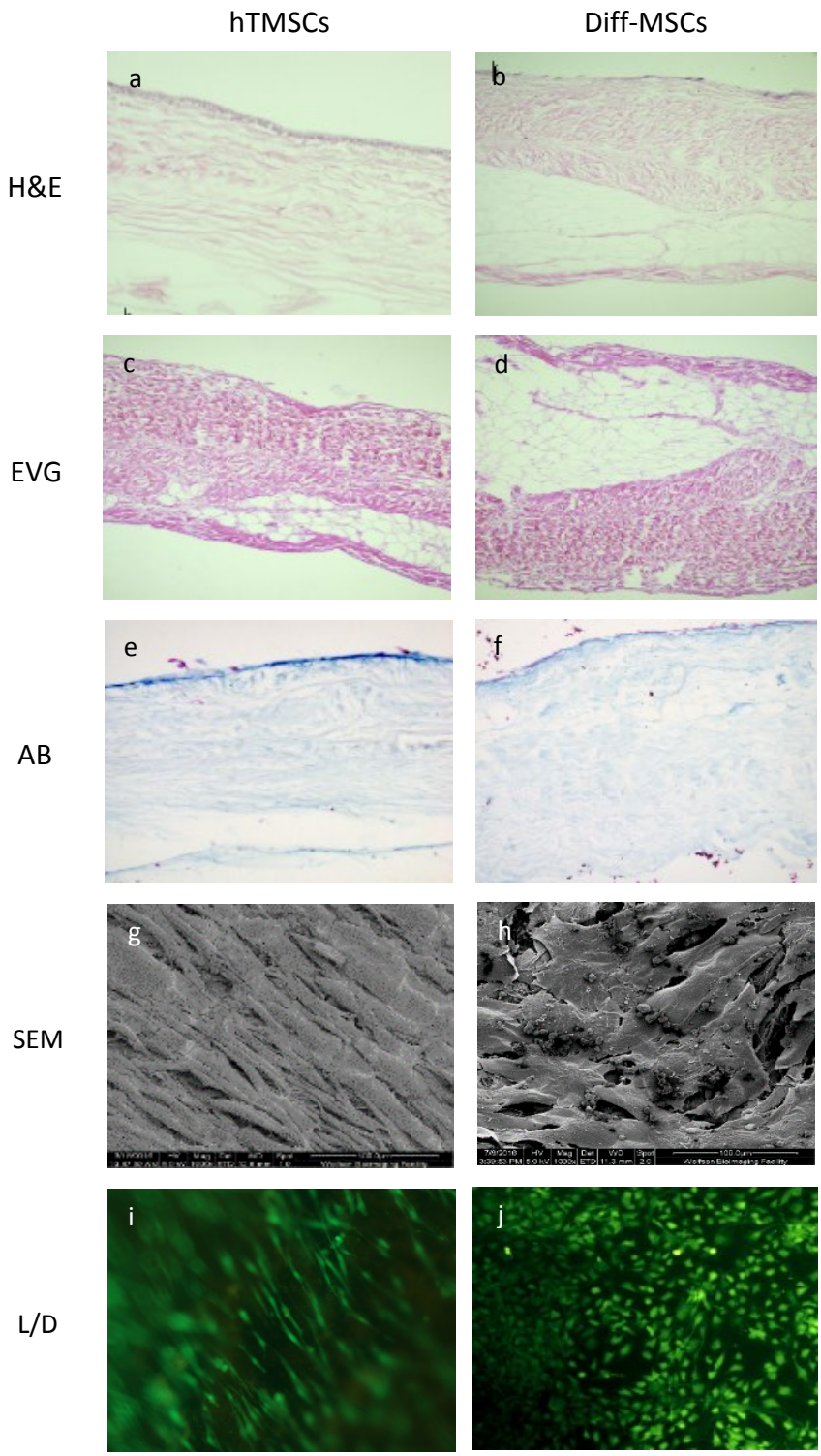

Figure 30 Recellularization of Try- decellularized pericardium with undifferentiated (hTMSCs) and cardiac-committed cells (diff-MSC). The H&E staining showed a well-defined layer of cells growing over the acellular scaffolds that were coloured in purple (a, b). The EVG staining confirmed the composition of the Try-decellularized pericardium as a tissue mainly made of collagen (c, d). The layer of cells was observed in the AB staining, where they were coloured in bright blue with pink dots (e, f). SEM images illustrated that the hTMSCs proliferated into a confluent and oriented monolayer, while the diff-MSCs did not arrange themselves into an oriented layer of cells (g, h). Live/Dead assay confirmed that most of the attached cells were alive (green fluorescence) over the scaffolds. Only a few dead cells were detected (red fluorescence) (i, j). Magnifications: 200x (a-f); 1000x (g, h); 100x (I, j).

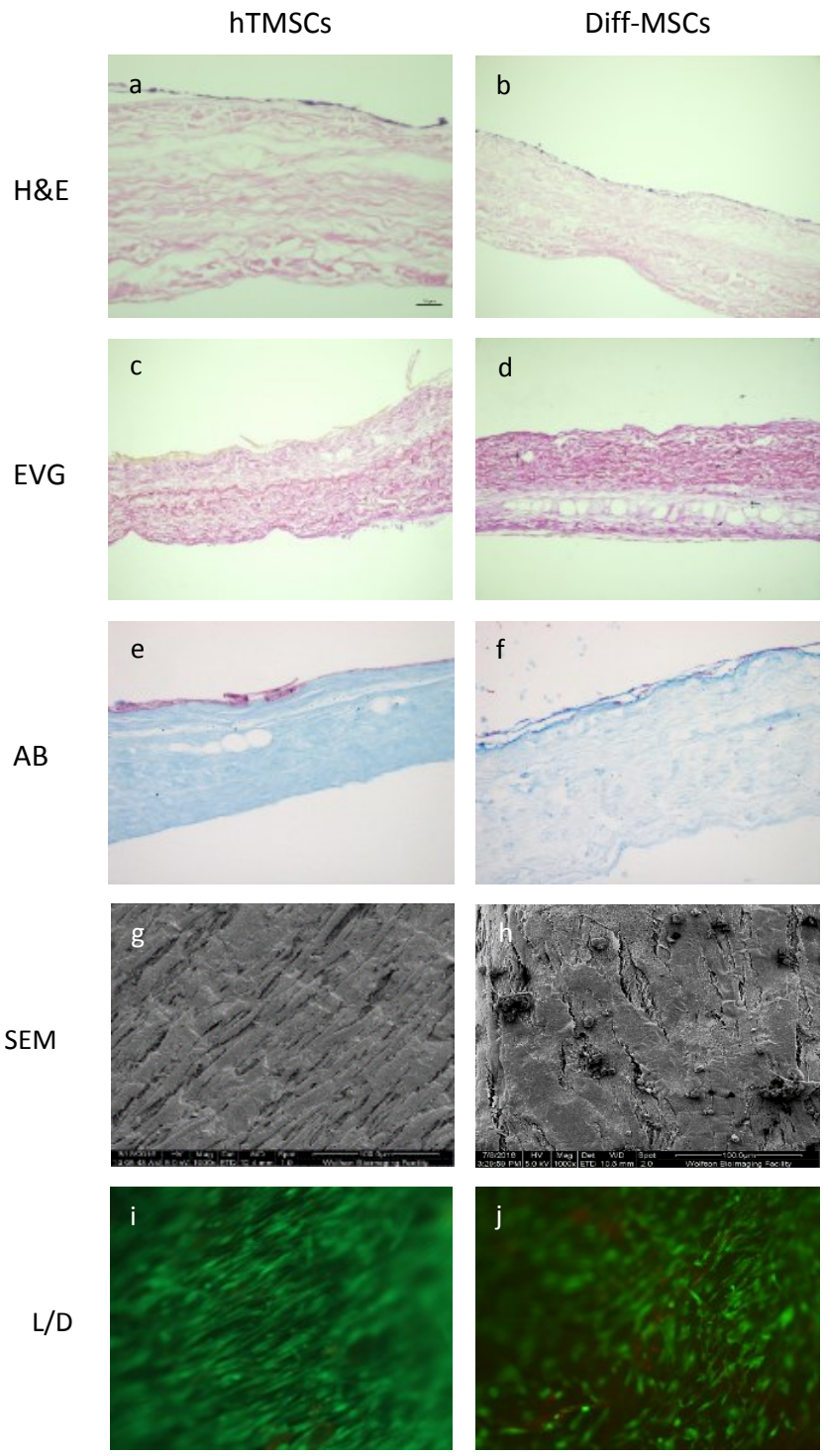

Figure 31 Recellularization of TX- decellularized pericardium with undifferentiated (hTMSCs) and cardiac-like cells (diff-MSC). The H&E staining showed a clear layer of blue nuclei growing over the tissue (a, b). EVG staining displayed the same cell layer in a pink/yellowish colour (c, d). AB staining confirmed the presence of GAG within the TX-decellularized pericardium and showed the cell layer coloured in pink (e, f). SEM images demonstrated that both cell lines proliferated into a confluent and oriented monolayer (g, h). The cardiac committed cells appeared to be shorter and wider than the undifferentiated cells. Live/Dead assay confirmed that the majority of the engrafted cells were alive (green fluorescence) over the scaffolds and just a few dead cells were detected (red fluorescence) (i, j). Magnifications: 200x (a-f); 1000x (g, h); 100x (i, j).

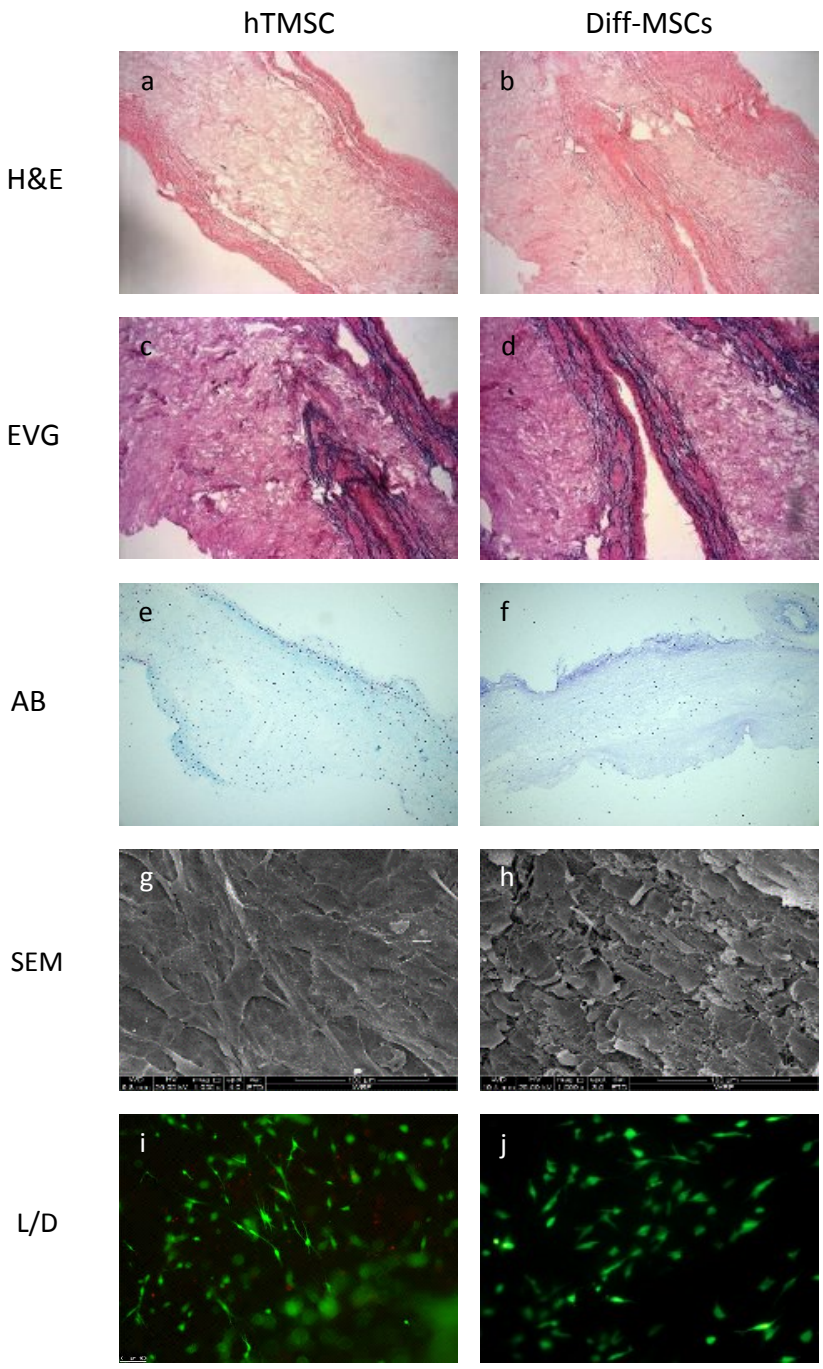

Figure 32 Recellularization of the SDS-decellularized myocardium with undifferentiated and cardiac-like cells (hTMSCs and diff-MSCs respectively). The H&E staining showed the presence of few hTMSCs and diff-MSCs growing on the acellular tissue (a, b). EVG staining confirmed the composition of the reseeded tissue, illustrating abundance of collagen and elastic fibers (c, d). Engrafted cells were also detected with the AB staining that illustrated several nuclei on the surface of the scaffold, as well as deeper in the tissue (e, f). SEM pictures demonstrated that both cell types adhered and proliferated over the scaffolds. The Live/Dead assay identified the majority of the seeded cells as alive (green fluorescent). Some dead undifferentiated cells were detected (red florescent) (i, j). Magnifications: 200x (a-f); 1000x (g, h); 100x (i, j).

SEM examination of the reseeded decellularized myocardium, confirmed the affinity of both cell lines with the scaffold. After two weeks of culture cells did not proliferate as much as they did over the decellularized pericardia. However, the viability/cytotoxicity assay demonstrated that most of the attached cells were viable over the acellular myocardium. Less dead differentiated cells were found on the surface of the tissue in comparison with the undifferentiated MSCs.

5.3. Cell seeding on a clinical-grade scaffold

The seeding potential of CorMx, a decellularized xenograft material, was similarly investigated. When we first started using the CorMx as scaffold to grow our cells, the material was completely acellular. H&E and DAPI stating of the unseeded CorMx showed absence of nuclei within the matrix, indicating that the decellularization process was successfully performed (Figure 33 a, c). However, over the time, we noticed that some lots of CorMx had a leftover of the cells within the material suggesting that the decellularization process was not complete (Figure 33 b, d). When we asked the manufacturer, we learned that the material is not completely acellular. However they guaranteed that any remaining cellular materials within the CorMx will not trigger an immune response in the humans. Since no issues have been reported from the clinical fields, we kept on using this material to develop cardiac-patch, even though not 100% acellular.

Differentiated and undifferentiated hTMSCs were seeded at high density on the CorMx and cultured for two weeks under static conditions. Successful recellularization of the material was illustrated with histological stainings, SEM and viability/cytoxicity assay. Examination of the engineered patches with H&E illustrated the presence of a clear layer of cells growing on the scaffold (Figure 34). No major differences were observed in regards to how the two cell lines have engrafted the material. EVG staining confirmed the presence of the cells growing over the CorMx by showing the very same layer with a yellowish colour. Analysis of the engineered patches with a SEM, demonstrated that the hTMSCs developed a confluent and monolayer of cells (Figure 35). SEM images of the seeded diff-hTMSCs showed that the committed cells did not reach confluency yet. However they established several contacts with the neighbour cells and according to their morphology, they seemed to be healthy. The viability of the seeded cells on the scaffolds was detected using a fluorescent viability/cytotoxicity assay, which

demonstrated that most of the undifferentiated and differentiated MSCs were viable on the CorMx (Figure 36).

In addition, dynamic conditions were applied to the engineered-CorMx. Differentiated and undifferentiated human MSCs and undifferentiated porcine MSCs, were cultured for one week under static conditions, followed by a week under dynamic conditions. The seeded CorMx was grown in a bioreactor to ensure maintenance of stability, sterility and the perfusion of culture media uniformly through the scaffold. From the H&E analyses of the engineered CorMx, a thick multilayer of purple nuclei was observed on the scaffolds seeded with all the three cell types (Figure 37). Few cells were observed within the CorMx but it was not clear if those nuclei belonged to the seeded cells or to the nuclei left over from the incomplete decellularization of the material. The EVG staining confirmed the presence of the cells growing on the matrix, which was coloured in pink for the hTMSCs and in yellowish for the diff-hTMSCs and pTMSCs. The pink coloration of the human undifferentiated cells may imply that those cells started to produce their own ECM made of collagen. Examination of the patches under SEM, showed a confluent layer of hTMSCs, diff-hMSCs and pTMSCs growing on the surface of the CorMx. Undifferentiated human and porcine cells were also aligned in the same direction, while the cardiac-committed cells were less organized (Figure 38). Cell viability on the surface of the scaffolds was demonstrated using a viability/cytotoxicity assay. In comparison with the engineered patches grown under static conditions, it appeared that these cells were more aligned, suggesting that the bioreactor helped the cells to organize into an orientated pattern (Figure 39).

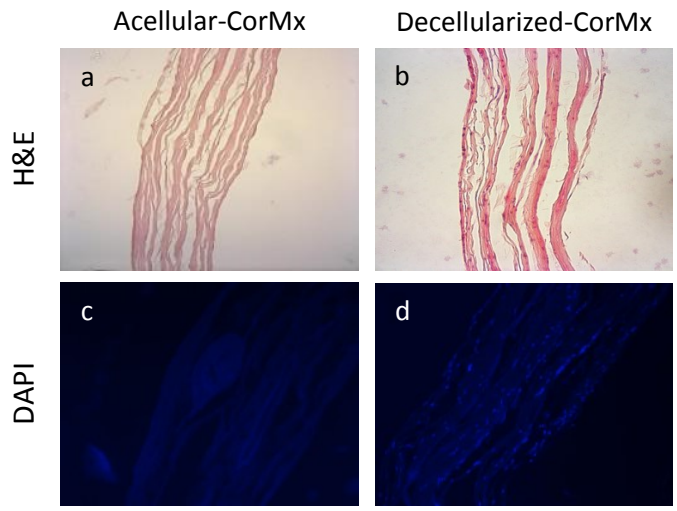

Figure 33 Unseeded CorMx stained for H&E (a, b) and DAPI (c, d). In the old lots of CorMx no nuclei were detected in the material, indicating that a fully decellularization was achieved. Some of the new lots of CorMx had a leftover of nuclei dispersed in the scaffold, indicating that the material was not fully acellular. Magnification: 200x.

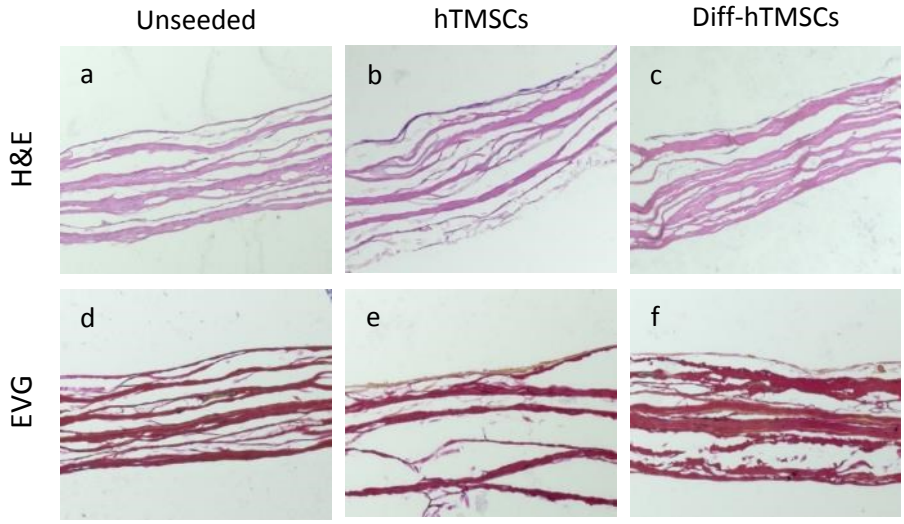

Figure 34 Histological analysis of the CorMx unseeded and engineered with undifferentiated and differentiated human thymus-derived MSCs that were cultured for two weeks under static conditions. H&E and EVG stainings showed absence of nuclei in and over the unseeded scaffold (a, d). The histological stainings of the hTMSCs-engineered CorMx demonstrated a thin layer of cells growing on the surface of the scaffold that was coloured in blue and yellow respectively in the H&E (b) and EVG staining (e). Cell engraftment was also observed on the surface of the CorMx engineered with cardiac-like cells that appeared blue and yellow respectively in the H&E (c) and EVG staining (f). Magnification: 200x.

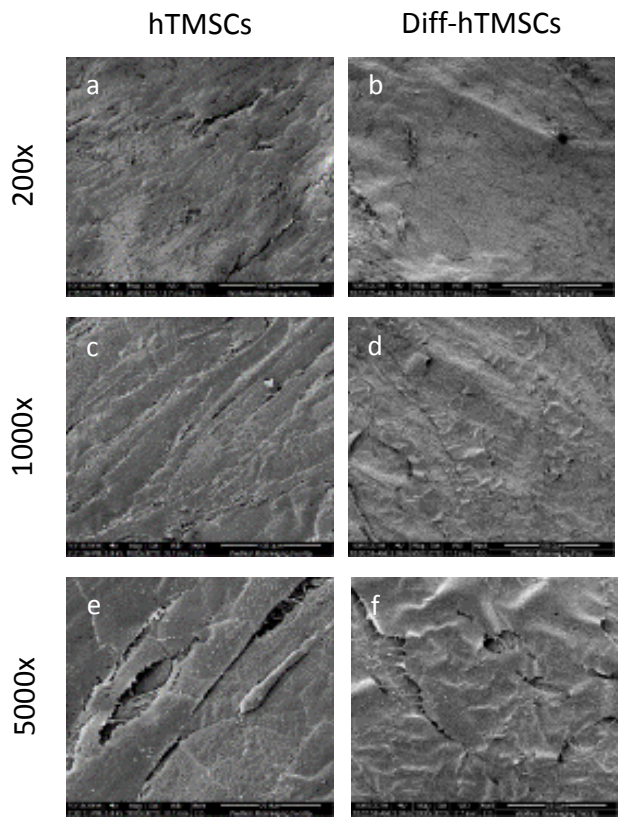

Figure 35 Scanning electron microscopy images of the CorMx seeded with undifferentiated (hTMSCs) and cardiac-committed cells (diff-MSC) that were cultured for two weeks under static conditions. (a, c, e) The hTMSCs attached and proliferated on the surface of the scaffold giving rise to a confluent and oriented carpet of cells. (b, d, f) The diff-MSCs grew on the scaffold but without reaching a confluent layer. Magnifications: 200x (a, b); 1000x (c, d); 5000x (e, f).

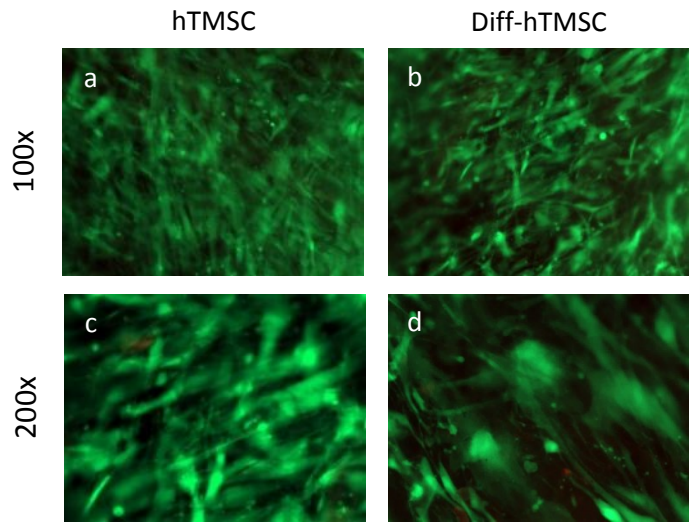

Figure 36 Live-cells imaging analysis of the undifferentiated (a, c) and differentiated MSC (b, d) viability on the CorMx cultured under static conditions. In the representative fluorescence images, live cells were indicated by the green fluorescence, while very rare dead cells were represented by red fluorescence. Cells were not organized in an oriented fashion, in fact they were growing with random orientations. Magnifications: 100x (a, b); 200x (c, d).

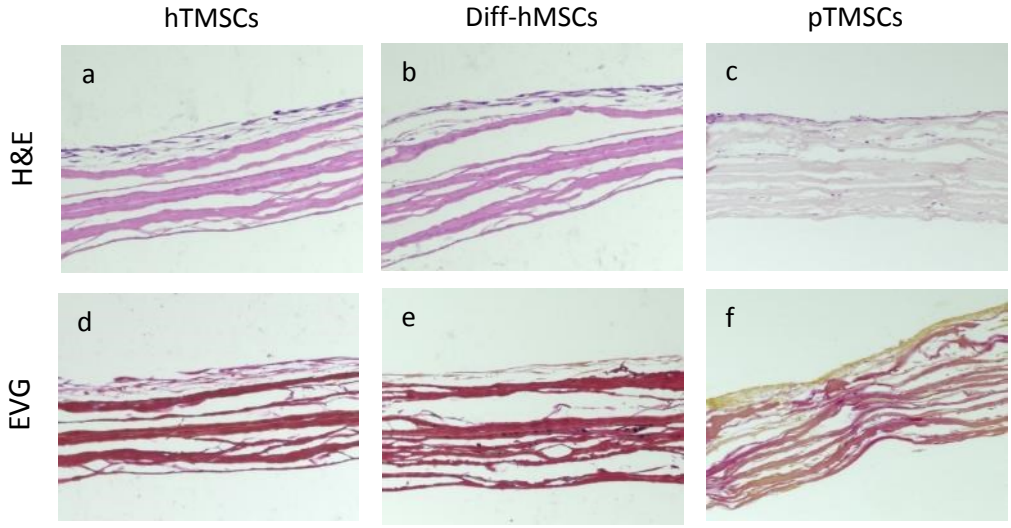

Figure 37 Histological examination of the engineered-CorMx grown for one week under static conditions and one week within a rotating bioreactor. The hTMSCs, diff-MSC and the pTMSCs seeded onto the CorMx successfully engrafted the scaffolds. The H&E stating showed a thick blue multilayer of both undifferentiated and differentiated human cells growing over the CorMx (a, b respectively). EVG analysis confirmed the presence of the cells showing a pink and yellow layer of hTMSCs (d) and diff-MSCs (e) respectively. The pTMSCs-engineered CorMx exhibited a thick and dense layer of cells growing on top of the scaffold. H&E staning showed a blue layer of cell nuclei (c) while in the EVG staining the layer appeared to be yellow (f). Magnification: 200x.

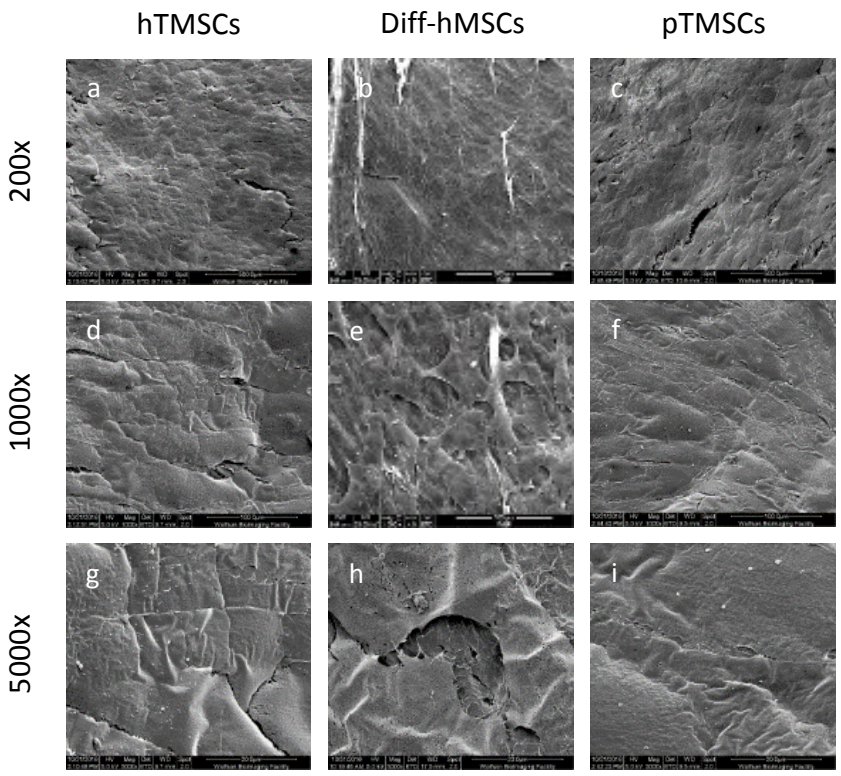

Figure 38 Scanning electron microscopy images of the CorMx seeded with undifferentiated (hTMSCs), human cardiac-committed MSC (diff-MSC) and porcine MSC (pTMSCs) cultured for one week under static conditions and one week under dynamic conditions. (a, d, g) The hTMSCs engrafted the scaffold and arranged themselves into a confluent and aligned layer of cells. (b, e, h) The diff-hMSCs grew on the surface of the CorMx and established several contacts with the adjacent cells (c, f, i). The pTMSCs proliferated on the scaffold giving rise to a confluent and oriented carpet of cells. Magnifications: 200x (a, b); 1000x (c, d); 5000x (e, f).

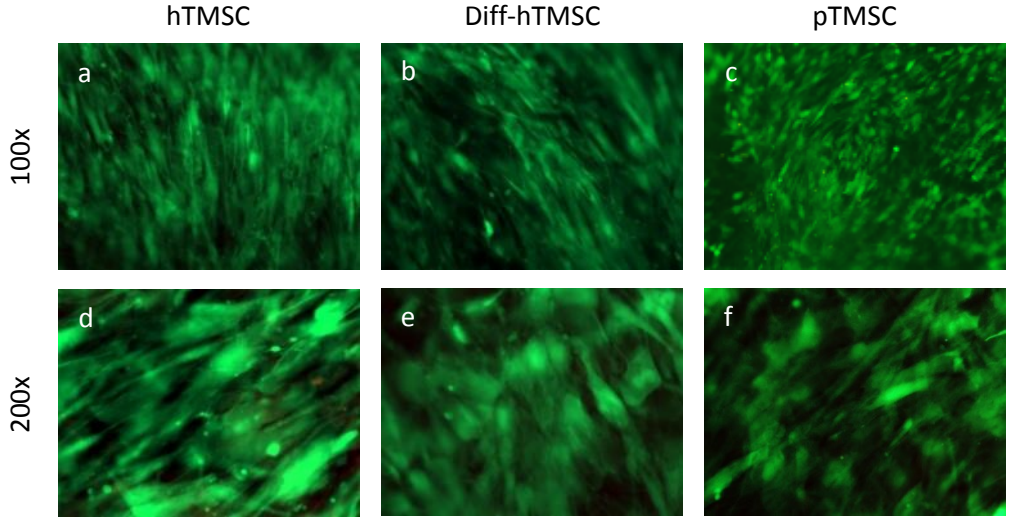

Figure 39 Live/Dead assay of the hTMSC-, diff-hMSC- and pTMSC -engineered CorMx cultured for one week under static conditions and one week in a rotating bioreactor. All the three cell types were viable on the surface of the scaffold, as shown by the green fluorescence. Very few dead cells were observed (red fluorescence). Human-derived cells appeared to be more organized then the porcine cells, as most of them were aligned in the same orientation. Magnifications: 100x (a, b, c); 200x (d, e, f).

CONCLUSIONS

Human and porcine MSCs were efficiently isolated from the thymus gland and expanded in vitro. The characterization of their surface markers demonstrated that the cells expressed all the main mesenchymal antigens. Additionally, a functional characterization confirmed that both cell lines were capable to differentiate into cells of the osteogenic, adipogenic and chondrogenic lineage, validating our isolation protocol of thymus-derived MSCs. Human and porcine cells successfully differentiated into cardiac-like cells. Thus, committed cells expressed cardiac-specific proteins and genes, whereas non-differentiated cells were negative for all the cardiac markers.

All cellular and nuclear materials were efficiently removed from the porcine pericardia and myocardia, while the ECM structure and composition were well preserved. The acellular scaffolds showed good biocompatibility properties. Indeed both the undifferentiated and differentiated MSCs seeded onto the scaffolds engrafted and proliferated on the surface of the materials. The TX-decellularized pericardium appeared to be the optimal scaffold in terms of preservation of the ECM and recellularization potential. Furthermore, the seeding potential of CorMx has been shown to allow cell's engraftment and growth with high efficiency, especially if the construct is cultured under dynamic conditions.

In conclusion, viable grafts have been developed using MSCs isolated from the thymus gland and scaffolds either generated through the decellularization of xenogeneic materials or available on the market.

CHAPTER 2: IN VIVO STUDY

OBJECTIVES

The purpose of the in vivo study was to establish a juvenile swine model suitable for testing the safety and feasibility of using engineered grafts for the RVOT reconstruction. Cell-seeded patches need to be tested in vivo in order to verify their strength, durability and biocompatibility. We aimed to implant the heart with either engineered patches or unseeded control scaffolds through a recovery CPB procedure, mimicking as close as possible the human surgical settings. We intended to recover the animals and to monitor their cardiac function with doppler echocardiography. Four months post-surgery we explanted and analyse the grafts in order to verify if angiogenesis, remodelling and regeneration occurred. We hypothesized that the engineered patch might trigger such processes better than the non-viable graft.

A swine model of CPB was established to assess the safety and practicability of the in vivo implantation of the engineered-CorMx. The cells used to engineer the scaffold were MSCs isolated from the thymus gland of newborn piglets, expanded in vitro and characterized for the expression of mesenchymal markers and for their ability to differentiate into cells of the mesodermal lineage (Figure 40). Cells were then seeded on the CorMx and cultured for one week under static conditions and one week in a rotating bioreactor. The constructs were then implanted into five-week-old piglets through a CPB procedure. The animals were recovered and regularly checked with echo. Four months after surgery, the pigs were terminated, the grafts dissected and analysed in the lab.

Two piglets were implanted with an engineered CorMx (TE-patch 24h and TE-patch 4m) and one piglet was implanted with a non-seeded CorMx (scaffold). Two animals successfully recovered from the surgical procedure and were terminated four months after the CPB. One of the two piglets implanted with an engineered-CorMx faced complications during the recovery and was sacrificed 24 hours after surgery.

Graft denomination	Graft composition	Time point	Weight at surgery (kg)	Weight at termination (kg)
Scaffold	CorMx	4 months	24	106
TE-patch 24h	pTMSC + CorMx	24 hours	25	25
TE-patch 4m	pTMSC + CorMx	4 months	21	105

Table 9. *Summary of the information about the three animals implanted so far, illustrating the name of the graft, its composition, when it was explanted and the weight of the pig on the day of surgery and termination.*

Prior to the implantation of the grafts into the animals, a little piece of patch was cut off and examined for histological stainings, SEM and viability assay (Figure 41). The H&E of the unseeded scaffold showed absence of nuclei on the surface of the CorMx and through its thickness. According to the EVG staining, the scaffold was mainly made of collagen fibers. The topography of the CorMx can be observed in the SEM image that show a flat surface with no cells. Histological examination of the seeded graft that has been explanted at 24 hours post-surgery (TE-patch 24h) demonstrated a thick layer of cell growing on top of the scaffold. No cells were detected deeper in the matrix.

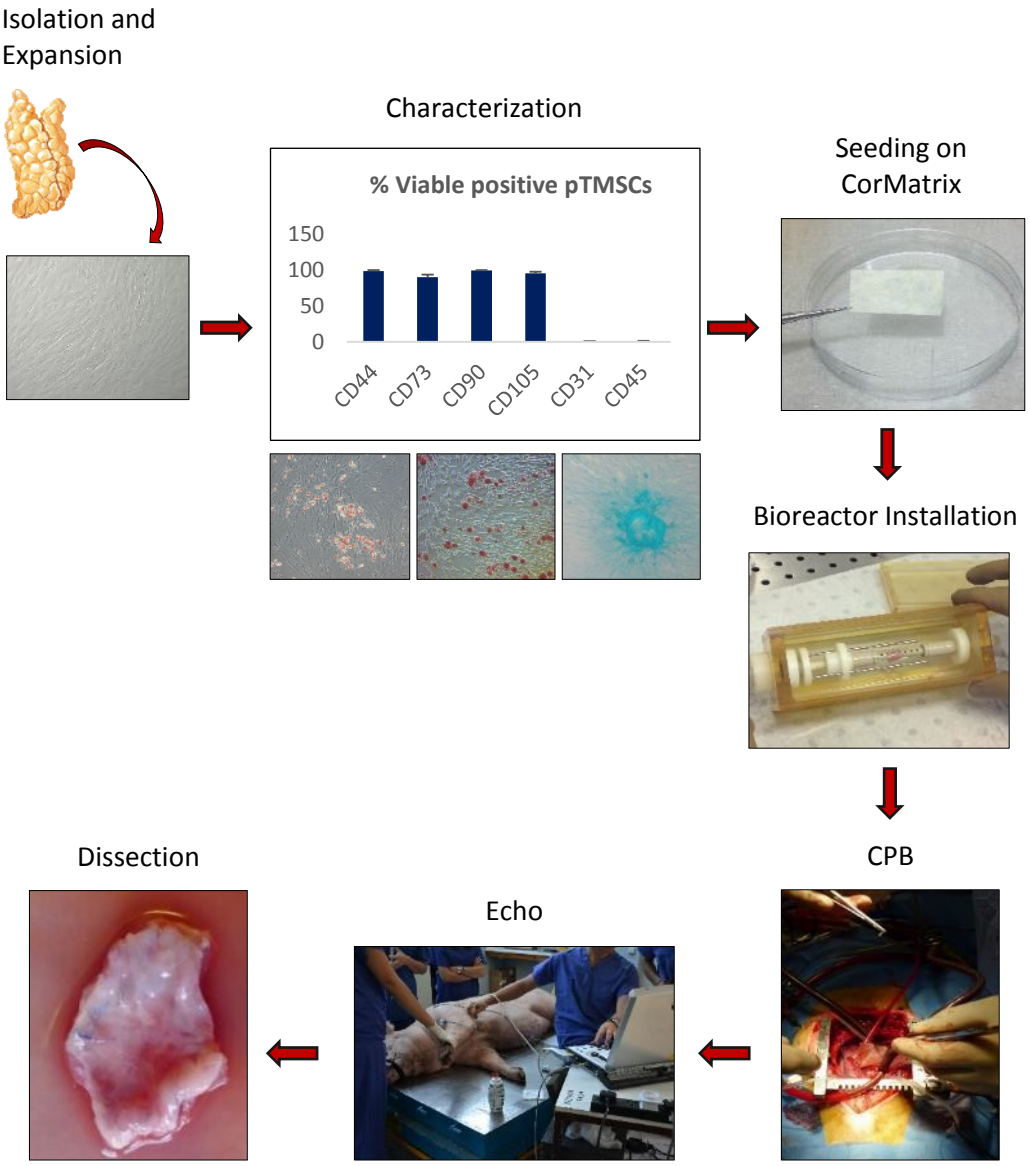

Figure 40 Schematic diagram illustrating the main steps of our methodology. MSCs were firstly isolated from the thymus gland of a newborn piglet and expanded in vitro. Cells' phenotype was characterized for the expression of surface markers by flow cytometry and cells were functionally characterized by their potential to differentiate into osteocyte, adipocyte and chondrocyte. MSCs were seeded onto the CorMx materials and cultured for one week under static conditions and one week in a rotating bioreactor. The graft was then patched to the RVOT of a piglet through a CPB procedure. The animal was regularly monitored with echocardiograms and terminated after four months. The graft was then explanted and analysed with histological and immunofluorescent stainings.

The live/dead staining showed a confluent and viable layer of cells attached to the CorMx. SEM examination confirmed the presence of a confluent and oriented layer of cells growing on the surface of the scaffold. H&E and EVG staining of the engineered CorMx that has been in vivo for 4 months, showed again a nice cell layer engrafted on top of the scaffold.

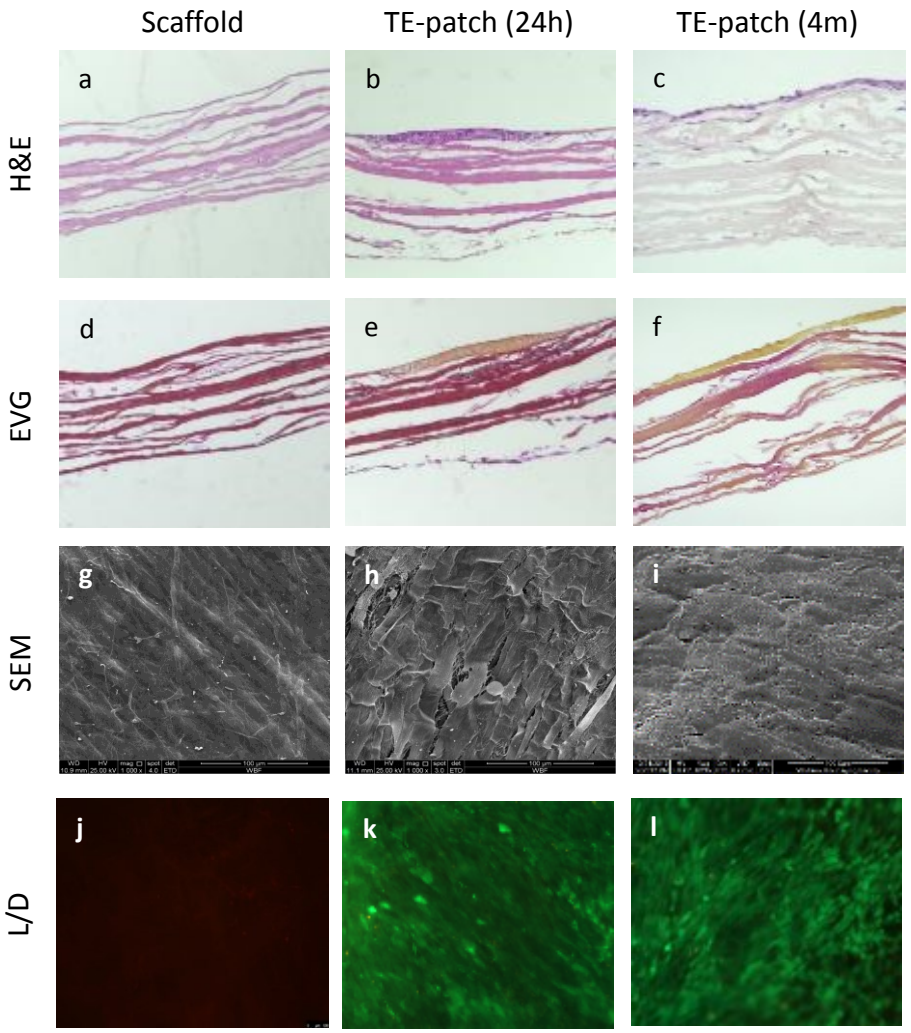

Figure 41 Grafts before in vivo implantation analysed by histological stainings (H&E and EVG) scanning electron microscopy (SEM) and live/dead staining (L/D). H&E examination of the unseeded scaffold showed a matrix lacking of nuclei (a), while the scaffolds engineered with pTMSCs showed a thick multilayer of cells growing on top of it (blue) (c, d). The EVG staining demonstrated absence of cells in the unseeded scaffold and that it is mainly made of collagen (pink) (d). The EVG of the TE-patch that have been in vivo for 24 hours and 4 month (respectively e and d) confirmed the presence of a clear layer of cells that have engrafted the surface of the scaffold (yellow). SEM images allowed to visualize the topography of the grafts: a flat and lack-of-cell surface is observed in the unseeded scaffold, while a confluent and oriented carpet of cells was present in the engineered patches (h, i). The live/dead staining demonstrated that the seeded cells were viable prior the in vivo implantation (green fluorescence) (k, l). Very few dead cells were detected (red fluorescence). Magnification: 200x (a-f); 1000x (g-i); 100x (j-l).

Few cells were detected within the matrix. The morphology of the cell layer can be observed in the SEM picture which displayed a carpet of cells covering the surface of the graft. The viability assay confirmed that the seeded cells were viable before the implantation in vivo. Only very few dead cells were detected.

1. DOPPLER-ECHOCARDIOGRAPHY

Two-dimensional echo was employed to monitor the animals' cardiac functions. Echos were recorded from the short-axis view to allow the visualization of the LV and RV, corresponding to where the graft was patched. Since the echo machine was bought only recently, no measurements were available for the first implanted pig, where the unseeded scaffold was used. A four-month-old pig that did not undergo surgical procedures was employed to compare the cardiac functions of the implanted pigs before termination with those exhibited by this control animal. The M-mode measuring allowed to calculate many parameters, including the EF (59%), the SV (26 ml) and the FS (30%) (Figure 42).

The animal implanted with the TE-patch that was sacrificed 24 hours after surgery, was examined with an echo immediately before surgery (Figure 43). The M-mode measurements showed an EF of 78%, an SV of 12 ml and a FS of 44%, indicating that the piglet displayed normal cardiac function.

The pig implanted with the TE-patch 4m, has been regularly monitored with echo until the end point. Analysis was performed before surgery (pre-op) and after two, three and four months (Figure 44). Between the first and the last measurements, it was observed an upward trend for most of the values calculated with the M-mode (Figure 45). For instance the SV pre-op was 12 ml, after 2 months was 23 ml, after 3 months was 24 ml and after 4 months was 42.5 ml. The EF and the SV pre-op were respectively 54% and 27%, after 2 months 81% and 48%, after 3 months 69% and 37% and after 4 months 72% and 41%. These results indicate that heart function and anatomy of the pig implanted with the TE-patch 4m were normal as compared to the non-operated control animal.

CTR 4 months

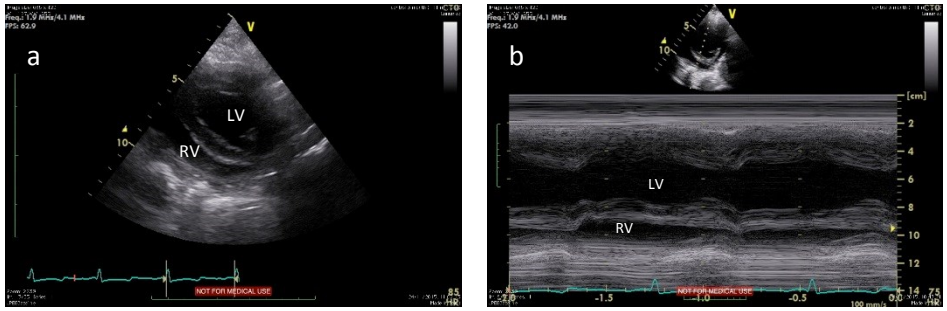

c

	CTR 4m
IVSd (cm)	1.7
IVSs (cm)	2.7
LVIDd (cm)	3.3
LVIDs (cm)	2.3
LVPWd (cm)	1.5
LVPWs (cm)	1.8
EDV (ml)	45
ESV (ml)	18
EF (%)	59
SV (ml)	26
FS (%)	30

Figure 42 Doppler-echocardiogram of a four-month-old pig that did not undergo surgery. The LV and RV were distinguished in the short-axis view (a). The M-mode image (b) allowed to observe the contraction of one area over time and to measure the cardiac parameters of interest (c).

Pre-op

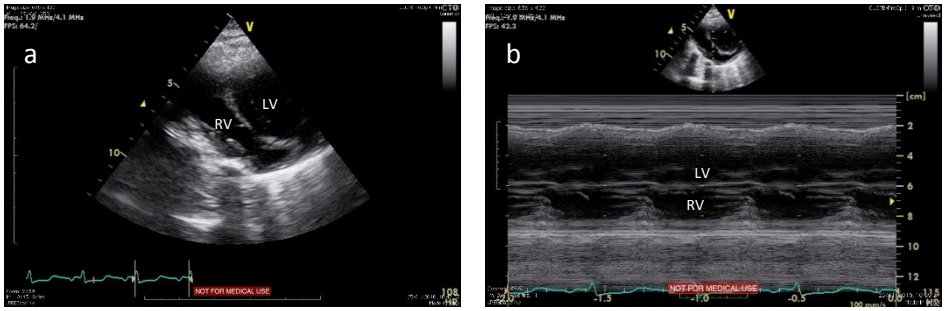

c

	pre-op
IVSd (cm)	1.1
IVSs (cm)	1.4
LVIDd (cm)	2.2
LVIDs (cm)	1.2
LVPWd (cm)	0.9
LVPWs (cm)	0.6
EDV (ml)	15
ESV (ml)	3
EF (%)	78
SV (ml)	12
FS (%)	44

Figure 43 Two-dimensional echocardiogram of the pig implanted with a TE-patch that was terminated 24 hours post-surgery (a). The echo was performed in short-axis and immediately before the CPB. With the M-mode function it was observed the contraction of the heart (b) and the values of interests were calculated (c).

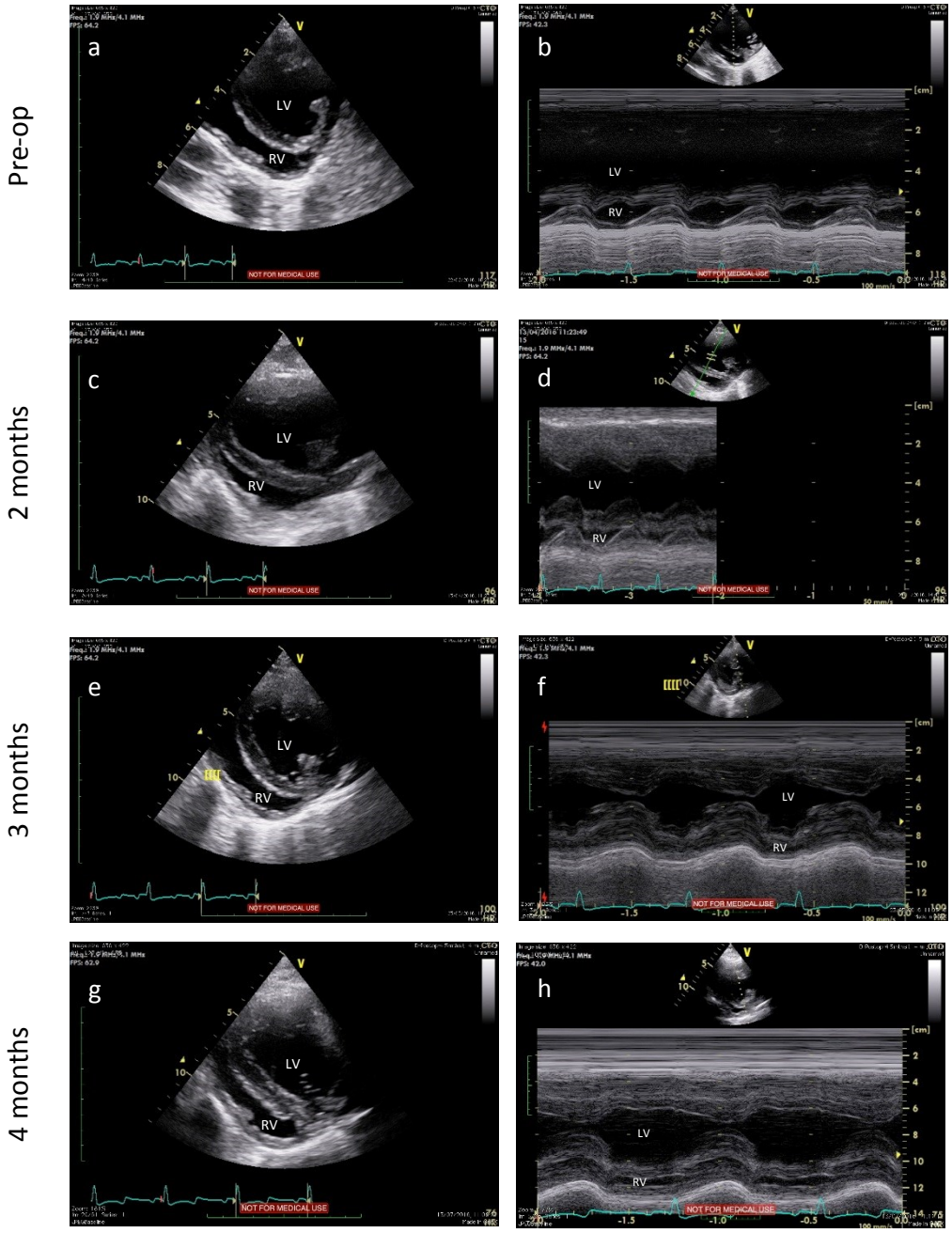

Figure 44 Doppler-echocardiograms in short axis of the pig implanted with a TE-patch. Echos were performed before surgery (a, b) and after two (c, d), three (e, f) and four months (g, h), when the animal was terminated. The M-mode measuring allowed to examine the cardiac function, the contractility of the heart and to visualise the cardiac structures (Figure 45).

	pre-op	2m	3m	4m
IVSd (cm)	0.6	1.5	1.7	1.3
IVSs (cm)	1.35	2.1	2.3	2.15
LVIDd (cm)	2.45	2.8	3	3.7
LVIDs (cm)	1.75	1.5	1.9	2.15
LVPWd (cm)	0.4	1	1.5	1.9
LVPWs (cm)	0.5	1.4	1.9	2.3
EDV (ml)	21	29	35	58
ESV (ml)	9	6	11	15.5
EF (%)	54	81	69	72
SV (ml)	12	23	24	42.5
FS (%)	27	48	37	41

Figure 45 Echo parameters of the pig implanted with the TE-patch 4m measured with the M-mode. Echo was performed immediately before surgery (pre-op) and after two (2m), three (3m) and four months (4m), corresponding to when the animal was terminated.

2. GROSS EXAMINATION OF THE EXPLANTS

When the animals were terminated the hearts were collected and the grafts explanted. A macroscopic evaluation of the explanted tissues showed good integration of the grafts within the surrounding cardiac tissue (Figure 46). The blue stitches used to patch the graft to the RV, were still visible after 4 months in vivo, allowing to identify the exact area of the implants. No major differences where observed at the microscopic level between the seeded and unseeded scaffolds. Both grafts were thinner than the myocardium, though they appeared to be well incorporated within it. The TE-patch that was explanted after 24h was dissected after having been in formalin for a long time. This probably caused the tissue to shrink, which size was smaller in comparison with the other two explants.

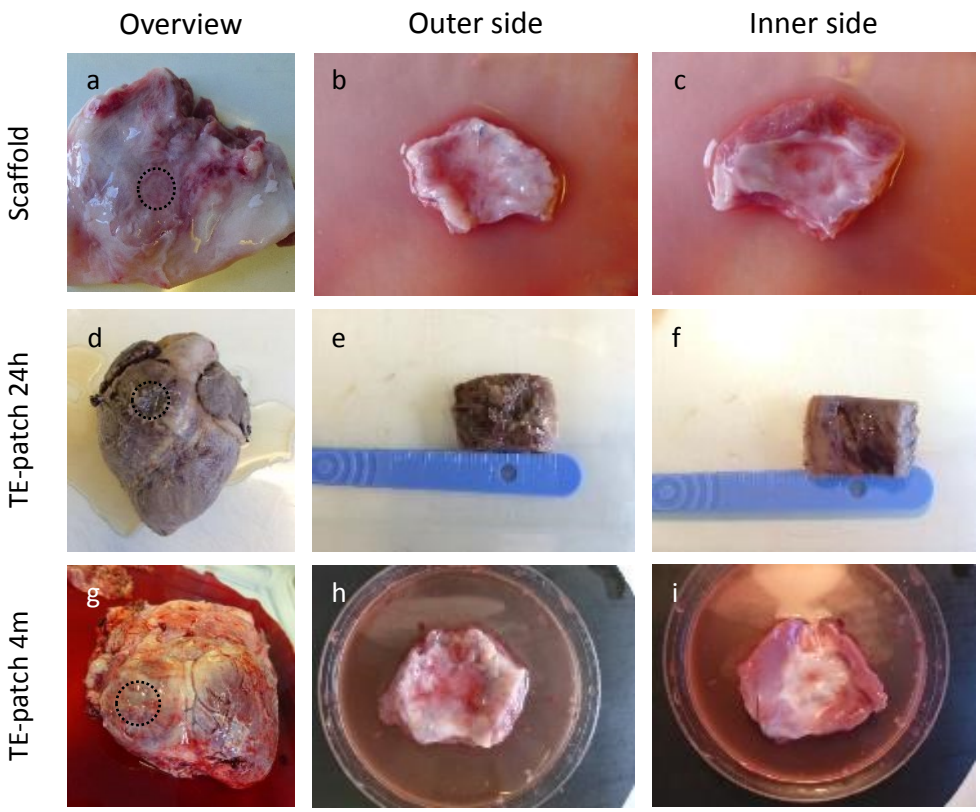

Figure 46 Macroscopic images of the dissected explants. Overview of the heart patched with the unseeded scaffold (a), outer (b) and inner side of the scaffold (c) where the blue stitches were still visible. The heart explanted after 24h (d) exhibited a brownish coloration due to the long time it has been in formalin prior to be examined. e and f show respectively the outer and inner side of the seeded graft. (g) Heart explanted after 4month that was patched with a TE-patch, outer (h) and inner side of the graft (i). The patch location is highlighted by the black dotted lines in the overview pictures.

3. HISTOLOGICAL EVATUATION OF THE EXPLANTS

H&E and EVG stainings were performed on the explanted grafts, on the adjacent cardiac tissue (RV) and on the LV. As shown by the histology of the unseeded scaffold analysed for histological stainings (Figure 47 and Figure 48), the CorMx is no longer detectable after 4 months in vivo. This observation indicates optimal integration of the scaffold with the surrounding tissue and complete degradation of the matrix. Yet, it is possible to distinguish between the native cardiac tissue and the newly formed tissue that built up from the implanted graft. The H&E staining showed that several cells migrated to the graft and populated the matrix. Although the architecture of the newly formed tissue was not equivalent to that of the cardiac tissue, few cardiac-like areas were detected within the graft-side of the explant. These “cardiac-pockets” were also found in the EVG

staining, being coloured in yellow as the muscle tissue. Based on the histology, the composition and architecture of the RV immediately adjacent to the graft, seemed to be equivalent to the LV far from the implant. Moreover, no inflammation was detected in the cardiac tissue, neither close to the graft, nor far in the LV. This imply that the scaffold alone is well tolerated by the host as it does not cause a long term immune response.

From the histological evaluation of the engineered CorMx explanted 24 hours after surgery (TE-patch 24h), it is possible to analyse the immediate effect of the patch on the host tissue, as well as the triggered inflammatory response and the retention of the seeded cells. The H&E and EVG stainings of the explant (Figure 49 and Figure 50) showed good integration of the TE-patch with the cardiac tissue. The CorMx appeared to be intact and no damaged area were detected. A thick layer of cells was built up over the inner side of the graft, which corresponded to where the cells were seeded. Based on these results, it not yet clear if this new cell layer was constituted of cells that have migrated from the surrounding cardiac tissue or if they have been attracted from the blood stream by the seeded cells. An intense inflammatory response was observed in the RV close to the implant. No inflammation was observed far from the graft, such as in the LV. The detected inflammatory response was likely to be physiological and due to the surgery performed.

The histology of the engineered CorMx explanted 4 months after surgery (TE-patch 4m) allowed us to evaluate the long term effect of the developed cardiac patch. As it happened in the scaffold implanted without seeded cells, the CorMx was no longer detectable in the explant. In fact over time, it has degraded leaving no trace of itself (Figure 51, Figure 52). The graft side of the explant can be recognized only because the new tissue that generated from the patch did not appear completely the same as the myocardium (identified by a pale pink colour in the H&E staining and by a bright pink colour in the EVG staining). Interestingly, the cardiac tissue adjacent to the graft, seemed to be penetrating in the graft as if it was attracted towards that direction. Several areas made of cardiac-like tissue were observed in the graft side of the explant (identified by a bright pink colour in the H&E staining and by a yellow colour in the EVG staining). These areas appeared to be more frequent in the TE-patch in comparison with the unseeded scaffold, suggesting that the seeded cells contributed in the remodelling of the implanted patch. According to the EVG staining, the newly formed tissue was prevalently made of collagen and a thick layer of elastin laid on the inner side of the

explant, corresponding to where the cells were seeded. This observation may imply that the engineered side of the patch helped the process of endothelialisation of the new tissue. No signs of inflammation were detected 4 months after implantation, indicating that the TE-patch was tolerated by the host and that the seeded cells did not rise any long term immune response, despite they were not autologous.

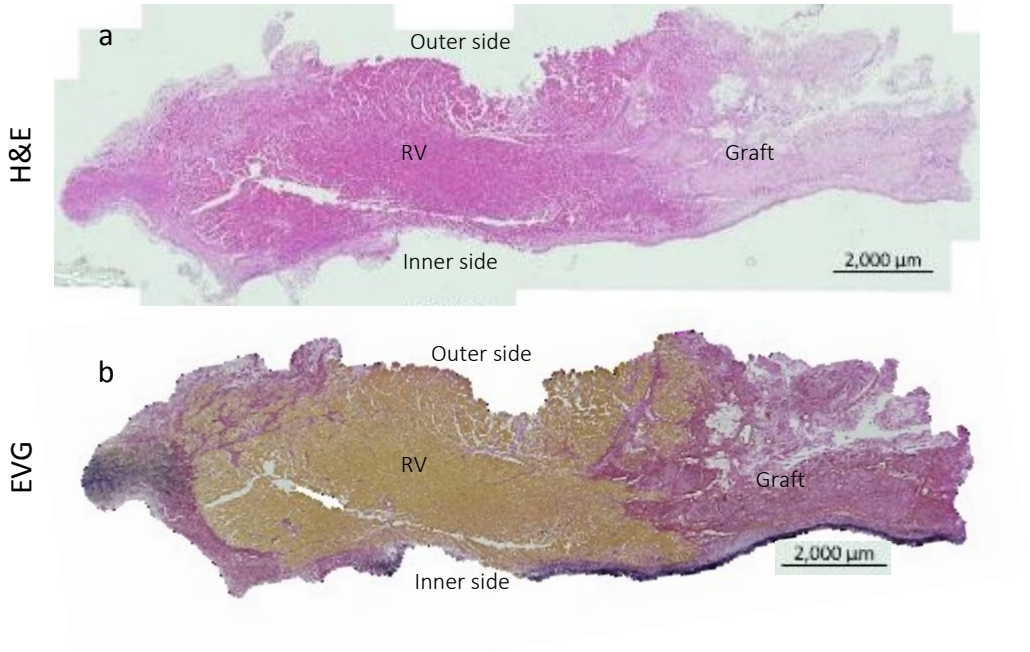

Figure 47 Reconstructed images of the H&E (a) and EVG (b) histological stainings of the unseeded scaffold explanted at 4 months post-surgery. The graft has perfectly integrated with the surrounding tissue and the CorMx was no longer detectable in the graft-side of the explants. The newly formed tissue was recognizable on the right-hand side of the sample, coloured in pale pink by the H&E staining (a) and in bright pink by the EVG staining (b). The EVG examination also showed a mature endothelialisation in the inner side of the explant. In the cardiac tissue of RV next to the scaffold, no inflammatory response was detected. Magnification: 100x.

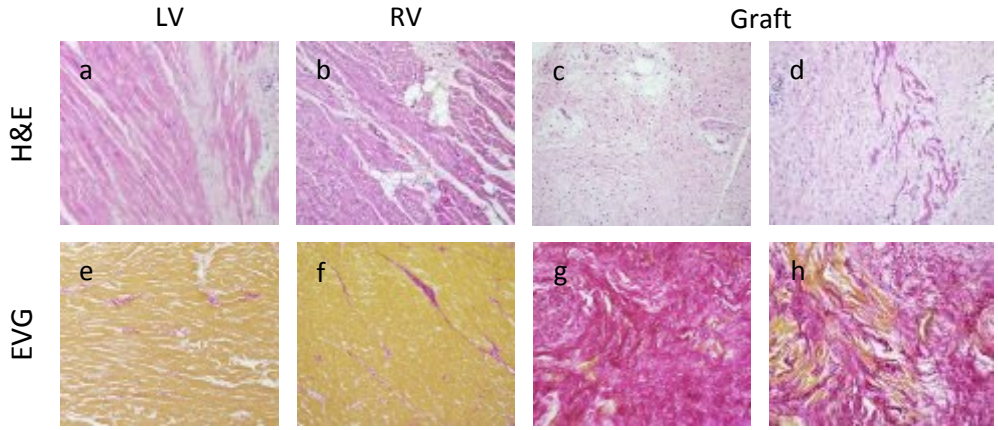

Figure 48 Images at higher magnification of the histological staining of the scaffold explanted 4 months post-op. (a, b) H&E staining of the LV and RV showed no differences between the myocardium next to the implant (RV) and myocardium far from it (LV). (c, d) H&E staining of the graft side of the explant demonstrated that several cells from the host have populated the scaffold and that a few cardiac-like tissue areas were detected in the newly formed tissue. (e, f) EVG analysis of the LV and RV confirmed that the cardiac tissue of the RV is equivalent to that of the LV. (g) The EVG staining of the graft side of the explant showed that the developed tissue was rich in collagen content (bright pink). (h) A few "cardiac-pockets" were also detected within the graft-side of the explant. Magnification: 200x.

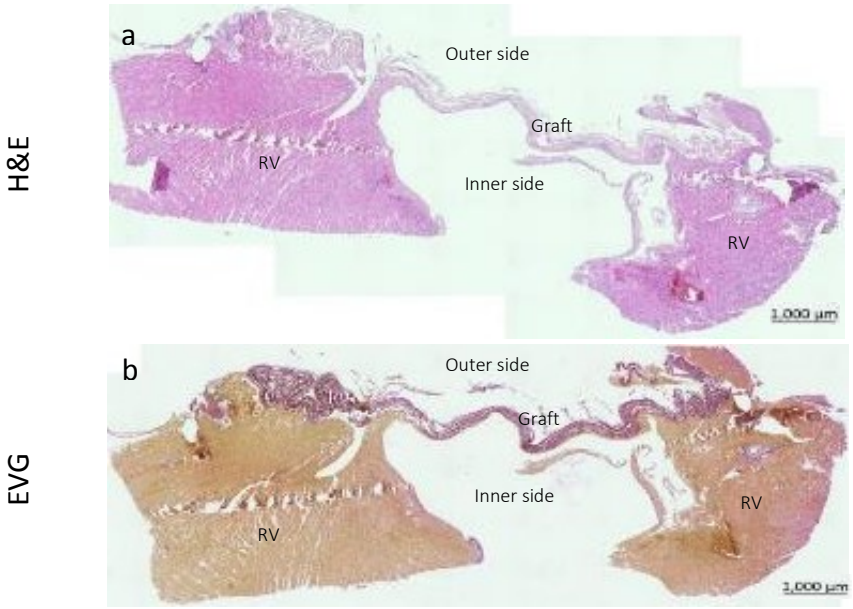

Figure 49 Imaging reconstruction of the H&E (a) and EVG (b) stainings of the TE-patch that was explanted 24 hours post-surgery. The seeded side of the graft faced the inner side of the heart, and a thick layer of cells was detected on that side of the implant. The CorMx was clearly identified as a multilayer of thin tissues coloured in pale pink and bright pink by the H&E and EVG staining respectively. The scaffold seemed to be nicely in contact with the cardiac tissue of the RV onto which it was stitched. A strong inflammatory response seemed to be occurring 24 hours after implantation. Magnification: 100x.

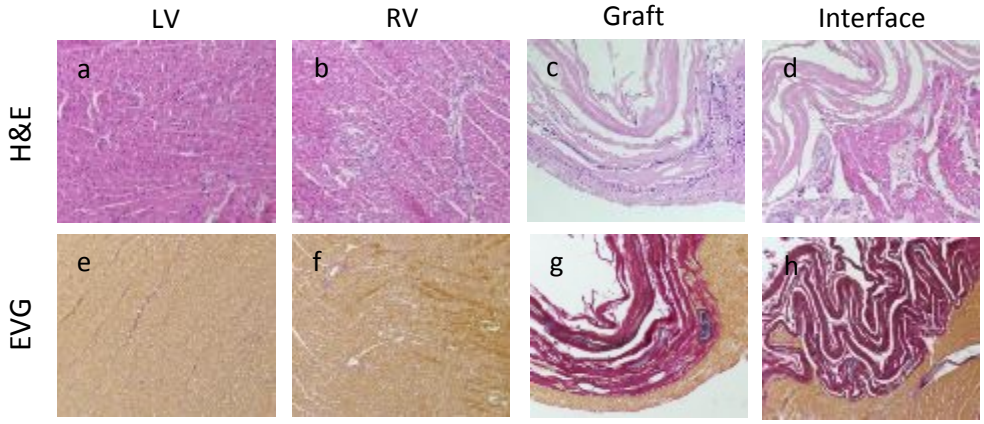

Figure 50 Higher magnification images of the histological staining of the TE-patch explanted 24 hours after bypass. H&E staining of the LV and RV demonstrated that no inflammation was detected far from from the implantation site (a), while many inflammatory cells were detected in the cardiac tissue next to the graft (b). In the H&E staining of the graft was identified a thick layer of cells growing over the inner side of the scaffold, where the cells were seeded (c). The interface between the CorMx and the myocardium displayed a nice integration of the graft with the host tissue (d). EVG examination of the LV and RV of the explant showed that the inflammatory response was present only near the RV of the implantation area (e, f). The EVG staining of the engineered graft confirmed the presence of a layer of cells proliferating in the inner side of the scaffold (coloured in yellow, g) and a nice and clean interface between the graft and the cardiac tissue. Magnification: 200x.

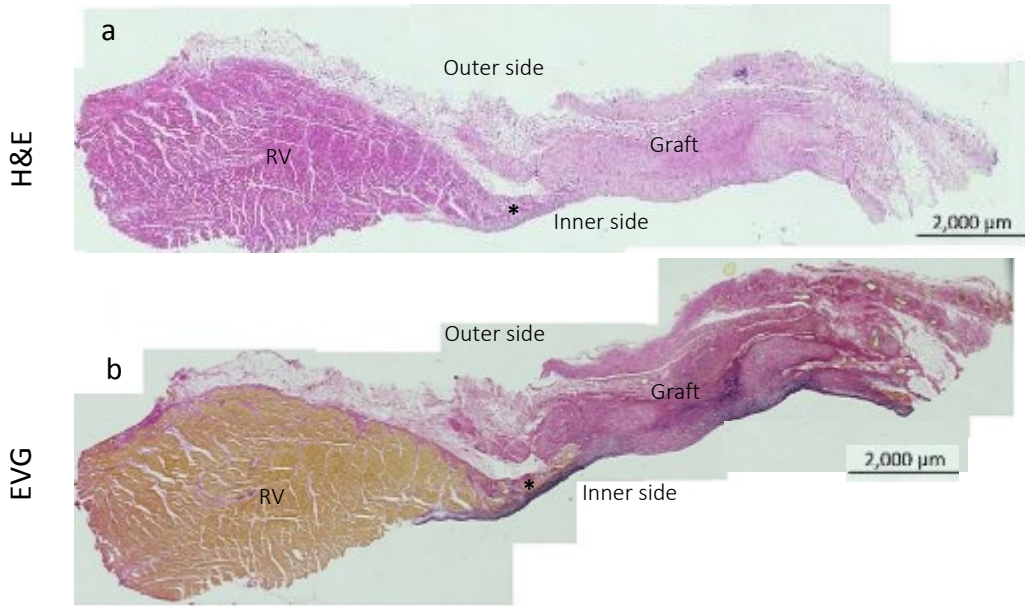

Figure 51 Reconstructed images of the H&E (a) and EVG (b) histological stainings of the engineered CorMx explanted 4 months after cardiopulmonary bypass. The patch has successfully integrated in the surrounding tissue and CorMx was no longer detectable in the graft-side of the explants (on the right-hand side of the sample, coloured in pale pink by the H&E and in bright pink by the EVG staining). In the cardiac-side of the graft (RV), no inflammation was observed and the newly formed tissue appeared to be penetrating into it (*). Magnification: 100x.

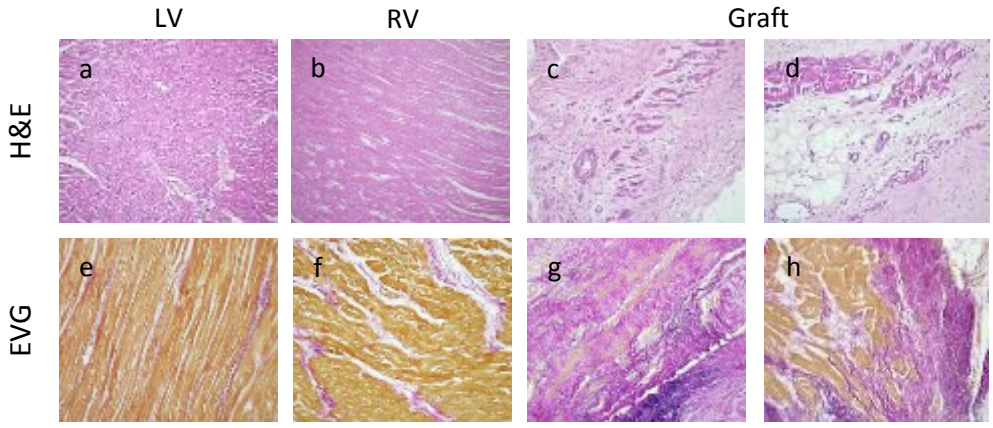

Figure 52 Detailed images of the histology of the TE-patch explanted 4 months post-op. (a, b) H&E staining of the LV and RV showed no major differences the cardiac tissue close to the implant (RV) and the cardiac tissue far from it (LV). (c, d) H&E staining of the graft side of the explant demonstrated high density of cells, no inflammation occurring and the presence of cardiac-like areas in the newly-formed tissue. (e, f) EVG examination of the LV and RV confirmed that the myocardium has not been altered from the implantation. (g, h) The EVG staining of the graft side of the explant showed a collagen- and elastin-rich tissue (coloured in pink and purple respectively), with several cardiac-resembling tissue areas populating the newly formed tissue. Magnification: 200x.

4. IMMUNOFLUORESCENT ANALYSIS OF THE EXPLANTS

Fluorescent immunohistological analysis was performed on the explanted tissue grafts and RV. The expression of the following markers was investigated: CX43, cMYH and Des as cardiac markers; aSMA and smMYH as smooth muscle cells indicator and Iso as endothelial marker. As shown in Figure 53 a double staining for smMYH and Des was performed on the unseeded scaffold, TE-patch 24h and TE-patch 4m as well as on the respective RV. Positivity for smMYH was detected mainly around the blood vessels, indicating that the smooth muscle cells were localized in correspondence of the vasculature. Based on this staining it appeared that the TE-patch 4m developed more blood vessels in the newly formed tissue in comparison with the unseeded scaffold. No positivity for the smooth muscle marker was detected in the graft side of the TE-patch 24h probably due to the longer time needed for angiogenesis.

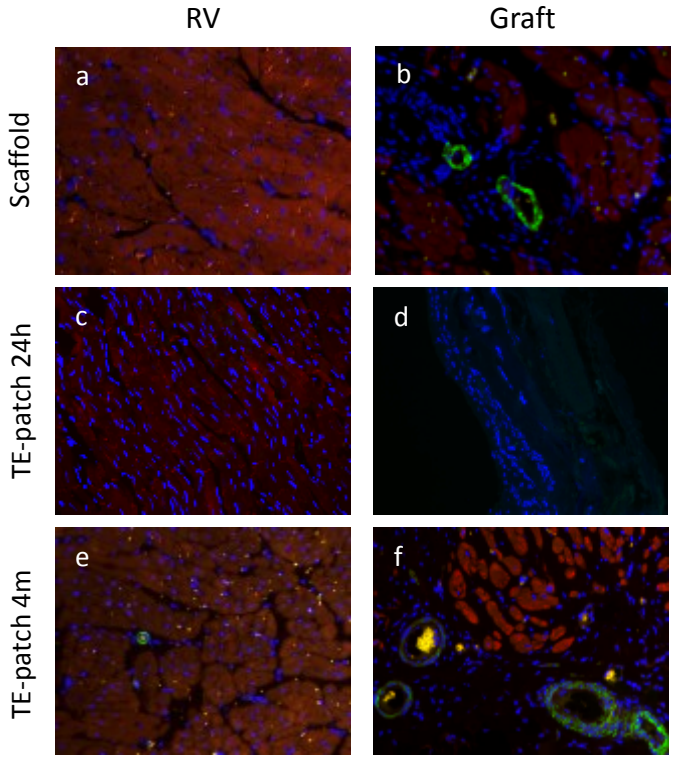

Figure 53 Immunohistological staining for the cardiac protein Desmin (Des, red fluorescence) and for the smooth muscle Myosin Heavy Chain (smMYH, green fluorescence) on the CorMx scaffold explanted 4 months post-surgery (b), the engineered scaffold explanted after 24 hours (TE-patch 24h) (d), the engineered graft explanted after 4 months (TE-patch 4m) (f) and the related right ventricles (RV) (a, c, e). All cardiac tissue was positive for Desmin. A few cardiac-like areas expressing Des were detected in the graft-side of the patches explanted after 4 months. Positivity for smMYH was observed around the blood vessels. Absence of expression of the two markers was present in the graft explanted after 24h post-surgery. Magnification: 200x.

Expression of Des was detected in the cardiac tissue that was present in all the explanted samples. The presence of this marker allowed us to characterize the areas indicated as “cardiac pockets”. In fact those regions of cardiac-like tissue were the only one that were expressing Des in the graft-side of the explants. A stronger expression of Des was observed in the pockets of the TE-patch 4m then in the unseeded scaffold, suggesting that the seeded cells have helped the development of cardiac-like tissue in the newly formed tissue. No expression of Des was detected in the graft that was explanted 24 hours post-surgery, while the adjacent RV was strongly positive for the cardiac protein.

A double fluorescent staining was carried out to investigate the expression of cMYH and CX43 (Figure 54) on the scaffold, TE-patch 24h, TE-patch 4m and on the relative RVs. The cardiac-specific markers were highly expressed by the myocardium of the three RVs. cMYH was also detected in the cardiac pockets present in the graft-side of both the unseeded scaffold and the TE-patch 4m. CX43 allowed to visualise the gap junctions present in between each muscle fibre. This protein was not detected in the cardiac pockets of the explanted unseeded scaffold, while it was expressed in some of the cardiac-like regions originated in the tissue that built up from the TE-patch (4m). Such observation confirmed that the cardiac pockets that developed in the TE-patch (4m) were more mature then those developed in the graft side of the unseeded scaffold. In regards of the TE-patch 24h, absence of both cMYH and CX43 was observed, most likely due to the lack of time needed to remodel the graft.

The expression of Iso and aSMA was investigated with a double staining performed on the three explanted grafts and the RVs (Figure 55 and Figure 56). High positivity for Iso was detected in correspondence of the edge of the inner side of both the unseeded scaffold and the TE-patch 4m, indicating that a good endothelialisation occurred in the inner side of the graft. A few smooth muscle cells were detected nearby the edge of the two explants. No differences were observed between the endothelialisation of the two samples, suggesting that the seeded cells did not make a detectable difference in this process. Moreover, the endothelium of the inner side of the RV resembled the new one developed from the implanted patches, confirming that the endothelialisation achieved after 4 month was successful. The edges of the TE-patch 24h, corresponded to the interface between the CorMx and the cardiac tissue. A good integration of the scaffold with the surrounding tissue was observed in this sample. Iso and aSMA were highly expressed in the graft side of both the scaffold alone and the TE-patch 4m. Although the

staining for Iso was not as bright as it was close to the edge or in the RV, its presence was homogenously detected throughout the newly formed tissue, whereas aSMA was localized specifically around the blood vessels. Positivity for Iso and aSMA was also detected in the TE-patch 24h. Most of the cells constituting the thick layer covering the inner side of the scaffold, were found to be positive for Iso. This finding may imply that the seeded cells had already recruited endothelial cells to start the process of endothelialisation after 24 hours from implantation.

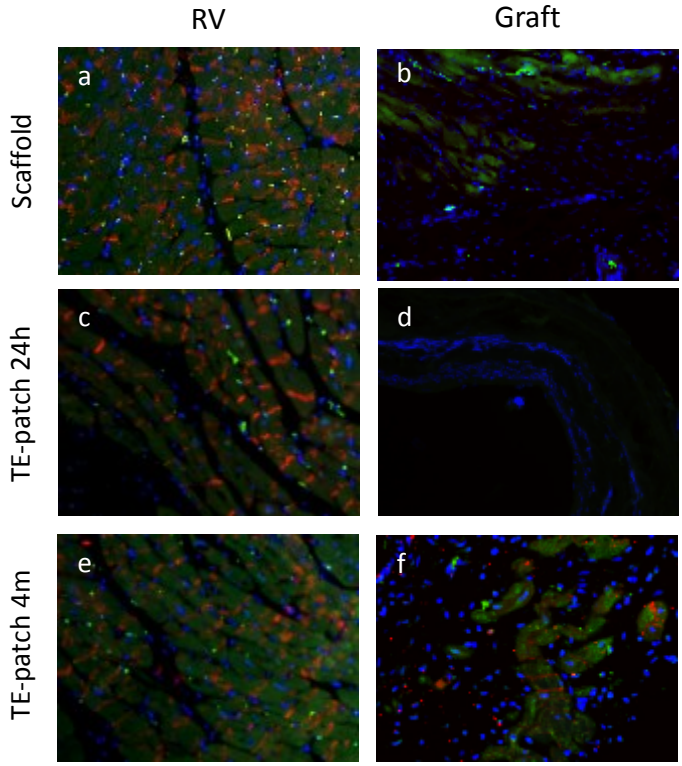

Figure 54 Immunofluorescent staining for the cardiac proteins cardiac Myosin Heavy Chain (cMYH, green fluorescence) and Connexin-43 (CX43, red fluorescence) on the unseeded scaffold explanted 4 months after surgery (b), the engineered graft explanted after 24 hours post-surgery (TE-patch 24h) (d), the seeded patch explanted after 4 months (TE-patch 4m) (f) and on the related right ventricles (RV) (a, c, e). Positivity for cMYH was observed all over the cardiac tissue of the RV and in some cardiac-like areas located in the graft side of the grafts explanted 4 months after implantation. CX43 was detected in correspondence of the gap junctions located in the cardiac tissue. A few cardiac pockets expressing the marker were found in the graft side of the TE-patch 4m. No positivity for the two cardiac proteins was observed in the TE-patch 24h. Magnification: 200x.

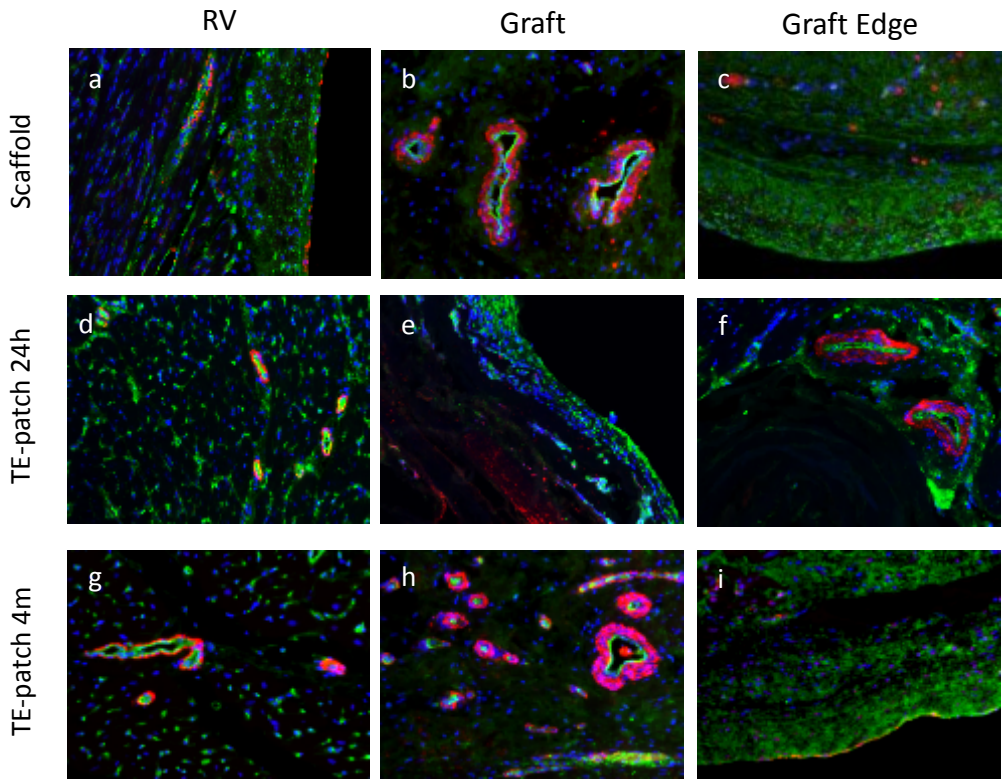

Figure 55 Immunohistological staining for the endothelial marker Isolectin B4 (Iso, green fluorescent signal) and the smooth muscle protein alpha-smooth muscle actin (a-SMA, red fluorescent signal) of the unseeded scaffold explanted 4 months post-op (scaffold) (b), the engineered scaffold explanted after 24 hours (TE-patch 24h) (e), the engineered graft explanted after 4 months (TE-patch 4m) (h), the relative RV (a, d, g) as positive controls and the inner side of edge of the grafts (c, f, i). The edge of the grafts explanted 4 months post-op showed strong positivity for Iso. Expression of aSMA was found only in the inner side of the TE-patch 4m. The RVs demonstrated high positivity for Iso through all the surface of the sample, while aSMA was located mainly around the blood vessels. The graft sides of the 4 month-explants expressed both markers, although more vasculature appeared to be present in the TE-patch 4m. Strong positivity for Iso was observed in the engineered graft explanted 24 hours after surgery, especially on the surface facing the inner side of the heart, where the cells were seeded. Some expression of aSMA was also detected on the graft of this sample. Magnification: 200x.

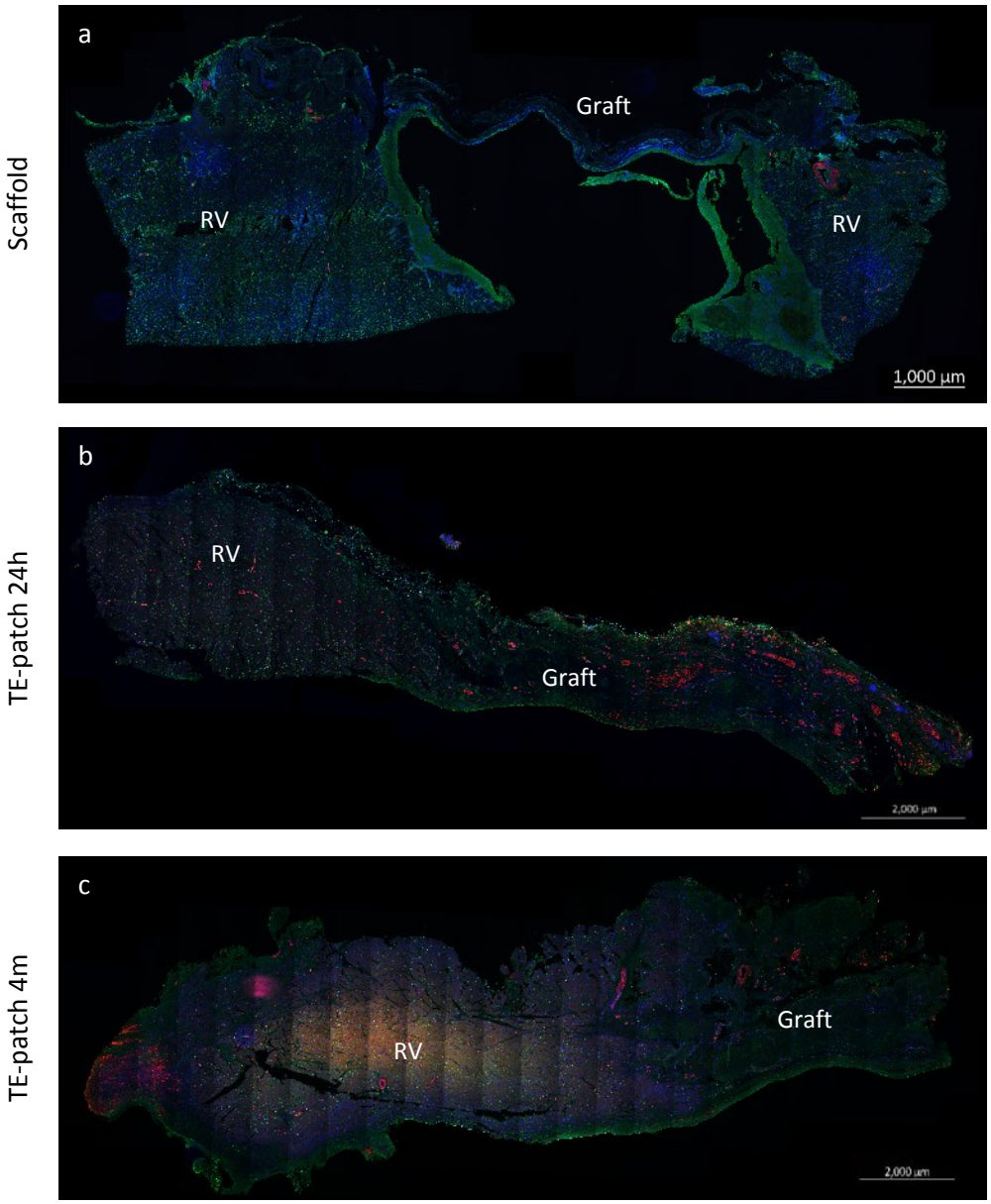

Figure 56 Image reconstruction of the fluorescent immunostaining for Isolectin B4 (Iso, green fluorescent signal) and alpha-smooth muscle actin (α-SMA, red fluorescent signal) of the unseeded scaffold explanted 4 months after surgery (scaffold) (a), the engineered scaffold explanted after 24 hours (TE-patch 24h) (b) and the engineered scaffold explanted after 4 months (TE-patch 4m) (c). Magnification: 100x.

5. BLOOD VESSELS QUANTIFICATION

The fluorescence immunostaining for Iso and aSMA allowed to compare the angiogenesis that occurred in the unseeded scaffold with the one that occurred in the TE-patch 4m, distinguishing between the greater vessels and the capillaries (Figure 57). Statistically significant difference was observed in the vascularization of the two explants. The number of both capillaries and greater vessels was significantly higher in the engineered patch then in the unseeded scaffold. Such a difference was also appreciated in the fluorescence image reconstruction of the analysed samples (Figure 56 b and c).

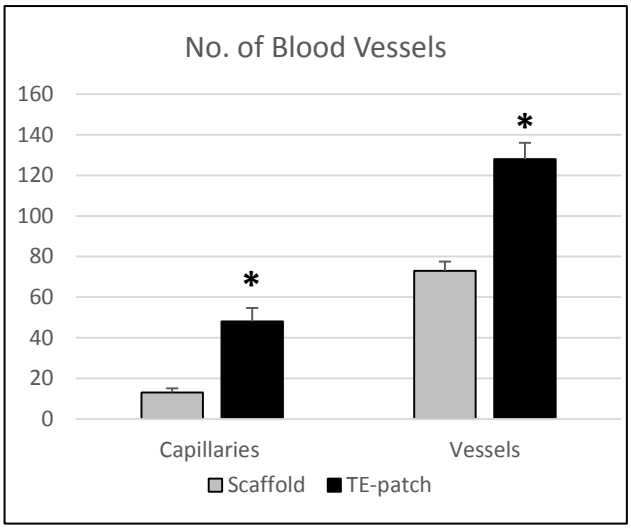

*Figure 57 Blood vessel quantification of the unseeded scaffold (grey bars) versus the engineered patch that has been in vivo for 4 months (black bars). A distinction between small blood vessels (capillaries) and great vessels was performed. The vascularization detected in the engineered patch was significantly higher in comparison with the one found in the unseeded graft. * $p < 0.05$.*

CONCLUSIONS

A novel large animal model was established to determine the practicability of using engineered grafts for RVOT reconstruction. CPB was set up by cannulating the ascending aorta and the superior and inferior vena cava. Two animals successfully recovered and grew up at standard rates. Two-dimensional echo showed that the pig implanted with engineered-patch did not develop heart failure and its cardiac functions were comparable to those of control pigs. Gross examination of the seeded and unseeded grafts explanted four months post-surgery showed good integration of the material with the surrounding tissue. Histological and immunofluorescence analysis demonstrated that the grafts remodelled. Indeed they were no longer detectable and cardiac-like areas were observed in correspondence to the implantation site. Angiogenesis occurred in both explants, however the vascularization found in the engineered-patch was significantly higher than in the unseeded scaffold and more remodelling appeared to be present. One animal implanted with a seeded graft was sacrificed 24 hours after surgery as the piglet became too anaemic during the recovery care. Examination of the explant showed that the graft was well integrated in the RV and an inflammatory response was detected only in the cardiac tissue close to the implantation site.

The validation of our CPB swine model is of great value for the preclinical studies focused on the treatment of CHD and heart failure.

DISCUSSION

CHDs represent the most common congenital anomalies in newborn babies with a reported percentage ranging from 6 to 13 per 1000 live birth (Tennant et al. 2010). In the United Kingdom alone there are approximately 4600 children born with CHD each year (Khoshnood et al. 2012). When treating these patients, surgical repairs often require the use of patches to close the septal defect or enlarge stenosed structures. For example the correction of TA includes a cardiac patch for the RVOT reconstruction. Most of the grafts currently used in cardiac surgery are synthetic materials such as polymers and Gore-Tex® or fixed xenograft and homografts. Because these materials are either synthetic or treated to remove the remaining cells, they consist of dead tissues that do not grow with the patient. In addition, they are not electromechanically integrated, they may become fibrotic at the site of implantation and pose the risk of calcification, thrombosis and stenosis (Steeds and Oakley 2004). The lack of contractility, electrical conductivity and mismatched mechanical properties could lead to loss of cardiac function. The combination of these various shortcomings might contribute to the risk of sudden cardiac death in children implanted with non-leaving patches (Silka et al. 1998). As CHD are usually treated in the early stage of life, additional surgeries are often required to replace the implants, increasing the risks of arrhythmia and many other complications related to an open-heart surgery (Du et al. 2002).

An engineered viable graft with contractility and conductivity properties matching the native tissue is the ultimate goal of cardiac tissue engineering. TE constructs have come to include cells and scaffolds as their key components in the purpose of guiding the repair and remodelling of damaged tissue. To date, major attention has been dedicated to cell therapy and TE for the treatment of heart diseases and heart failure. New evidences suggest that TE therapy could potentially offer a new treatment for patients suffering from CHD (Wehman and Kaushal 2015; Maeda and Ruel 2015). Thus, engineered-graft could be designed so that they could incorporate with the native tissue, facilitate the healing process and above all, grow with the patient.

With this study we aimed to develop a viable cardiac patch with the potential to be used in the correction of CHD. As a living graft could grow in parallel with the recipient organ, repeated surgeries might be avoided for patients that have received an engineered viable patch.

We have firstly isolated, expanded and characterized MSCs from the thymus gland of children undergoing to open-heart surgeries. When a baby is diagnosed postnatally with

a CHD, a palliative surgery is normally performed soon after birth, in order to intervene with the complete surgical correction when the patient has gained more weight and strength. During this palliative surgery the thymus is discharged to have a better access to the heart. This procedure makes convenient to use the gland as a source of autologous stem cells. Indeed, in the gap between the palliative surgery and the second operation, it is possible to isolate and expand the thymus-derived MSC and use them to engineer a cardiac patch. Flow cytometry characterization of our hTMSCs showed that the cells express most of the mesenchymal markers, including CD29, CD44, CD73, CD90 and CD105. They have also been shown to be negative for leukocyte, immunocytes, endothelial and hematopoietic markers such as CD14, CD31, CD34, CD45 and HLA-DR. Moreover, a functional characterization demonstrated that the TMSCs are capable to differentiate into the three main mesodermal phenotypes: osteocyte, adipocytes and chondrocytes. These data confirmed that the cell population isolated from the thymus gland is made of functional mesenchymal stem cells. Based on this results, the same isolation protocol was applied to obtain MSCs from the thymus of newborn piglets, in order to use porcine cells into our swine model of CHD. Although the availability of FACS porcine antibodies was a limitation in the characterization of this cell line, we showed that pTMSCs highly expressed the essential mesenchymal surface markers, including CD44, CD73, CD90 and CD105, while they did not express endothelial and hematopoietic cell markers (respectively CD31 and CD45). These porcine cells also successfully differentiated into cells of the three main mesodermal phenotypes, indicating that they are functionally efficient stem cells. All the following experiments were carried out in parallel for the human and porcine-derived MSCs in order to test both cell lines and validate them for the subsequent in vivo application: the pTMSCs for the pre-clinical studies in the swine model and the hTMSCs for future potential clinical trials.

Many evidences in the literature support the potential of MSCs to differentiate into cardiac-like cells either in vitro or in vivo (Xu et al. 2004; Labovsky et al. 2010; Toma et al. 2002; Kawada et al. 2004; Fukuhara et al. 2003). We have applied several protocols and different techniques in an attempt to differentiate the MSCs into cardiac-committed cells and generate engineered grafts coherent with the native tissue's phenotype. Three differentiation strategies were optimized: a protocol based on a combination of growth factors (T1), one that employed a medium conditioned by cardiomyocytes (T2) and one based on culturing the stem cells with cardiomyocytes (T3). The rationale of T1 was to demonstrate the capability of the MSCs to differentiate into cardiac-like cells if

adequately stimulated towards the myocardial pathway. T2 was performed to show that the CCM in combination with an epigenetic modifier favouring the differentiation, can generate cardiac committed cells. According to the literature, this effect is due to the factors present in the medium previously used to culture the CMs (Xie et al. 2006; Rangappa et al. 2003). Lastly, we demonstrated the feasibility of obtaining differentiated cells by simply coculturing the MSCs with mature CMs. The success of T3 indicates that the cytokines and growth factors freshly released by the CMs can efficiently stimulate the cardiac differentiation of stem cells without the need of adding any supplements. This data suggest that by implanting undifferentiated cells in vivo, it could be possible to obtain cells committed to the phenotype of the cardiac surrounding environment. The differentiation outcome was assessed by immunofluorescent stainings and qPCR analysis for cardiac-specific markers. The ICC showed that the human and porcine cells treated with all the applied protocols were highly positive for the proteins SaA, cMYH and Des, while no positivity was detected in the untreated MSCs. The analysis of the gene expression of the committed cells demonstrated that the level of the cardiac genes GATA-4, ACTA1, cMYH and DES strongly increased at the end of the differentiation with T1, T2 and T3. From these results it appeared that the most efficient protocols for both the human and the porcine cells were T2 and T3, suggesting that the interaction between the factors released by the CMs and the MSCs is crucial to promote the differentiation of the stem cells into cardiac-committed cells. Although we did not obtain beating cardiomyocytes as some research groups did by simply treating their cells with the demethylating agent 5-Aza (Lian et al. 2012; Kadivar et al. 2006; Nartprayut et al. 2013), we managed to produce committed cells with similar phenotype and gene expression as mature cardiomyocytes.

The second part of this study was focused on generating and testing different types of scaffolds. Decellularized materials have been shown to have great potential as template for cell growth (Gardin et al. 2015; Mirsadraee et al. 2006). The decellularization consists of a process finalized at isolating the ECM of a tissue from its inhabiting cells, preserving the ECM architecture and composition. Many evidences demonstrated the biocompatibility of the acellular pericardium and myocardium both in vivo and in vitro (Pagoulatou et al. 2012; Mendoza-Novelo et al. 2011; Rajabi-Zeleti et al. 2014; Ott et al. 2008). We have optimized and compared two protocols to remove the cellular content from the pericardial membrane collected from adult pigs. The first protocol employed the enzyme Trypsin while the second one employed the detergent TritonX. Both

strategies were followed by a treatment with a nuclease in order to remove the residual nuclear materials. A successful decellularization was achieved applying both protocols; all cellular and nuclear content were removed from the tissues and the ECM was well preserved. No major differences were observed between the Trypsin- and TritonX-decellularized pericardia. The reseeding potential of the developed scaffolds was tested with undifferentiated and differentiated MSCs that were cultured for two weeks under static conditions. Both cell types efficiently engrafted and proliferated on the surface of the two acellular scaffolds. The TritonX-decellularized pericardium appeared to be more biocompatible then the Trypsin-decellularized pericardium as the seeded cells generated a confluent and oriented cell layer. A third protocol was developed to decellularize pieces of porcine myocardium. This approach was based on the action of two detergents: SDS and TritonX. Although the cellular content was efficiently removed from the native tissue, the architecture of the resulting ECM was slightly damaged. Cells successfully attached to the decellularized myocardium, however they did not proliferate into a confluent layer. Many different protocols were tested but only with the one reported in this thesis we succeeded in recellularing the acellular scaffold. We hypothesized that the SDS was not completely washed away, resulting in a matrix with a certain component of toxicity. Ott et al. demonstrated how to decellularize and recellularize a whole rat heart by perfusing the organ rather than immerging it into the solutions required (Ott et al. 2008). This represents an interesting approach to improve our technique and develop a more suitable matrix for cell growth. Comparing the pericardium decellularized with Trypsin and TritonX with the SDS-decellularized myocardium, it appears that the TritonX-decellularized pericardium is the most promising option to generate engineered patches.

A commercially available material was also tested to investigate whether it represents a suitable scaffold for cell growth. CorMx is an ECM patch derived from decellularized porcine small intestinal submucosa that is already used in corrective surgery as a non-living graft. Several publications have reported good results regarding its application in clinical studies for the treatment of CHDs (Witt et al. 2013; Zaidi et al. 2014; Woo, Fishbein, and Reemtsen 2016). However, very few works have been published about the application of engineered CorMx in vivo. We sought to develop an engineered graft by seeding either differentiated or undifferentiated MSCs on the scaffold and culturing them for two weeks under different conditions. Cell attachment and growth over the CorMx was found to be more efficient then when the same cells were seeded on the

decellularized pericardia and myocardium. Two different growing conditions were compared: culturing the graft for two weeks under static conditions versus culturing it for one week under static conditions and one week under dynamic conditions. In the second case the graft was stitched to the rotating arm of a bioreactor to provide mechanical stimuli and to ensure a homogeneous distribution of the oxygen and nutrients through the scaffold. As expected, the proliferation rate was higher for the cells cultured in the dynamic system. Thus, a confluent and aligned multilayer of cells was observed on the surface of the scaffold, while just a monolayer of cells was found over the graft grown under static conditions. Although the CorMx is said to be decellularized, few nuclei of cells within the unseeded scaffold were clearly visible in some lots of the material by microscopic examination. This makes it difficult to define whether the nuclei found within the scaffold belong to the seeded cells or to the decellularization leftover. As expected, viability assay showed that these cells were not viable and the evaluation of the scaffold explanted after three and four months in a swine model, showed no sign of an inflammatory response due to the incomplete decellularization.

CorMx material has shown good outcome in many preclinical studies that have demonstrated minimal scar formation and eventual remodelling of the graft following implantation (Valentin et al. 2006; Badylak et al. 2008). A study performed in rats showed that the RVOT reconstitution with CorMx resulted in new cardiac tissue formation in the patched area and ventricular dimension close to the normal baseline values when compared with Dacron reconstruction of the RVOT, which resulted in significant ventricular dilatation (Wainwright et al. 2012). Most of the preclinical studies that have shown new cardiac tissue formation during the CorMx remodelling, also suggest that there might be a chance for growth and reconstitution of the native tissue, which is particularly desirable among the paediatric patients. To date, only a few studies have attempted to create engineered patches with CorMx. For instance, it has been shown that cardiac pericytes can colonize the scaffold and efficiently penetrate into it after three weeks of culturing under dynamic conditions (Avolio et al. 2015). Tanaka et al. showed that CorMx enhanced with controlled released of fibroblast growth factor enabled in situ constructive myocardial remodelling when surgically implanted into the porcine RV (Tanaka et al. 2015). Most of the obtained in vivo results did not met the expectations and a few issues were reported, including unfavourable inflammatory response, calcification, low seeded cell survival and electrical uncoupling of the seeded

cells to the host tissue (Wendel et al. 2014; Leor et al. 2000). Despite these unfavourable outcomes, we did not observe any inflammatory response nor calcification process associated to the implantation of either the engineered CorMx or the unseeded control after 4 months in vivo.

With this study we demonstrated the security and feasibility to use either unseeded CorMx or cell-seeded CorMx for RVOT reconstruction. A novel swine model of CPB with recovery of the animal was developed to test such constructs. The pigs were treated like pediatric patients, in order to mimic as close as possible the clinical operating conditions. Three juvenile pigs underwent CPB to perform a RVOT reconstruction using a CorMx patch. Two animals successfully recovered and were terminated 4 months post-surgery. One of these piglets was implanted with a TE-patch, while the other was patched with the unseeded scaffold. The third pig was implanted with a TE-patch and was sacrificed 24 hours after surgery. Doppler-echocardiography showed that the operated animals had normal cardiac function and anatomy in comparison with non-operated control pigs.

Histological examinations of the grafts explanted 4 months post-operation, showed complete degradation of the CorMx as the scaffold was no longer detectable in the RV. New tissue formation was found in the patched area and a mature endothelialisation was detected in the inner side of both the seeded and unseeded explants. In fact the immunostaining for endothelial and smooth muscle markers of the inner layer of the explants was similar to what was observed in the native tissue. Tissue remodelling was also observed in both explants as some cardiac-like areas were identified in the graft-side of the two explants. However, the remodelling present in the TE-patch appeared to be more intense. In fact more “cardiac pockets” were found in the engineered graft and some of them expressed CX43, that being marker of mature cardiomyocytes (Halbach et al. 2007; Severs et al. 2008), it may imply that these areas were closer to the phenotype of the native tissue. Additionally, a quantification study of the vasculature present in the newly formed tissue, demonstrated that the TE-patch was significantly more vascularized than the unseeded scaffold, suggesting that the presence of the seeded cells might have triggered the angiogenesis. Indeed, it has been well established that the MSCs play a key role in promoting angiogenesis and would healing (Sasaki et al. 2008; Nguyen et al. 2010; King et al. 2014). The histological evaluation of the TE-patch that was explanted 24 hours post-op, showed an acute inflammation of the cardiac tissue surrounding the implanted patch. However, a specific staining for inflammatory markers

has not been performed yet, thus our conclusions are based on histological stainings of the tissue. We reckon that this intense inflammatory response was not due to the patch itself, but rather to the surgery performed the day before. A thick layer of cells expressing endothelial markers was observed in the inner side of the scaffold (where the seeded cells were growing). Based on these preliminary results it not clear yet whether these cells have migrated from the adjacent tissue or if they have been recruited from the blood stream as endothelial progenitor cells (EPCs) and have attached to the graft. The interaction between MSCs and EPCs has been extensively investigated. For example, the coculture of BM-MSCs with EPCs has been demonstrated to induce angiogenic differentiation and tubulogenesis (Rouwkema et al. 2009). Moreover cotransplantation of MSCs and EPCs has been shown to significantly improve diabetic would healing (Sukpat et al. 2013) and improve healing of complex bone defects (Keramaris et al. 2012). Based on our preliminary results, we believe that it is more probable that the EPCs and endothelial cells found on the graft have migrated from the surrounding native tissue rather than being recruited from the blood stream, for this latter option consisting of a longer process. Further experiments both in vitro and in vivo have been planned to clarify the interaction between the MSCs and the endothelial cells. For example, we will coculture the MSCs and the EPCs in a system that keeps the two cells line separate but would allow the migration of the EPCs only. This in vitro model should clarify the chemoattraction carried out from the MSCs towards the EPCs.

This in vivo study represents a proof of concept for the feasibility of our approach. The results obtained so far are by no mean conclusive on the subject, they are rather considered as initial data leading to further investigations. More animals need to be implanted, in order to have at least three unseeded control-pigs and three with engineered-patch grafting. To date, one further piglet has been implanted with an engineered-patch. The animal recovered well and will be terminated in four months.

In conclusion, we provided a method to isolate, expand and commit human and porcine mesenchymal stem cells derived from the thymus gland, into cardiac-like phenotype. The use of this cell type is of high clinical relevance as the starting material is normally discharged during palliative surgery and allows the application of autologous stem cells. We have also established three protocols to efficiently decellularize porcine pericardium and myocardium in order to generate biocompatible scaffolds that allow cellular engraftment and proliferation. In addition, we have demonstrated that our cells can be used to engineer CorMx, a material that holds great promises as scaffold in cardiac TE being relatively inexpensive, easy to handle, biodegradable and off-the-shelf. Its safety has already been proven for clinical application in many organs, including the heart (Zaidi et al. 2014; Holubec et al. 2015) and the FDA has already approved its surgical use. Lastly, we performed a preclinical proof-of-concept study demonstrating that our novel CPB methodology is safe and feasible. The validation of our large animal model is of major importance to investigate the suitability of a cardiac patch for RVOT reconstruction in a paediatric setting.

REFERENCES

Al-Halees, Z., F. Pieters, F. Qadoura, M. Shahid, M. Al-Amri, and F. Al-Fadley. 2002. 'The Ross procedure is the procedure of choice for congenital aortic valve disease', *J Thorac Cardiovasc Surg*, 123: 437-41; discussion 41-2.

Alsoufi, B. 2014. 'Aortic valve replacement in children: Options and outcomes', *J Saudi Heart Assoc*, 26: 33-41.

Anderson, R. H., and N. A. Brown. 1996. 'The anatomy of the heart revisited', *Anat Rec*, 246: 1-7.

Anderson, R. H., and B. R. Wilcox. 1992. 'The surgical anatomy of ventricular septal defect', *J Card Surg*, 7: 17-35.

Avolio, E., I. Rodriguez-Arabaolaza, H. L. Spencer, F. Riu, G. Mangialardi, S. C. Slater, J. Rowlinson, V. V. Alvino, O. O. Idowu, S. Soyombo, A. Oikawa, M. M. Swim, C. H. Kong, H. Cheng, H. Jia, M. T. Ghorbel, J. C. Hancox, C. H. Orchard, G. Angelini, C. Emanueli, M. Caputo, and P. Madeddu. 2015. 'Expansion and characterization of neonatal cardiac pericytes provides a novel cellular option for tissue engineering in congenital heart disease', *J Am Heart Assoc*, 4: e002043.

Badylak, S. F., J. E. Valentin, A. K. Ravindra, G. P. McCabe, and A. M. Stewart-Akers. 2008. 'Macrophage phenotype as a determinant of biologic scaffold remodeling', *Tissue Eng Part A*, 14: 1835-42.

Badylak, S., K. Kokini, B. Tullius, A. Simmons-Byrd, and R. Morff. 2002. 'Morphologic study of small intestinal submucosa as a body wall repair device', *J Surg Res*, 103: 190-202.

Barry, F. P., and J. M. Murphy. 2004. 'Mesenchymal stem cells: clinical applications and biological characterization', *Int J Biochem Cell Biol*, 36: 568-84.

Bell, P. E., and G. T. Diffee, Jr. 1991. 'Cardiopulmonary bypass. Principles, nursing implications', *AORN J*, 53: 1480-96.

Beltrami, A. P., L. Barlucchi, D. Torella, M. Baker, F. Limana, S. Chimenti, H. Kasahara, M. Rota, E. Musso, K. Urbanek, A. Leri, J. Kajstura, B. Nadal-Ginard, and P. Anversa. 2003. 'Adult cardiac stem cells are multipotent and support myocardial regeneration', *Cell*, 114: 763-76.

Brennan, M. P., A. Dardik, N. Hibino, J. D. Roh, G. N. Nelson, X. Papademitris, T. Shinoka, and C. K. Breuer. 2008. 'Tissue-engineered vascular grafts demonstrate evidence of growth and development when implanted in a juvenile animal model', *Ann Surg*, 248: 370-7.

Brown, B. N., J. E. Valentin, A. M. Stewart-Akers, G. P. McCabe, and S. F. Badylak. 2009. 'Macrophage phenotype and remodeling outcomes in response to biologic scaffolds with and without a cellular component', *Biomaterials*, 30: 1482-91.

Burkhart, H. M., M. Y. Qureshi, S. C. Peral, P. W. O'Leary, T. M. Olson, F. Cetta, T. J. Nelson, and Group Wanek Program Clinical Pipeline. 2015. 'Regenerative therapy for hypoplastic left heart syndrome: first report of intraoperative intramyocardial injection of autologous umbilical-cord blood-derived cells', *J Thorac Cardiovasc Surg*, 149: e35-7.

Cantero Peral, S., H. M. Burkhart, S. Oommen, S. Yamada, S. L. Nyberg, X. Li, P. W. O'Leary, A. Terzic, B. C. Cannon, T. J. Nelson, and Group Wanek Program Porcine Pipeline. 2015. 'Safety and feasibility for pediatric cardiac regeneration using epicardial delivery of autologous umbilical cord blood-derived mononuclear cells established in a porcine model system', *Stem Cells Transl Med*, 4: 195-206.

Carrier, R. L., M. Papadaki, M. Rupnick, F. J. Schoen, N. Bursac, R. Langer, L. E. Freed, and G. Vunjak-Novakovic. 1999. 'Cardiac tissue engineering: cell seeding, cultivation parameters, and tissue construct characterization', *Biotechnol Bioeng*, 64: 580-9.

Cheema, F. H., G. Polvani, M. Argenziano, and M. Pesce. 2012. 'Combining stem cells and tissue engineering in cardiovascular repair -- a step forward to derivation of

novel implants with enhanced function and self-renewal characteristics', *Recent Pat Cardiovasc Drug Discov*, 7: 10-20.

Cook, J. L., and D. B. Fox. 2007. 'A novel bioabsorbable conduit augments healing of avascular meniscal tears in a dog model', *Am J Sports Med*, 35: 1877-87.

Crick, S. J., M. N. Sheppard, S. Y. Ho, L. Gebstein, and R. H. Anderson. 1998. 'Anatomy of the pig heart: comparisons with normal human cardiac structure', *J Anat*, 193 (Pt 1): 105-19.

Dai, W., J. Dong, G. Chen, and T. Uemura. 2009. 'Application of low-pressure cell seeding system in tissue engineering', *Biosci Trends*, 3: 216-9.

Davies, B., N. J. Elwood, S. Li, F. Cullinane, G. A. Edwards, D. F. Newgreen, and C. P. Brizard. 2010. 'Human cord blood stem cells enhance neonatal right ventricular function in an ovine model of right ventricular training', *Ann Thorac Surg*, 89: 585-93, 93 e1-4.

Dean, E. W., B. Udelsman, and C. K. Breuer. 2012. 'Current advances in the translation of vascular tissue engineering to the treatment of pediatric congenital heart disease', *Yale J Biol Med*, 85: 229-38.

Dimarino, A. M., A. I. Caplan, and T. L. Bonfield. 2013. 'Mesenchymal stem cells in tissue repair', *Front Immunol*, 4: 201.

Dohmen, P. M., F. da Costa, S. Yoshi, S. V. Lopes, F. P. da Souza, R. Vilani, A. F. Wouk, M. da Costa, and W. Konertz. 2006. 'Histological evaluation of tissue-engineered heart valves implanted in the juvenile sheep model: is there a need for in-vitro seeding?', *J Heart Valve Dis*, 15: 823-9.

Dominici, M., K. Le Blanc, I. Mueller, I. Slaper-Cortenbach, F. Marini, D. Krause, R. Deans, A. Keating, Dj Prockop, and E. Horwitz. 2006. 'Minimal criteria for defining multipotent mesenchymal stromal cells. The International Society for Cellular Therapy position statement', *Cytotherapy*, 8: 315-7.

Donmez, A., and O. Yurdakok. 2014. 'Cardiopulmonary bypass in infants', *J Cardiothorac Vasc Anesth*, 28: 778-88.

Drukker, M., G. Katz, A. Urbach, M. Schuldiner, G. Markel, J. Itskovitz-Eldor, B. Reubinoff, O. Mandelboim, and N. Benvenisty. 2002. 'Characterization of the expression of MHC proteins in human embryonic stem cells', *Proc Natl Acad Sci U S A*, 99: 9864-9.

Du, Z. D., Z. M. Hijazi, C. S. Kleinman, N. H. Silverman, K. Larntz, and Investigators Amplatzer. 2002. 'Comparison between transcatheter and surgical closure of secundum atrial septal defect in children and adults: results of a multicenter nonrandomized trial', *J Am Coll Cardiol*, 39: 1836-44.

Eschenhagen, T., C. Fink, U. Remmers, H. Scholz, J. Wattchow, J. Weil, W. Zimmermann, H. H. Dohmen, H. Schafer, N. Bishopric, T. Wakatsuki, and E. L. Elson. 1997. 'Three-dimensional reconstitution of embryonic cardiomyocytes in a collagen matrix: a new heart muscle model system', *FASEB J*, 11: 683-94.

Field, M. L., B. Al-Alao, N. Mediratta, and A. Sosnowski. 2006. 'Open and closed chest extrathoracic cannulation for cardiopulmonary bypass and extracorporeal life support: methods, indications, and outcomes', *Postgrad Med J*, 82: 323-31.

Fuchs, J. R., S. Terada, E. R. Ochoa, J. P. Vacanti, and D. O. Fauza. 2002. 'Fetal tissue engineering: in utero tracheal augmentation in an ovine model', *J Pediatr Surg*, 37: 1000-6; discussion 00-6.

Fukuhara, S., S. Tomita, S. Yamashiro, T. Morisaki, C. Yutani, S. Kitamura, and T. Nakatani. 2003. 'Direct cell-cell interaction of cardiomyocytes is key for bone marrow stromal cells to go into cardiac lineage in vitro', *J Thorac Cardiovasc Surg*, 125: 1470-80.

Gabbieri, D., P. M. Dohmen, J. Linneweber, A. Lembcke, J. P. Braun, and W. Konertz. 2007. 'Ross procedure with a tissue-engineered heart valve in complex congenital aortic valve disease', *J Thorac Cardiovasc Surg*, 133: 1088-9.

Gao, Y., and J. G. Jacot. 2015. 'Stem Cells and Progenitor Cells for Tissue-Engineered Solutions to Congenital Heart Defects', *Biomark Insights*, 10: 139-46.

Gardin, C., S. Ricci, L. Ferroni, R. Guazzo, L. Sbricoli, G. De Benedictis, L. Finotti, M. Isola, E. Bressan, and B. Zavan. 2015. 'Decellularization and Delipidation Protocols of Bovine Bone and Pericardium for Bone Grafting and Guided Bone Regeneration Procedures', *PLoS One*, 10: e0132344.

Gardner, R. L. 2002. 'Stem cells: potency, plasticity and public perception', *J Anat*, 200: 277-82.

Gelb, B. D., and W. K. Chung. 2014. 'Complex Genetics and the Etiology of Human Congenital Heart Disease', *Cold Spring Harbor Perspectives in Medicine*, 4.

Ghanbari, H., H. Viatge, A. G. Kidane, G. Burriesci, M. Tavakoli, and A. M. Seifalian. 2009. 'Polymeric heart valves: new materials, emerging hopes', *Trends Biotechnol*, 27: 359-67.

Gnecchi, M., P. Danieli, and E. Cervio. 2012. 'Mesenchymal stem cell therapy for heart disease', *Vascul Pharmacol*, 57: 48-55.

Gnecchi, M., H. He, N. Noiseux, O. D. Liang, L. Zhang, F. Morello, H. Mu, L. G. Melo, R. E. Pratt, J. S. Ingwall, and V. J. Dzau. 2006. 'Evidence supporting paracrine hypothesis for Akt-modified mesenchymal stem cell-mediated cardiac protection and functional improvement', *FASEB J*, 20: 661-9.

Halbach, M., K. Pfannkuche, F. Pillekamp, A. Ziomka, T. Hannes, M. Reppel, J. Hescheler, and J. Muller-Ehmsen. 2007. 'Electrophysiological maturation and integration of murine fetal cardiomyocytes after transplantation', *Circ Res*, 101: 484-92.

Hasan, A., R. Waters, B. Roula, R. Dana, S. Yara, T. Alexandre, and A. Paul. 2016. 'Engineered Biomaterials to Enhance Stem Cell-Based Cardiac Tissue Engineering and Therapy', *Macromol Biosci*, 16: 958-77.

Hecker, L., and R. K. Birla. 2007. 'Engineering the heart piece by piece: state of the art in cardiac tissue engineering', *Regen Med*, 2: 125-44.

Hemli, J. M., N. C. Patel, and V. A. Subramanian. 2012. 'Increasing surgical experience with off-pump coronary surgery does not mitigate the morbidity of emergency conversion to cardiopulmonary bypass', *Innovations (Phila)*, 7: 259-65.

Hibino, N., E. McGillicuddy, G. Matsumura, Y. Ichihara, Y. Naito, C. Breuer, and T. Shinoka. 2010. 'Late-term results of tissue-engineered vascular grafts in humans', *J Thorac Cardiovasc Surg*, 139: 431-6, 36 e1-2.

Hirt, M. N., A. Hansen, and T. Eschenhagen. 2014. 'Cardiac tissue engineering: state of the art', *Circ Res*, 114: 354-67.

Hoashi, T., G. Matsumiya, S. Miyagawa, H. Ichikawa, T. Ueno, M. Ono, A. Saito, T. Shimizu, T. Okano, N. Kawaguchi, N. Matsuura, and Y. Sawa. 2009. 'Skeletal myoblast sheet transplantation improves the diastolic function of a pressure-overloaded right heart', *J Thorac Cardiovasc Surg*, 138: 460-7.

Holubec, T., E. Caliskan, S. H. Sundermann, C. T. Starck, A. Plass, D. Bettex, V. Falk, and F. Maisano. 2015. 'Use of extracellular matrix patches in cardiac surgery', *J Card Surg*, 30: 145-8.

In 't Anker, P. S., S. A. Scherjon, C. Kleijburg-van der Keur, W. A. Noort, F. H. Claas, R. Willemze, W. E. Fibbe, and H. H. Kanhai. 2003. 'Amniotic fluid as a novel source of mesenchymal stem cells for therapeutic transplantation', *Blood*, 102: 1548-9.

Ishigami, S., S. Ohtsuki, S. Tarui, D. Ousaka, T. Eitoku, M. Kondo, M. Okuyama, J. Kobayashi, K. Baba, S. Arai, T. Kawabata, K. Yoshizumi, A. Tateishi, Y. Kuroko, T. Iwasaki, S. Sato, S. Kasahara, S. Sano, and H. Oh. 2015. 'Intracoronary autologous

cardiac progenitor cell transfer in patients with hypoplastic left heart syndrome: the TICAP prospective phase 1 controlled trial', *Circ Res*, 116: 653-64.

Jacobs, M. L. 2000a. 'Congenital Heart Surgery Nomenclature and Database Project: tetralogy of Fallot', *Ann Thorac Surg*, 69: S77-82.

———. 2000b. 'Congenital Heart Surgery Nomenclature and Database Project: truncus arteriosus', *Ann Thorac Surg*, 69: S50-5.

Kadivar, M., S. Khatami, Y. Mortazavi, M. A. Shokrgozar, M. Taghikhani, and M. Soleimani. 2006. 'In vitro cardiomyogenic potential of human umbilical vein-derived mesenchymal stem cells', *Biochem Biophys Res Commun*, 340: 639-47.

Kadner, A., S. P. Hoerstrup, G. Zund, K. Eid, C. Maurus, S. Melnitchouk, J. Grunenfelder, and M. I. Turina. 2002. 'A new source for cardiovascular tissue engineering: human bone marrow stromal cells', *Eur J Cardiothorac Surg*, 21: 1055-60.

Kalavrouziotis, G., M. Purohit, G. Ciotti, A. F. Corno, and M. Pozzi. 2006. 'Truncus arteriosus communis: Early and midterm results of early primary repair', *Annals of Thoracic Surgery*, 82: 2200-06.

Kalfa, D., and E. Bacha. 2013. 'New technologies for surgery of the congenital cardiac defect', *Rambam Maimonides Med J*, 4: e0019.

Kaushal, S., J. P. Jacobs, J. G. Gossett, A. Steele, P. Steele, C. R. Davis, E. Pahl, K. Vijayan, A. Asante-Korang, R. J. Boucek, C. L. Backer, and L. E. Wold. 2009. 'Innovation in basic science: stem cells and their role in the treatment of paediatric cardiac failure--opportunities and challenges', *Cardiol Young*, 19 Suppl 2: 74-84.

Kawada, H., J. Fujita, K. Kinjo, Y. Matsuzaki, M. Tsuma, H. Miyatake, Y. Muguruma, K. Tsuboi, Y. Itabashi, Y. Ikeda, S. Ogawa, H. Okano, T. Hotta, K. Ando, and K. Fukuda. 2004. 'Nonhematopoietic mesenchymal stem cells can be mobilized and differentiate into cardiomyocytes after myocardial infarction', *Blood*, 104: 3581-7.

Keramaris, N. C., S. Kaptanis, H. L. Moss, M. Loppini, S. Pneumaticos, and N. Maffulli. 2012. 'Endothelial progenitor cells (EPCs) and mesenchymal stem cells (MSCs) in bone healing', *Curr Stem Cell Res Ther*, 7: 293-301.

Kern, S., H. Eichler, J. Stoeve, H. Kluter, and K. Bieback. 2006. 'Comparative analysis of mesenchymal stem cells from bone marrow, umbilical cord blood, or adipose tissue', *Stem Cells*, 24: 1294-301.

Khoshnood, B., N. Lelong, L. Houyel, A. C. Thieulin, J. M. Jouannic, S. Magnier, A. L. Delezoide, J. F. Magny, C. Rambaud, D. Bonnet, F. Goffinet, and Epicard Study Group. 2012. 'Prevalence, timing of diagnosis and mortality of newborns with congenital heart defects: a population-based study', *Heart*, 98: 1667-73.

King, A., S. Balaji, S. G. Keswani, and T. M. Crombleholme. 2014. 'The Role of Stem Cells in Wound Angiogenesis', *Adv Wound Care (New Rochelle)*, 3: 614-25.

Krasuski, R. A., and T. M. Bashore. 2016. 'Congenital Heart Disease Epidemiology in the United States: Blindly Feeling for the Charging Elephant', *Circulation*, 134: 110-3.

Krause, K., C. Schneider, K. H. Kuck, and K. Jaquet. 2010. 'Stem cell therapy in cardiovascular disorders', *Cardiovasc Ther*, 28: e101-10.

Labovsky, V., E. L. Hofer, L. Feldman, V. Fernandez Vallone, H. Garcia Rivello, A. Bayes-Genis, A. Hernando Insua, M. J. Levin, and N. A. Chasseing. 2010. 'Cardiomyogenic differentiation of human bone marrow mesenchymal cells: Role of cardiac extract from neonatal rat cardiomyocytes', *Differentiation*, 79: 93-101.

Lacour-Gayet, F., A. Serraf, T. Komiya, M. Sousa-Uva, J. Bruniaux, A. Touchot, D. Roux, P. Neuville, and C. Planche. 1996. 'Truncus arteriosus repair: influence of techniques of right ventricular outflow tract reconstruction', *J Thorac Cardiovasc Surg*, 111: 849-56.

Laflamme, M. A., K. Y. Chen, A. V. Naumova, V. Muskheli, J. A. Fugate, S. K. Dupras, H. Reinecke, C. Xu, M. Hassanipour, S. Police, C. O'Sullivan, L. Collins, Y. Chen, E. Minami, E. A. Gill, S. Ueno, C. Yuan, J. Gold, and C. E. Murry. 2007. 'Cardiomyocytes derived from human embryonic stem cells in pro-survival factors enhance function of infarcted rat hearts', *Nat Biotechnol*, 25: 1015-24.

Laflamme, M. A., and C. E. Murry. 2005. 'Regenerating the heart', *Nat Biotechnol*, 23: 845-56.

Lambert, V., E. Gouadon, A. Capderou, E. Le Bret, M. Ly, S. Dinanian, J. F. Renaud, M. Puceat, and C. Rucker-Martin. 2015. 'Right ventricular failure secondary to chronic overload in congenital heart diseases: benefits of cell therapy using human embryonic stem cell-derived cardiac progenitors', *J Thorac Cardiovasc Surg*, 149: 708-15 e1.

Lee, M. Y., B. Sun, S. Schliffke, Z. Yue, M. Ye, J. Paavola, E. C. Bozkulak, P. J. Amos, Y. Ren, R. Ju, Y. W. Jung, X. Ge, L. Yue, B. E. Ehrlich, and Y. Qyang. 2012. 'Derivation of functional ventricular cardiomyocytes using endogenous promoter sequence from murine embryonic stem cells', *Stem Cell Res*, 8: 49-57.

Leor, J., S. Aboulafia-Etzion, A. Dar, L. Shapiro, I. M. Barbash, A. Battler, Y. Granot, and S. Cohen. 2000. 'Bioengineered cardiac grafts: A new approach to repair the infarcted myocardium?', *Circulation*, 102: III56-61.

Lian, X., C. Hsiao, G. Wilson, K. Zhu, L. B. Hazeltine, S. M. Azarin, K. K. Raval, J. Zhang, T. J. Kamp, and S. P. Palecek. 2012. 'Robust cardiomyocyte differentiation from human pluripotent stem cells via temporal modulation of canonical Wnt signaling', *Proc Natl Acad Sci U S A*, 109: E1848-57.

Lian, X., J. Zhang, S. M. Azarin, K. Zhu, L. B. Hazeltine, X. Bao, C. Hsiao, T. J. Kamp, and S. P. Palecek. 2013. 'Directed cardiomyocyte differentiation from human pluripotent stem cells by modulating Wnt/beta-catenin signaling under fully defined conditions', *Nat Protoc*, 8: 162-75.

Liu, H., E. B. Slamovich, and T. J. Webster. 2006. 'Less harmful acidic degradation of poly(lacticco-glycolic acid) bone tissue engineering scaffolds through titania nanoparticle addition', *Int J Nanomedicine*, 1: 541-5.

Lu, L., S. J. Peter, M. D. Lyman, H. L. Lai, S. M. Leite, J. A. Tamada, S. Uyama, J. P. Vacanti, R. Langer, and A. G. Mikos. 2000. 'In vitro and in vivo degradation of porous poly(DL-lactic-co-glycolic acid) foams', *Biomaterials*, 21: 1837-45.

Lyons, F. G., A. A. Al-Munajjed, S. M. Kieran, M. E. Toner, C. M. Murphy, G. P. Duffy, and F. J. O'Brien. 2010. 'The healing of bony defects by cell-free collagen-based scaffolds compared to stem cell-seeded tissue engineered constructs', *Biomaterials*, 31: 9232-43.

Maeda, K., and M. Ruel. 2015. 'The clinical application potential of extracellular matrix in cardiac tissue engineering', *J Thorac Cardiovasc Surg*, 150: 1290-1.

Majumdar, M. K., M. Keane-Moore, D. Buyaner, W. B. Hardy, M. A. Moorman, K. R. McIntosh, and J. D. Mosca. 2003. 'Characterization and functionality of cell surface molecules on human mesenchymal stem cells', *J Biomed Sci*, 10: 228-41.

Maltsev, V. A., A. M. Wobus, J. Rohwedel, M. Bader, and J. Hescheler. 1994. 'Cardiomyocytes differentiated in vitro from embryonic stem cells developmentally express cardiac-specific genes and ionic currents', *Circ Res*, 75: 233-44.

Martin, I., D. Wendt, and M. Heberer. 2004. 'The role of bioreactors in tissue engineering', *Trends Biotechnol*, 22: 80-6.

Mayshar, Y., U. Ben-David, N. Lavon, J. C. Biancotti, B. Yakir, A. T. Clark, K. Plath, W. E. Lowry, and N. Benvenisty. 2010. 'Identification and classification of

chromosomal aberrations in human induced pluripotent stem cells', *Cell Stem Cell*, 7: 521-31.

Mendoza-Novelo, B., E. E. Avila, J. V. Cauich-Rodriguez, E. Jorge-Herrero, F. J. Rojo, G. V. Guinea, and J. L. Mata-Mata. 2011. 'Decellularization of pericardial tissue and its impact on tensile viscoelasticity and glycosaminoglycan content', *Acta Biomater*, 7: 1241-8.

Mirsadraee, S., H. E. Wilcox, S. A. Korossis, J. N. Kearney, K. G. Watterson, J. Fisher, and E. Ingham. 2006. 'Development and characterization of an acellular human pericardial matrix for tissue engineering', *Tissue Eng*, 12: 763-73.

Momma, K. 2010. 'Cardiovascular anomalies associated with chromosome 22q11.2 deletion syndrome', *Am J Cardiol*, 105: 1617-24.

Mosala Nezhad, Z., A. Poncelet, L. de Kerchove, C. Fervaille, X. Banse, X. Bollen, J. P. Dehoux, G. El Khoury, and P. Gianello. 2016. 'CorMatrix valved conduit in a porcine model: long-term remodelling and biomechanical characterization', *Interact Cardiovasc Thorac Surg*.

Murphy, C. M., M. G. Haugh, and F. J. O'Brien. 2010. 'The effect of mean pore size on cell attachment, proliferation and migration in collagen-glycosaminoglycan scaffolds for bone tissue engineering', *Biomaterials*, 31: 461-6.

Murphy, C. M., and F. J. O'Brien. 2010. 'Understanding the effect of mean pore size on cell activity in collagen-glycosaminoglycan scaffolds', *Cell Adh Migr*, 4: 377-81.

Nartprayut, K., U. Pratya Y, P. Kheolamai, S. Manochantr, M. Chayosumrit, S. Issaragrisil, and A. Supokawej. 2013. 'Cardiomyocyte differentiation of perinatallyderived mesenchymal stem cells', *Mol Med Rep*, 7: 1465-9.

Neumann, A., S. Cebotari, I. Tudorache, A. Haverich, and S. Sarikouch. 2013. 'Heart valve engineering: decellularized allograft matrices in clinical practice', *Biomed Tech (Berl)*, 58: 453-6.

Nguyen, B. K., S. Maltais, L. P. Perrault, J. F. Tanguay, J. C. Tardif, L. M. Stevens, M. Borie, F. Harel, S. Mansour, and N. Noiseux. 2010. 'Improved function and myocardial repair of infarcted heart by intracoronary injection of mesenchymal stem cell-derived growth factors', *J Cardiovasc Transl Res*, 3: 547-58.

Nolan, K., Y. Millet, C. Ricordi, and C. L. Stabler. 2008. 'Tissue engineering and biomaterials in regenerative medicine', *Cell Transplant*, 17: 241-3.

Nora, J. J., and A. H. Nora. 1990. 'Etiology of Congenital Heart-Diseases Revisited - Genetic Core Lesions, Genetic-Environmental Interactions, Developmental Mechanisms, and Chance', *Developmental Cardiology*: 549-56.

O'Brien, F. J., B. A. Harley, I. V. Yannas, and L. J. Gibson. 2005. 'The effect of pore size on cell adhesion in collagen-GAG scaffolds', *Biomaterials*, 26: 433-41.

Okita, K., M. Nakagawa, H. Hyenjong, T. Ichisaka, and S. Yamanaka. 2008. 'Generation of mouse induced pluripotent stem cells without viral vectors', *Science*, 322: 949-53.

Ott, H. C., T. S. Matthiesen, S. K. Goh, L. D. Black, S. M. Kren, T. I. Netoff, and D. A. Taylor. 2008. 'Perfusion-decellularized matrix: using nature's platform to engineer a bioartificial heart', *Nat Med*, 14: 213-21.

Pagoulatou, E., I. E. Triantaphyllidou, D. H. Vynios, D. J. Papachristou, E. Koletsis, D. Deligianni, and D. Mavrilas. 2012. 'Biomechanical and structural changes following the decellularization of bovine pericardial tissues for use as a tissue engineering scaffold', *J Mater Sci Mater Med*, 23: 1387-96.

Patel, D. M., J. Shah, and A. S. Srivastava. 2013. 'Therapeutic potential of mesenchymal stem cells in regenerative medicine', *Stem Cells Int*, 2013: 496218.

Pelech, A. N., and U. Broeckel. 2005. 'Toward the etiologies of congenital heart diseases', *Clinics in Perinatology*, 32: 825-+.

Pradines, M., I. Masson, R. Portero, C. Giroux, and J. M. Gracies. 2016. 'Muscle lengthening and structural changes in the muscle-tendon complex of triceps surae after 1 year of rehabilitation including a daily self-stretch program in patients with chronic hemiparesis', *Ann Phys Rehabil Med*, 59S: e73.

Quarti, A., S. Nardone, M. Colaneri, G. Santoro, and M. Pozzi. 2011. 'Preliminary experience in the use of an extracellular matrix to repair congenital heart diseases', *Interact Cardiovasc Thorac Surg*, 13: 569-72.

Rajabi-Zeleti, S., S. Jalili-Firoozinezhad, M. Azarnia, F. Khayyatan, S. Vahdat, S. Nikeghbalian, A. Khademhosseini, H. Baharvand, and N. Aghdami. 2014. 'The behavior of cardiac progenitor cells on macroporous pericardium-derived scaffolds', *Biomaterials*, 35: 970-82.

Rangappa, S., J. W. Entwistle, A. S. Wechsler, and J. Y. Kresh. 2003. 'Cardiomyocyte-mediated contact programs human mesenchymal stem cells to express cardiogenic phenotype', *J Thorac Cardiovasc Surg*, 126: 124-32.

Razzouk, A. J., and L. L. Bailey. 2014. 'Heart transplantation in children for end-stage congenital heart disease', *Semin Thorac Cardiovasc Surg Pediatr Card Surg Annu*, 17: 69-76.

Reubinoff, B. E., M. F. Pera, C. Y. Fong, A. Trounson, and A. Bongso. 2000. 'Embryonic stem cell lines from human blastocysts: somatic differentiation in vitro', *Nat Biotechnol*, 18: 399-404.

Roufosse, C. A., N. C. Direkze, W. R. Otto, and N. A. Wright. 2004. 'Circulating mesenchymal stem cells', *Int J Biochem Cell Biol*, 36: 585-97.

Roura, S., C. Galvez-Monton, and A. Bayes-Genis. 2014. 'Umbilical cord blood-derived mesenchymal stem cells: new therapeutic weapons for idiopathic dilated cardiomyopathy?', *Int J Cardiol*, 177: 809-18.

Rouwkema, J., P. E. Westerweel, J. de Boer, M. C. Verhaar, and C. A. van Blitterswijk. 2009. 'The use of endothelial progenitor cells for prevascularized bone tissue engineering', *Tissue Eng Part A*, 15: 2015-27.

Rowlands, A. S., S. A. Lim, D. Martin, and J. J. Cooper-White. 2007. 'Polyurethane/poly(lactic-co-glycolic) acid composite scaffolds fabricated by thermally induced phase separation', *Biomaterials*, 28: 2109-21.

Rupp, S., C. Jux, H. Bonig, J. Bauer, T. Tonn, E. Seifried, S. Dimmeler, A. M. Zeiher, and D. Schranz. 2012. 'Intracoronary bone marrow cell application for terminal heart failure in children', *Cardiol Young*, 22: 558-63.

Sadegh, A. B., E. Basiri, A. Oryan, and P. Mirshokraei. 2014. 'Wrapped omentum with periosteum concurrent with adipose derived adult stem cells for bone tissue engineering in dog model', *Cell Tissue Bank*, 15: 127-37.

Said, S. M., and H. M. Burkhart. 2014. 'When repair is not feasible: prosthesis selection in children and adults with congenital heart disease', *Semin Thorac Cardiovasc Surg Pediatr Card Surg Annu*, 17: 22-9.

Sanganalmath, S. K., and R. Bolli. 2013. 'Cell therapy for heart failure: a comprehensive overview of experimental and clinical studies, current challenges, and future directions', *Circ Res*, 113: 810-34.

Sasaki, M., R. Abe, Y. Fujita, S. Ando, D. Inokuma, and H. Shimizu. 2008. 'Mesenchymal stem cells are recruited into wounded skin and contribute to wound repair by transdifferentiation into multiple skin cell type', *J Immunol*, 180: 2581-7.

Scharn, D. M., W. J. Oyen, P. L. Klemm, M. H. Wijnen, and J. A. vanderVliet. 2002. 'Assessment of prosthetic vascular graft thrombogenicity using the technetium-99m labeled glycoprotein IIb/IIIa receptor antagonist DMP444 in a dog model', *Cardiovasc Surg*, 10: 566-9.

Schneider, R. K., J. Anraths, R. Kramann, J. Bornemann, M. Bovi, R. Knuchel, and S. Neuss. 2010. 'The role of biomaterials in the direction of mesenchymal stem cell properties and extracellular matrix remodelling in dermal tissue engineering', *Biomaterials*, 31: 7948-59.

Scholl, F. G., M. M. Boucek, K. C. Chan, L. Valdes-Cruz, and R. Perryman. 2010. 'Preliminary experience with cardiac reconstruction using decellularized porcine extracellular matrix scaffold: human applications in congenital heart disease', *World J Pediatr Congenit Heart Surg*, 1: 132-6.

Severs, N. J., A. F. Bruce, E. Dupont, and S. Rothery. 2008. 'Remodelling of gap junctions and connexin expression in diseased myocardium', *Cardiovasc Res*, 80: 9-19.

Shimizu, T., M. Yamato, Y. Isoi, T. Akutsu, T. Setomaru, K. Abe, A. Kikuchi, M. Umezu, and T. Okano. 2002. 'Fabrication of pulsatile cardiac tissue grafts using a novel 3-dimensional cell sheet manipulation technique and temperature-responsive cell culture surfaces', *Circ Res*, 90: e40.

Shin'oka, T., Y. Imai, and Y. Ikada. 2001. 'Transplantation of a tissue-engineered pulmonary artery', *N Engl J Med*, 344: 532-3.

Shinoka, T., C. K. Breuer, R. E. Tanel, G. Zund, T. Miura, P. X. Ma, R. Langer, J. P. Vacanti, and J. E. Mayer, Jr. 1995. 'Tissue engineering heart valves: valve leaflet replacement study in a lamb model', *Ann Thorac Surg*, 60: S513-6.

Siebzehnrubl, F. A., V. Vedam-Mai, H. Azari, B. A. Reynolds, and L. P. Deleyrolle. 2011. 'Isolation and characterization of adult neural stem cells', *Methods Mol Biol*, 750: 61-77.

Silka, M. J., B. G. Hardy, V. D. Menashe, and C. D. Morris. 1998. 'A population-based prospective evaluation of risk of sudden cardiac death after operation for common congenital heart defects', *J Am Coll Cardiol*, 32: 245-51.

Smit, F. E., and P. M. Dohmen. 2015. 'Cardiovascular tissue engineering: where we come from and where are we now?', *Med Sci Monit Basic Res*, 21: 1-3.

Sojak, V., J. Lugo, D. Koolbergen, and M. Hazekamp. 2012. 'Surgery for truncus arteriosus', *Multimed Man Cardiothorac Surg*, 2012: mms011.

Steeds, R. P., and D. Oakley. 2004. 'Predicting late sudden death from ventricular arrhythmia in adults following surgical repair of tetralogy of Fallot', *QJM*, 97: 7-13.

Steele, A., and P. Steele. 2006. 'Stem cells for repair of the heart', *Curr Opin Pediatr*, 18: 518-23.

Steinert, A. F., C. Hendrich, and U. Zimmermann. 2001. '[Tissue engineering of cartilage replacement tissue in an improved alginate matrix]', *Z Orthop Ihre Grenzgeb*, 139: M94-5.

Sukpat, S., N. Isarasena, J. Wongphoom, and S. Patumraj. 2013. 'Vasculoprotective effects of combined endothelial progenitor cells and mesenchymal stem cells in diabetic wound care: their potential role in decreasing wound-oxidative stress', *Biomed Res Int*, 2013: 459196.

Sun, R., M. Liu, L. Lu, Y. Zheng, and P. Zhang. 2015. 'Congenital Heart Disease: Causes, Diagnosis, Symptoms, and Treatments', *Cell Biochem Biophys*, 72: 857-60.

Suzuki, Y., A. C. Yeung, and F. Ikeno. 2011. 'The representative porcine model for human cardiovascular disease', *J Biomed Biotechnol*, 2011: 195483.

Takahashi, K., K. Tanabe, M. Ohnuki, M. Narita, T. Ichisaka, K. Tomoda, and S. Yamanaka. 2007. 'Induction of pluripotent stem cells from adult human fibroblasts by defined factors', *Cell*, 131: 861-72.

Tanaka, A., K. Kawaji, A. R. Patel, Y. Tabata, M. C. Burke, M. P. Gupta, and T. Ota. 2015. 'In situ constructive myocardial remodeling of extracellular matrix patch

enhanced with controlled growth factor release', *J Thorac Cardiovasc Surg*, 150: 1280-90 e2.

Taniguchi, H., A. Sugioka, K. Fukao, and H. Nakauchi. 1997. 'Characterization of hematopoietic stem cells in the adult liver', *Transplant Proc*, 29: 1212-3.

Tarui, S., S. Sano, and H. Oh. 2014. 'Stem cell therapies in patients with single ventricle physiology', *Methodist Debakey Cardiovasc J*, 10: 77-81.

Tchervenkov, C. I., M. L. Jacobs, and S. A. Tahta. 2000. 'Congenital Heart Surgery Nomenclature and Database Project: hypoplastic left heart syndrome', *Ann Thorac Surg*, 69: S170-9.

Tennant, P. W., G. J. Gibson, L. Parker, and M. S. Pearce. 2010. 'Childhood respiratory illness and lung function at ages 14 and 50 years: childhood respiratory illness and lung function', *Chest*, 137: 146-55.

Thiene, G., and C. Frescura. 2010. 'Anatomical and pathophysiological classification of congenital heart disease', *Cardiovasc Pathol*, 19: 259-74.

Thompson, D. 1984. 'Anatomy of the heart', *Nurs Mirror*, 159: 28-34.

Thompson, L. D., D. B. McElhinney, V. M. Reddy, E. Petrossian, N. H. Silverman, and F. L. Hanley. 2001. 'Neonatal repair of truncus arteriosus: Continuing improvement in outcomes', *Annals of Thoracic Surgery*, 72: 391-95.

Thomson, J. A., J. Itskovitz-Eldor, S. S. Shapiro, M. A. Waknitz, J. J. Swiergiel, V. S. Marshall, and J. M. Jones. 1998. 'Embryonic stem cell lines derived from human blastocysts', *Science*, 282: 1145-7.

Toma, C., M. F. Pittenger, K. S. Cahill, B. J. Byrne, and P. D. Kessler. 2002. 'Human mesenchymal stem cells differentiate to a cardiomyocyte phenotype in the adult murine heart', *Circulation*, 105: 93-8.

Uccelli, A., L. Moretta, and V. Pistoia. 2008. 'Mesenchymal stem cells in health and disease', *Nat Rev Immunol*, 8: 726-36.

Urban, A. E., N. Sinzobahamvya, A. M. Brecher, J. Wetter, and S. Malorny. 1998. 'Truncus arteriosus: ten-year experience with homograft repair in neonates and infants', *Ann Thorac Surg*, 66: S183-8.

Utzon, F. 1976. '[Transposition of the great vessels. Corrective surgery by Mustard's method in 5 children]', *Ugeskr Laeger*, 138: 2127-32.

Valentin, J. E., J. S. Badylak, G. P. McCabe, and S. F. Badylak. 2006. 'Extracellular matrix bioscaffolds for orthopaedic applications. A comparative histologic study', *J Bone Joint Surg Am*, 88: 2673-86.

van der Bom, T., A. C. Zomer, A. H. Zwinderman, F. J. Meijboom, B. J. Bouma, and B. J. Mulder. 2011. 'The changing epidemiology of congenital heart disease', *Nat Rev Cardiol*, 8: 50-60.

Van Mierop, L. H. 1965. 'Anatomy of the heart', *Clin Symp*, 17: 67-90.

Van Praagh, R., and S. Van Praagh. 1965. 'The anatomy of common aorticopulmonary trunk (truncus arteriosus communis) and its embryologic implications. A study of 57 necropsy cases', *Am J Cardiol*, 16: 406-25.

Vincentelli, A., F. Wautot, F. Juthier, O. Fouquet, D. Corseaux, S. Marechaux, T. Le Tourneau, O. Fabre, S. Susen, E. Van Belle, F. Mouquet, C. Decoene, A. Prat, and B. Jude. 2007. 'In vivo autologous recellularization of a tissue-engineered heart valve: are bone marrow mesenchymal stem cells the best candidates?', *J Thorac Cardiovasc Surg*, 134: 424-32.

Wainwright, J. M., R. Hashizume, K. L. Fujimoto, N. T. Remlinger, C. Pesyna, W. R. Wagner, K. Tobita, T. W. Gilbert, and S. F. Badylak. 2012. 'Right ventricular outflow tract repair with a cardiac biologic scaffold', *Cells Tissues Organs*, 195: 159-70.

Wang, H. S., S. C. Hung, S. T. Peng, C. C. Huang, H. M. Wei, Y. J. Guo, Y. S. Fu, M. C. Lai, and C. C. Chen. 2004. 'Mesenchymal stem cells in the Wharton's jelly of the human umbilical cord', *Stem Cells*, 22: 1330-7.

Wehman, B., and S. Kaushal. 2015. 'The emergence of stem cell therapy for patients with congenital heart disease', *Circ Res*, 116: 566-9.

Weiland, A. P., and W. E. Walker. 1986. 'Physiologic principles and clinical sequelae of cardiopulmonary bypass', *Heart Lung*, 15: 34-9.

Wendel, J. S., L. Ye, P. Zhang, R. T. Tranquillo, and J. J. Zhang. 2014. 'Functional consequences of a tissue-engineered myocardial patch for cardiac repair in a rat infarct model', *Tissue Eng Part A*, 20: 1325-35.

Whiting, D., K. Yuki, and J. A. DiNardo. 2015. 'Cardiopulmonary bypass in the pediatric population', *Best Pract Res Clin Anaesthesiol*, 29: 241-56.

Williams, K. J., A. A. Picou, S. L. Kish, A. M. Giraldo, R. A. Godke, and K. R. Bondioli. 2008. 'Isolation and characterization of porcine adipose tissue-derived adult stem cells', *Cells Tissues Organs*, 188: 251-8.

Witt, R. G., G. Raff, J. Van Gundy, M. Rodgers-Ohlau, and M. S. Si. 2013. 'Short-term experience of porcine small intestinal submucosa patches in paediatric cardiovascular surgery', *Eur J Cardiothorac Surg*, 44: 72-6.

Wold, L. E., W. Dai, C. Sesti, S. L. Hale, J. S. Dow, B. J. Martin, and R. A. Kloner. 2004. 'Stem cell therapy for the heart', *Congest Heart Fail*, 10: 293-301.

Woo, J. S., M. C. Fishbein, and B. Reemtsen. 2016. 'Histologic examination of decellularized porcine intestinal submucosa extracellular matrix (CorMatrix) in pediatric congenital heart surgery', *Cardiovasc Pathol*, 25: 12-7.

Woodward, C. S. 2011. 'Keeping children with congenital heart disease healthy', *J Pediatr Health Care*, 25: 373-8.

Xie, X. J., J. A. Wang, J. Cao, and X. Zhang. 2006. 'Differentiation of bone marrow mesenchymal stem cells induced by myocardial medium under hypoxic conditions', *Acta Pharmacol Sin*, 27: 1153-8.

Xu, W., X. Zhang, H. Qian, W. Zhu, X. Sun, J. Hu, H. Zhou, and Y. Chen. 2004. 'Mesenchymal stem cells from adult human bone marrow differentiate into a cardiomyocyte phenotype in vitro', *Exp Biol Med (Maywood)*, 229: 623-31.

Yamanaka, S., J. Li, G. Kania, S. Elliott, R. P. Wersto, J. Van Eyk, A. M. Wobus, and K. R. Boheler. 2008. 'Pluripotency of embryonic stem cells', *Cell Tissue Res*, 331: 5-22.

Yannas, I. V., E. Lee, D. P. Orgill, E. M. Skrabut, and G. F. Murphy. 1989. 'Synthesis and characterization of a model extracellular matrix that induces partial regeneration of adult mammalian skin', *Proc Natl Acad Sci U S A*, 86: 933-7.

Yap, K. H., R. Murphy, M. Devbhandari, and R. Venkateswaran. 2013. 'Aortic valve replacement: is porcine or bovine valve better?', *Interact Cardiovasc Thorac Surg*, 16: 361-73.

Ye, L., Y. H. Chang, Q. Xiong, P. Zhang, L. Zhang, P. Somasundaram, M. Lepley, C. Swingen, L. Su, J. S. Wendel, J. Guo, A. Jang, D. Rosenbush, L. Greder, J. R. Dutton, J. Zhang, T. J. Kamp, D. S. Kaufman, Y. Ge, and J. Zhang. 2014. 'Cardiac repair in a porcine model of acute myocardial infarction with human induced pluripotent stem cell-derived cardiovascular cells', *Cell Stem Cell*, 15: 750-61.

Young, H. E., and A. C. Black, Jr. 2004. 'Adult stem cells', *Anat Rec A Discov Mol Cell Evol Biol*, 276: 75-102.

Yu, J., M. A. Vodyanik, K. Smuga-Otto, J. Antosiewicz-Bourget, J. L. Frane, S. Tian, J. Nie, G. A. Jonsdottir, V. Ruotti, R. Stewart, Slukvin, II, and J. A. Thomson. 2007. 'Induced pluripotent stem cell lines derived from human somatic cells', *Science*, 318: 1917-20.

Zaidi, A. H., M. Nathan, S. Emani, C. Baird, P. J. del Nido, K. Gauvreau, M. Harris, S. P. Sanders, and R. F. Padera. 2014. 'Preliminary experience with porcine intestinal submucosa (CorMatrix) for valve reconstruction in congenital heart disease: histologic evaluation of explanted valves', *J Thorac Cardiovasc Surg*, 148: 2216-4, 25 e1.

Zhang, J., G. F. Wilson, A. G. Soerens, C. H. Koonce, J. Yu, S. P. Palecek, J. A. Thomson, and T. J. Kamp. 2009. 'Functional cardiomyocytes derived from human induced pluripotent stem cells', *Circ Res*, 104: e30-41.

Ziolkowska, L., W. Kawalec, A. Turska-Kmiec, M. Krajewska-Walasek, G. Brzezinska-Rajszys, J. Daszkowska, B. Maruszewski, and P. Burczynski. 2008. 'Chromosome 22q11.2 microdeletion in children with conotruncal heart defects: frequency, associated cardiovascular anomalies, and outcome following cardiac surgery', *Eur J Pediatr*, 167: 1135-40.